SN-140

196p.

INVESTIGATION OF RELATIONS BETWEEN SOLAR VARIATIONS AND WEATHER ON EARTH AS SHOWN BY SATELLITE DATA

FINAL REPORT

CONTRACT No. NASw-724

CODE-1

NASA CR 52182

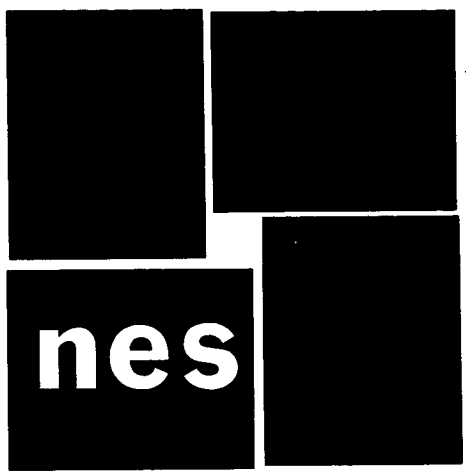

OCTOBER 1963

NATIONAL ENGINEERING SCIENCE CO.

PREPARED FOR

NATIONAL AERONAUTICS AND SPACE ADMINISTRATION

WASHINGTON, D.C.

INVESTIGATION OF RELATIONS BETWEEN SOLAR VARIATIONS AND WEATHER ON EARTH AS SHOWN BY SATELLITE DATA

Final Report
(NASA CR 52682; SN-140)

OTS: $12.50 phs
$5.48 mf

Prepared by

John C. Freeman, Jr.,
Leon F. Graves, and
W. H. Portig

Prepared for

NATIONAL AERONAUTICS AND SPACE ADMINISTRATION
Washington, D. C.

Final Report
(NASA Contract ~~No.~~ NASw-724)

October 1963 176p

NATIONAL ENGINEERING SCIENCE ~~COMPANY~~
914 Main Street, Houston ~~2~~, ~~Texas~~

PREFACE

Dr. B. J. O'Brien speaks of solar system measurements, especially solar wind and related measurements, as "solar weather observations." This is an attractive nomenclature and we would like to take this opportunity to endorse it. We might also try to introduce the term "icarology" or "acticology"[1] as the "scientific" name of the study of solar weather.

The present report is made up of several original papers written during the duration of the NESCO project SN-140, sponsored by the National Aeronautics and Space Administration under contract No. NASw-624. There is one paper (not previously published but read in 1958) important to this study and for which only the drafting was done at this time on this contract. Another paper is not yet available but will be in the Proceedings of Hurricane Conference in Mexico City, June 1963; it illustrates one point effectively enough to be included in this report.

The data from TIROS III was to form an important part of this study as originally conceived; however, the data (ordered two months before the study started) was received only six weeks prior to the end of the contract period. This unfortunate timing is reflected in the text and illustration of this report. It is hoped that we can continue our study of these data.

---

1 Many an ic'a-rologist or ic'a-rologer is a meteorologist in disguise. (To emphasize solar emanations rather than Icanian wings, Dr. Martin S. Day, Professor of English, University of Houston, coined acticology.)

In carrying out the work we have made use of the terminology and conventions for the high atmosphere recommended in June 1962 by the World Meteorological Organization[1]:

"The successive regions of the upper atmosphere will be known as the stratosphere, mesosphere and thermosphere, separated respectively by the stratopause and mesopause, all as broadly defined below:

a) Stratosphere: Region (situated between the tropopause and stratopause) in which the temperature generally increases with height.

b) Stratopause: The top of the inversion layer in the upper stratosphere (usually around 50 to 55 km).

c) Mesosphere: Region (situated between stratopause and mesopause) in which temperature generally decreases with height.

d) Mesopause: The base of the inversion at the top of the mesosphere (usually found at 80 to 85 km).

e) Thermosphere: Region above the mesopause in which temperature generally increases with height."

---

1 Bull. Amer. Meteor. Soc., 44, p. 429.

Solar heating of the mesophere has an almost instantaneous effect on the wind systems of the mesosphere and very high stratosphere. Since this heating effect depends strongly on time and position of the earth with respect to the sun, an attempt has been made to separate it from seasonal effects and evaluate it in this report.

TABLE OF CONTENTS

	Page
PREFACE	iii
TABLE OF CONTENTS	vii
LIST OF FIGURES	x
ABSTRACT	xiii
PART A:	
SOLAR WEATHER AND EARTH WEATHER IN AUGUST AND SEPTEMBER 1961 AS SHOWN BY SATELLITES AND OTHER OBSERVATIONS	1
REFERENCES	24
SOURCES OF WEATHER ANALYSES	27
LIST OF SYMBOLS	29
PART B:	
A MODEL OF THE ATMOSPHERE FOR INVESTIGATING THE INTERACTION WITH THE SUN THROUGH THE SOLAR WIND	31
REFERENCES	51
LIST OF SYMBOLS	53
APPENDIX I:	
THICKNESS OF A SHOCK WAVE IN THE SOLAR WIND	I-1
REFERENCES	I-5
LIST OF SYMBOLS	I-7
APPENDIX II:	
A POSSIBLE OSCILLATION OF THE WINDS IN THE EQUATORIAL STRATOSPHERE WITH A PERIOD OF 24 TO 27 MONTHS	II-1

	Page
REFERENCES	II-11
LIST OF SYMBOLS	II-13
APPENDIX III:	
A POSSIBLE INERTIAL OSCILLATION OF THE EQUATORIAL STRATOSPHERE	III-1
REFERENCES	III-6
LIST OF SYMBOLS	III-7
APPENDIX IV:	
A THEORY FOR ATMOSPHERIC CROSS SECTIONS	IV-1
REFERENCES	IV-37
LIST OF SYMBOLS	IV-39
APPENDIX V:	
SELECTION OF KEY DAYS	V-1
REFERENCES	V-6
LIST OF SYMBOLS	V-7
APPENDIX VI:	
INDICES OF SOLAR ACTIVITY	VI-1
REFERENCES	VI-4
LIST OF SYMBOLS	VI-5
APPENDIX VII:	
A MODEL OF EQUATORIAL FLOW	VII-1
REFERENCES	VII-16
LIST OF SYMBOLS	VII-17

Page

APPENDIX VIII:

THOUGHTS DEVELOPED AFTER A DISCUSSION OF SOLAR WEATHER WITH THE STAFF MEMBERS OF THE SOUTHWEST CENTER FOR ADVANCED STUDIES VIII-1

REFERENCES VIII-7

LIST OF FIGURES

FIGURE		Page
1	SOLAR AND MAGNETIC DATA	8
2	SOLAR AND MAGNETOSPHERE DATA	10
3	IONOSPHERE DATA	11
4	WIND AND MAGNETIC DATA	13
5	CLOUD ANALYSIS AFTER TIROS III AND WEATHER ANALYSIS, 30 AUGUST 1961	21
6	CLOUD ANALYSIS AFTER TIROS III AND WEATHER ANALYSIS, 2 SEPTEMBER 1961	22
7	WEATHER ANALYSES FOR 30 AUGUST, 3 SEPTEMBER, AND 11 SEPTEMBER 1961	(in pocket)
8	VISIBLE CORONA AND SOLAR WIND	33
9	EARTH'S MAGNETIC CAVITY	35
10	ATMOSPHERIC MODEL	37
11	RESPONSE OF THE POLAR TROPOPAUSE TO HEATING	40
12	RESPONSE OF THE POLAR TROPOPAUSE TO HEATING	49
13	RESPONSE OF THE POLAR TROPOPAUSE TO HEATING	50
II-1	VERTICAL WAVE MODEL	II-4
II-2	BANDS OF VORTICITY	II-5
III-1	VERTICAL WAVE MODEL	III-2
III-2	BANDS OF VORTICITY	III-3
IV-1	ISOTACHS AND ISENTROPES	IV-9
IV-2	THE DISTURBED WIND FIELD	IV-10

FIGURE		Page
IV-3	THE GRAPHICAL COMPUTER	IV-11
IV-4	THE GRAPHICAL COMPUTER	IV-12
IV-5	THE NEW STEADY STATE	IV-13
IV-6	INTERFACE CONDITIONS	IV-15
IV-7	FRONT IN ANTICYCLONIC VORTICITY	IV-16
IV-8	JET STREAM AND FRONT	IV-17
IV-9	VORTICITY DISTRIBUTION	IV-18
IV-10	MODEL JET STREAM AND FRONT	IV-19
IV-11	DIFFUSION OF VORTICITY	IV-20
IV-12	LAYERS ON A SLOPING GROUND	IV-31
IV-13	STABLE AND ADIABATIC LAYERS	IV-32
VII-1	TROPICAL VORTICITY BANDS	VII-3
VII-2	OUTLINE OF A BLOCK	VII-5
VII-3	WINDS IN A BLOCK	VII-9
VII-4	ISOBARS IN A BLOCK	VII-10
VIII-1	THE TURBULENT SOLAR SYSTEM	VIII-2
VIII-2	THE SPIRAL MAGNETIC FIELD	VIII-3
VIII-3	STORM HYDROMAGNETIC SHOCK	VIII-4

ABSTRACT

Data from satellites, especially that from Explorer XII, Mariner II and satellite drag estimates of temperature and density, were used to gain secondary measures of the solar wind and to show that a pressure increase at very high altitude is to be expected with increased solar activity.

A theory of response to pressure changes in the polar atmosphere at 80 to 100 km is presented showing that inertia waves should transmit wind changes downward in three to six days. It is also shown theoretically that the stable polar atmosphere should have about 17% of the pressure gradient change at 20 km that an autobarotropic fluid would have.

These combined observed and theoretical results lend credence to the "blind" correlations of magnetic indices and weather indices.

We have evidence that an increase in solar wind causes the westerlies to increase in about five days and then to decrease in 13 to 20 days and that this result is to be expected from mesopheric observations and from theory.

PART A

SOLAR WEATHER AND EARTH WEATHER IN AUGUST AND SEPTEMBER 1961 AS SHOWN BY SATELLITES AND OTHER OBSERVATIONS

by

John C. Freeman, Jr., Leon F. Graves,
and W. H. Portig

SOLAR WEATHER AND EARTH WEATHER IN AUGUST AND SEPTEMBER 1961 AS SHOWN BY SATELLITES AND OTHER OBSERVATIONS

When the writer's desire to study solar effects on the atmosphere (troposphere) by means of satellite data was originally transmitted to NASA in 1962, the satellite data for August and September 1961 was not available in the literature and consideration of data for any later date was out of the question. By May, 1963 the 1961 data was appearing in published reports. One of the primary measures of the solar wind (by Mariner II) (Snyder, et al, 1963) and the high correlation between solar wind (as measured by Mariner II) and the K_p index for that time was well known among space scientists.

This gives us some basis for estimating the solar wind during the period August and September, 1961. The work of J. W. Freeman (1963) in which he estimates the radial distance to the magnetopause from Van Allen radiation data gives us another secondary measure of the solar wind during this period. (It is interesting to note that there is not a high correlation between these two observations. This point will be discussed later.)

The solar wind is most attractive as a link between disturbances on the sun and disturbances in the normal condition of earth's atmosphere. Several points of attraction are:

1. The solar wind increases to a few hundred per cent of its

minimum value (Snyder, et al, 1963).

2. The solar wind varies most significantly by the day rather than by the second or by the month (similar to the weather) (Snyder, et al, 1863).

3. The sun's disturbances are visible in eight minutes but an effect on the earth carried by the solar winds occurs 24 to 72 hours later. This is good for predictability. The effect of the sun on radio propagation is accepted and well known and it has this lag. See, for example, Akasofu and Chapman, 1960.

4. The solar wind limits the "earth and atmosphere" to a cavity so that we can say that the earth's atmosphere ends at the magnetopause and the sun's atmosphere or corona exists beyond. This cavity is a natural link in solar earth relationships.

5. The solar wind carries hydromagnetic waves (Dessler and Parker, 1959) and so does the earth's magnetic field (Dessler, 1959) so the cavity boundary which has an area exposed to the sun which is 25 to 100 times that of the earth itself is an effective energy catcher.

6. The theories advanced by Dessler (1959) for heating of the lower ionosphere by dissipating hydromagnetic waves are

sound and consistent with many observations.

7. The heating is thought by Dessler (1959) to occur near the poles which is one of the meteorologist's favorite central areas. Also since the heating is local as opposed to the general heating from electromagnetic radiation, we expect higher gradients.

For these reasons, we have emphasized the solar wind as the element of solar "weather" that we will study for weather effects in the troposphere.

It was first pointed out to us by Rao (Snyder, Neugebauer and Rao, 1963) that there is such a high correlation between the solar wind and the K_p index that the K_p index can be used as a measure of the solar wind. Since we had accepted the solar wind as the principle solar-earth link to study, we have used the K_p index as our basic measure of solar effects. This led us naturally to the most recent literature on correlations between magnetic (and other solar) indices and pressure patterns. Most of these are statistical studies based on weather data from large areas of the earth. Since we are working with only one weather situation and are using the case history method, we must depend heavily on these reports for indications of possible statistical significance of our results. Papers of Willett (1961), Shapiro (1958, 1959), Shapiro and Ward (1962a, 1962b) and the work of Woodbridge, Macdonald and Pohrte (1958), along with the constant goading since 1954 of Roberts (e.g. Macdonald and Roberts, 1960) have

been important in this study.

After a survey of these reports we chose the following working hypothesis.

Shapiro and Ward's (1962a) analysis of several years of data and our preliminary analysis of the data for 1961 show that there is a positive correlation between the K_p index and the zonal wind with a 5-day lag and a negative correlation with a 14-day lag.

We offer the following explanation for this:

1. The solar wind is disturbed and turbulent (C. W. Snyder, Marcia Neugebauer and U. R. Rao, 1963).

2. The variation of the solar wind caused the magnetopause to move. (A. J. Dessler, 1962; A. J. Dessler and E. N. Parker, 1959)

3. The stronger the solar wind, the closer the magnetopause is to the earth and the movements have more energy. (Ronald Blum, 1963.)

4. The moving magnetopause causes hydromagnetic waves in the earth's magnetic field. (A. J. Dessler and E. N. Parker, 1959.)

5. The K_p index seems to be a good measure of this disturbance and therefore of the solar wind. (C. W. Snyder, Marcia Neugebauer and U. R. Rao, 1963.)

6. The stronger solar wind results in a larger energy source for the hydromagnetic waves. (More potential energy in the compressed magnetic field.)

7. These waves heat the atmosphere in the dark (Warwick, 1959; Harris, et al, 1962) near the poles (Dessler, 1959) at 100 to 120 km and higher. They are most effective when the pole is dark all 24 hours and least effective when the pole is light.

8. The net result is to cause a warmer pole with higher pressure and a new east wind component at 100 to 120 km (Gas Law and Thermal Wind Equation).

9. This east wind is transmitted downward by means of vibrations of ribbons of constant potential vorticity (refer to papers by J. C. Freeman, 1963). This process can be very fast if the wind speed is large and the gradient of wind with altitude is small and especially inertial waves are the chief mode of travel. (By very fast we mean that some aspects of it can travel from 50 to 15 km in two or three days. There are some instantaneous effects carried by gravity waves.) We assume it travels from 100 km to 50 km "instantaneously" (in 1 to 3 hours) because of the low stability of the mesosphere. (F. S. Johnson, 1961.)

10. This east wind begins to affect the tropopause in 2 to 4 days (N. J. Macdonald and W. O. Roberts, 1960) by pulling it up.

11. The first tropospheric effect is to increase relative vorticity of the tropospheric polar vortex and allow the westerlies and cyclonic vorticities to increase.

12. Macdonald and Roberts (1960) note the increase in the relative vorticity of disturbances (or troughs) in the Gulf of Alaska and Shapiro and Ward (1962a) describe increased westerlies.

13. The final effect (being most pronounced in about 14 days) is the decrease in the west wind as the thermal wind balance of the heated pole asserts itself in the troposphere. Meirs (1963) shows wind changes propagating downward at 1 to 5 km per day and we are postulating movement of 40 to 50 km in 12 to 15 days.

With this hypothesis in mind we have prepared graphs of solar, ionosphere high atmosphere and tropospheric data for the period August and September, 1961.

We will describe the scales and outlines of those figures along with credit for their source.

Because we are concerned with solar-earth weather effects, each Figure 1-4 has the plot of the K_p magnetic index which we take to be

a measure of the solar wind area and a plot of $Z1_p$ the west wind at 700 mb. (Since this is still summer we use the polar zonal index which we will see later contains most of the westerlies.)

Figure 1

SSN the sun spot numbers as reported by Lincoln (1961, 1962). The vertical lines on the graphs denote weeks. The vertical scale for SSN is the observed relative sun spot number.

C_p the planetary magnetic character index from Bartels (1962). The vertical scale is the accepted value of the index. It is a measure of magnetic disturbance.

A_p the planetary magnetic A index from Bartels (1962). This is essentially an expanded K index but has its accepted scale and method of measurement from a magnetogram.

$Z1_p$ the polar zonal index of westerly wind speeds as used and reported by the Extended Forecast Section of the U. S. Weather Bureau. The dotted line is the five day running mean of this quantity plotted three times a week on the day the period ends.

K_p is the planetary magnetic K index from Bartels (1962) summed for the day indicated. This quantity has an accepted scale and we use it as a measure of the solar wind for the day. The dotted line is the 5 day running mean of K_p quantity plotted daily on the last day of the period.

Figure 2

F_{10} the flux of 10.7 cm wave length radio waves as reported by

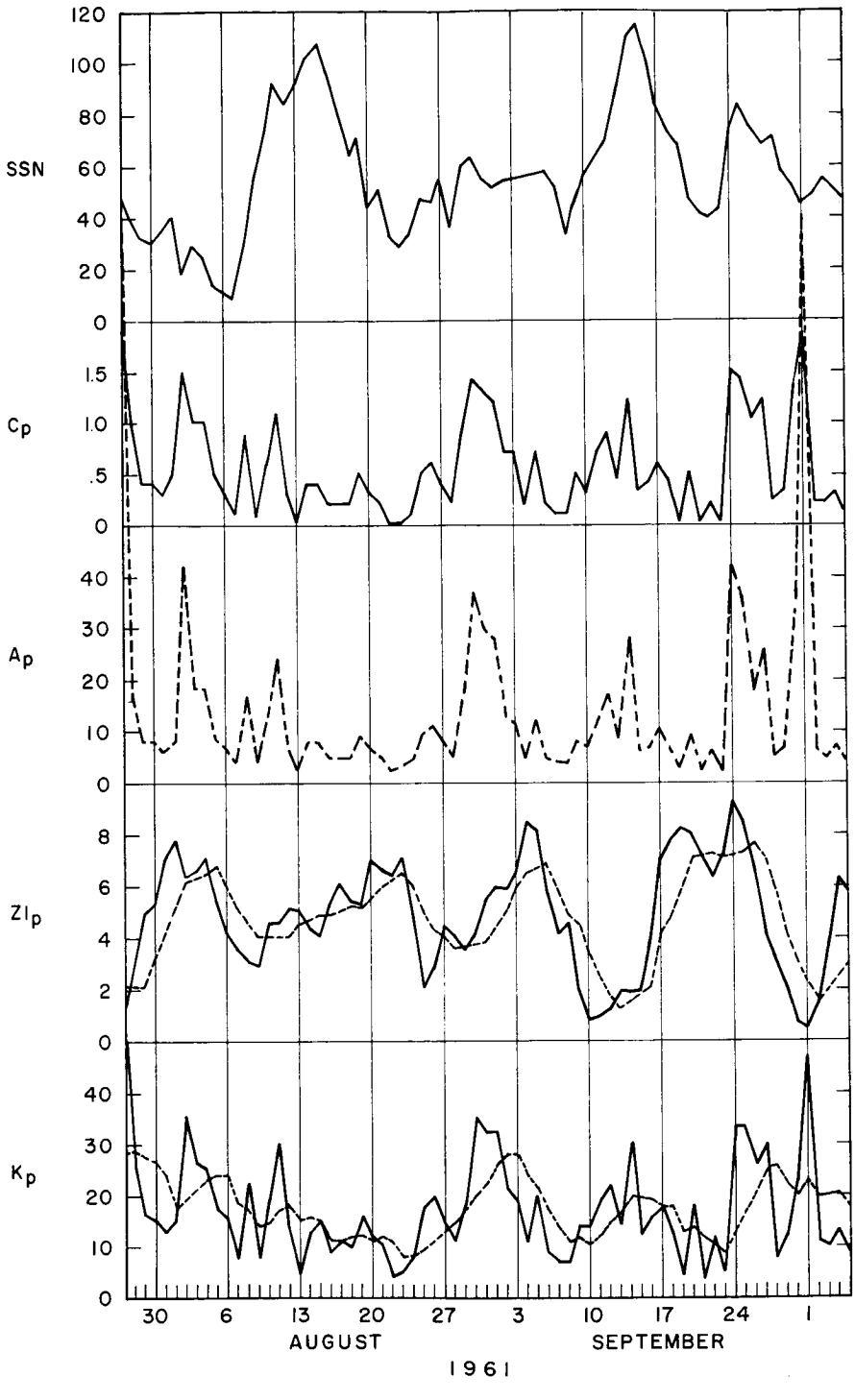

FIGURE 1
SOLAR AND MAGNETIC DATA

Jacchia (1963). He relates these waves to satellite drag and high atmosphere temperature as did King-Hele (1963). The vertical scale is in units of 10^{-22} W/m^2 c/s band width.

F_{20} the flux of 20 cm wave length radio waves.

D_{ST} This is the D_{ST} (H) from the San Juan and Honolulu computed by J. W. Freeman (1963) after Akasofu. This is a special magnetic index used as a measure of the intensity of individual magnetic storms. Note that the maximum deviation of $-100\ \gamma$ occurred in the magnetic storm of September 29 and 30.

R_M J. W. Freeman's (1963) measures the distance (on the sun side of the earth) in which there is a sharp cutoff in the count rate of the S_pL* charged particle detector. He assumes this is the boundary of the magnetosphere (and since it is practically the discovery observation, he is probably right). The figure for our period is plotted here. The units are km x 10^3.

R_M is taken as a measure of the solar wind. (This measure would be influenced by the preceding shock wave in the solar wind.)

Figure 3

$\dot{P}_R - \dot{P}$ The corrected drag on the satellite 1961 δ_1 during the period indicated. Jacchia (1963) takes this as the best summary of satellite drag measurement made on six satellites during this period.

---

* S_pL. An electron energy spectrometer channel with pass band 90 kev to 50 kev.

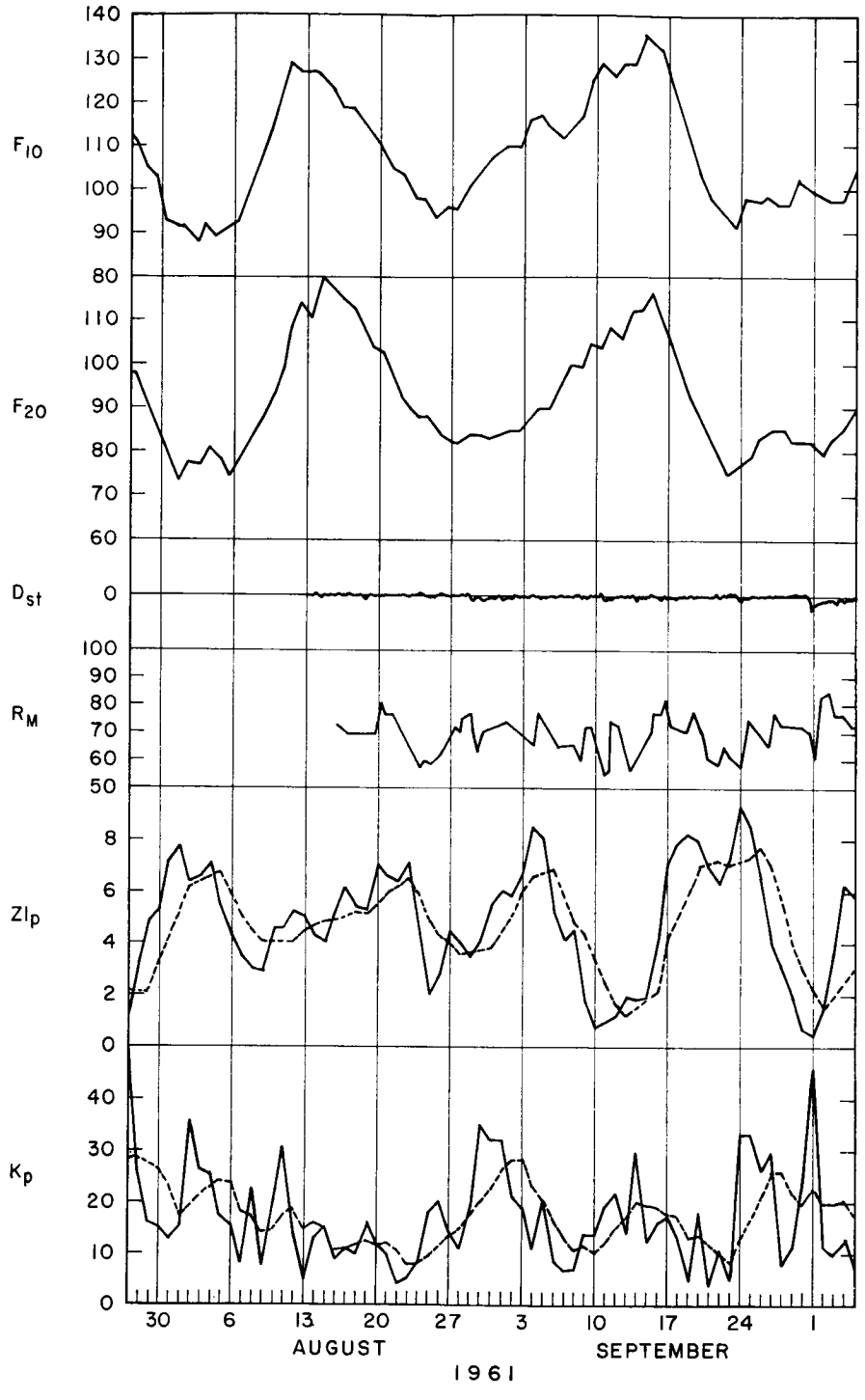

FIGURE 2

SOLAR AND MAGNETOSPHERE DATA

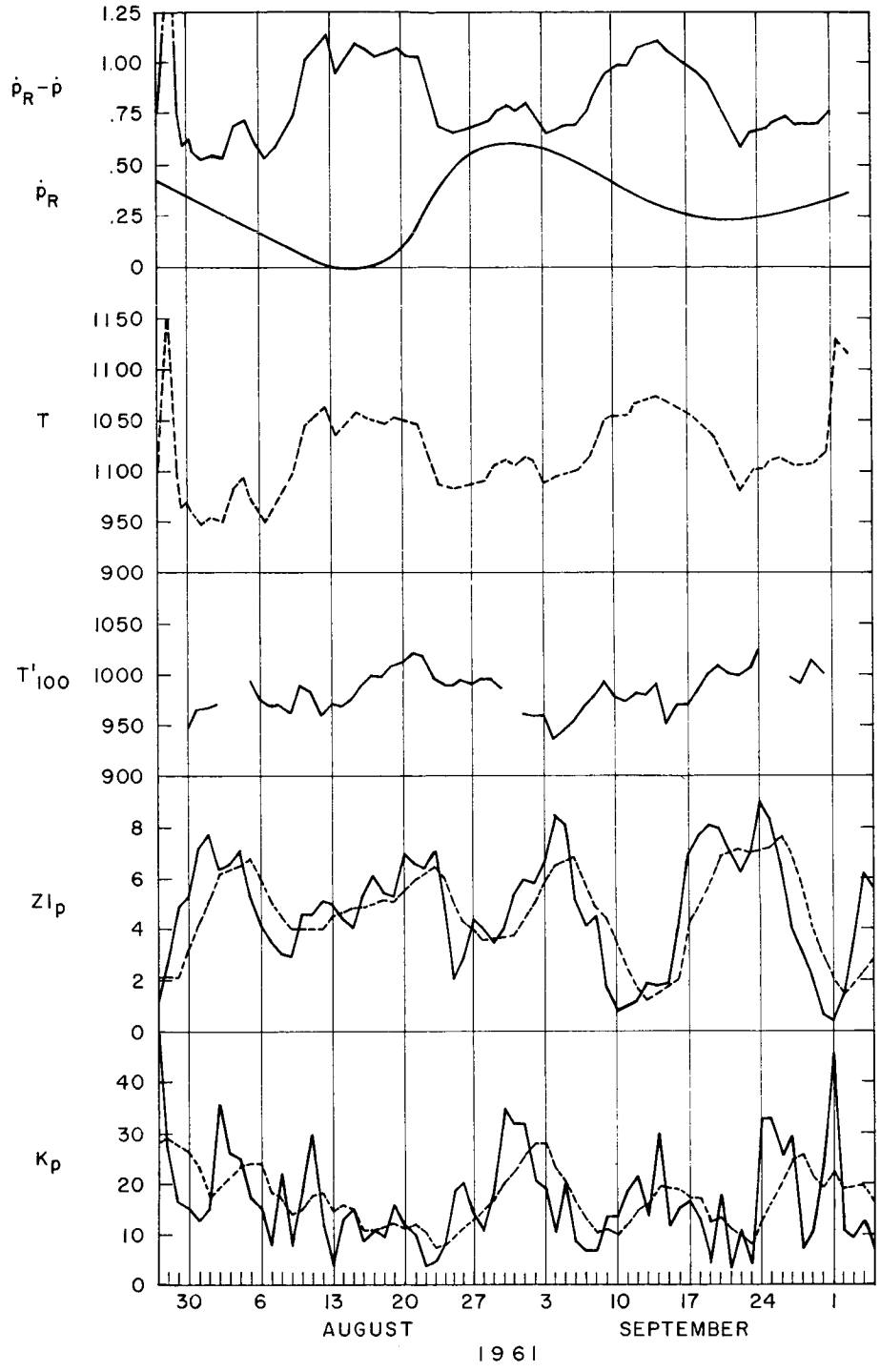

FIGURE 3
IONOSPHERE DATA

The radiation pressure is subtracted and the drag inverted in order to correlate with temperature. High temperature results in high drag. The satellites were at 350 to 650 km.

P_R Radiation pressure drag. The scale is torrs/sec.

T Jacchia's estimate of the temperature at satellite altitude. This would be the temperature in the high ionosphere in ^{o}K.

T'_{100} Jacchia's (1963) standardized temperature. The temperature is "corrected" to $A_p = 0$ and 10.7 cm flux = 100. This is a measure of the accuracy of the fit of his method of temperature estimate.

Figure 4

L An indication of the dates on which certain events are expected according to Shapiro (1959). As you go up three days you find a period of increased persistence begins. In five days a period of increased westerlies begins and in 13 days a period of decreased persistence and westerlies begins.

Δlat Is the difference between the mean latitude of the 18,200 feet height contour at 500 mb and the 19,200 feet height contour at 500 mb (when they define the north and south boundaries of the westerlies). This is expected to vary inversely with the speed of the westerlies.

W-E The maximum easterlies (usually near 80^{o}) are subtracted from the maximum westerlies to get the dotted curve. The solid curve is the mean zonal wind in the ring between 850 and 500 mb and

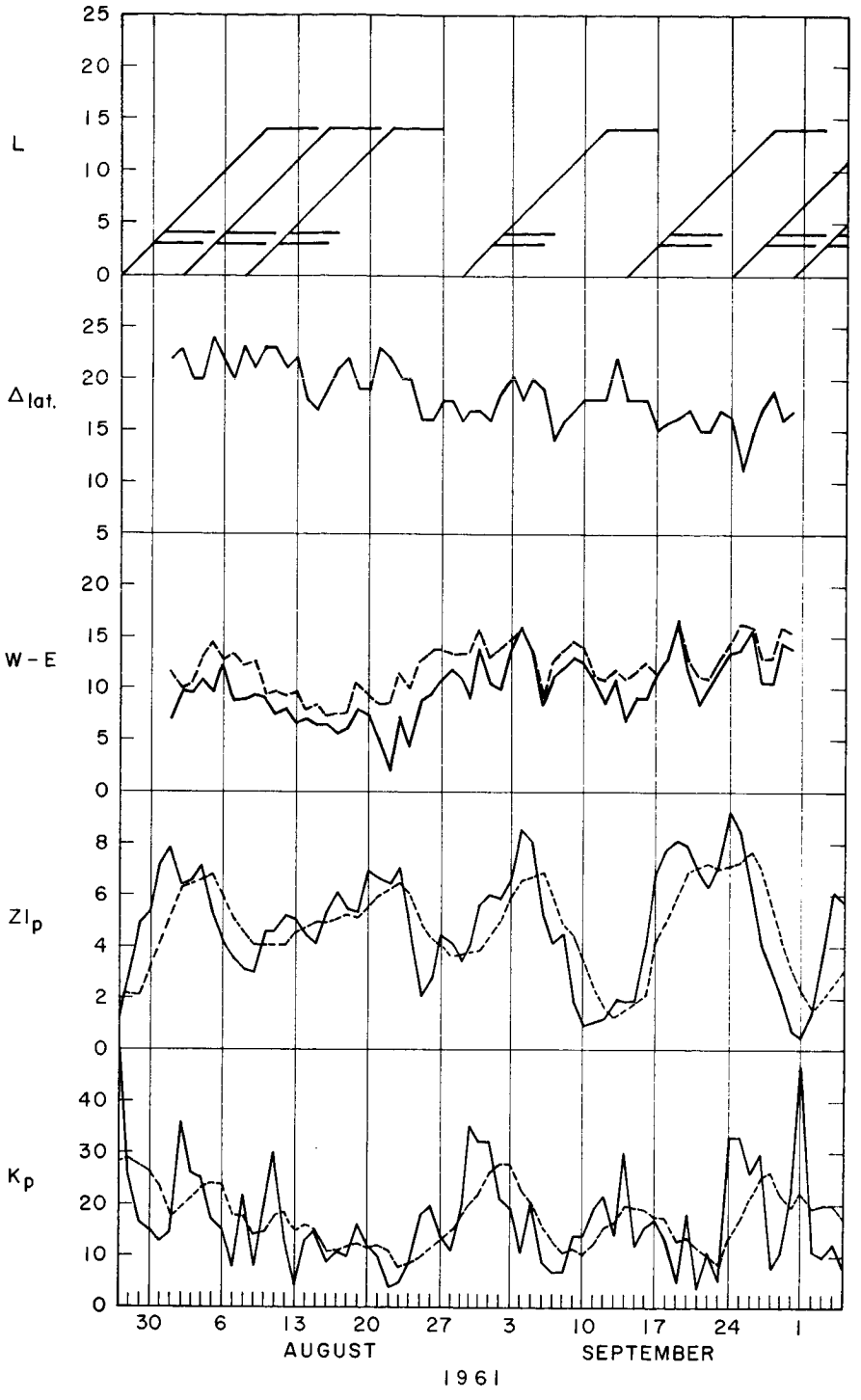

FIGURE 4

WIND AND MAGNETIC DATA

between 50°N and 55°N minus the mean zonal wind in the ring between 850 and 500 mb and between 80°N and 85°N. The figure is based on computation furnished by A. Kreuger of the National Weather Satellite Center of the U. S. Weather Bureau.

In addition to these graphs, we made several subjective studies of the weather patterns at various levels over the whole world. We decided that the pattern of September 10 and 11 was vastly different than that of August 29 and 30. The southern and northern hemisphere flows at 500 mb were mostly strong westerlies on August 29 and 30. The 10 mb chart of Scherhag (1962) showed zonal flow with a ring of high pressure. On September 10 and 11 there were several blocks and cut-off highs and lows. Hurricanes and typhoons were a prominent feature of the map. The 10 mb flow showed a definite two cell pattern on September 10 and 11. (The two cell pattern at 10 mb was firmly established by September 4 and at that time the surface high cell was over the magnetic pole. It progressed from east to west between September 4 and 11.)

These differences and the occurrence of a peak in the K_p index near August 29 led to the choice of August 30, September 3 and September 11 as days to emphasize in the study.

We made some quantitative studies of the differences between these days. The surface pressure distribution in the Northern Hemisphere north of 15° shows that the total weight of air on August 27 and September 10 was the same but that 50% of it was north

of 34.2° on August 27 and 50% of it was north of 34.2° on September 10. Thus there was a pressure increase at the poles during this period and a pressure decrease in lower latitudes.

Even though the choice of September 10 and 11, 1961 by a laboratory in Houston as a day of significance in the weather is understandable (the landfall of Hurricane Carla occurred at this time), it also turned out to be a very fortunate choice. We were led back to August 29 as the day of arrival of an impulse at the magnetosphere, and the highest value of K_p for the period occurred during this magnetic storm. In addition, the other effects on ionospheric temperature postulated by Jacchia (1963) are all small (see Figure 2).

The period August 29 to September 12 is one of the few periods in these two months when neither the beginning nor the end of the expected solar wind effect is influenced by another solar wind storm or other solar effect.

The maximum 5-day running mean of K_p for August and September occurs in association with a disturbance that reached its peak August 30, 1961 (see Figure 1). There were no very large values of K_p between August 11 and September 14; hence, this K_p increase event was comparatively isolated in time. The sun spot numbers show a flat disturbed minimum during this period (Figure 1) and the 10 cm solar flux stays below 110 from August 20 to September 3. The radius of the magnetosphere is a minimum on the day the K_p index reaches a peak. Both of these are accepted indications of a strong solar wind. We assume that there was a marked increase in the solar wind on

August 30.

At a time when the 10 cm solar flux value (see Figure 3) indicates that a minimum should be expected in temperature (as measured by satellite drag), there is a small maximum which reaches its peak with the K_p index and R_M (see Figure 2). Since solar corpuscular effects are generally accepted as the heating mechanism for this kind of temperature change, we shall assume that it caused this heating. Since the satellite was not in the auroral zone we can surmise that this heating was more pronounced at the poles. Since the effects we study depend on gradients of temperature we are not too unhappy to see a small temperature change.

Accepting that the polar atmosphere at about 100 km and above was heated on August 29 or 30, what do we expect to happen to the lower layers? Following Ward and Shapiro we would expect persistence of patterns to be great starting the third day after the event and continuing for six days. This would be the period September 1-6. According to "Die Grosswetterlagen Mitteleuropas" of Amtsblatt des Deutschen Wetterdienstes, the same basic pattern lasted from August 26 to September 7. The analysis of Shapiro (1959) predicts (as the "lag flag" of Figure 4 indicates) that the period from September 12 to September 17 should be a period of change. The description from Germany says there were moderate westerly winds from September 8 to 13. They broke down on September 14 and became a marked meridional pattern. This independent observation of Shapiro's persistences probably adds to the significance of his study. However, since we are concerned

with only one case we are not in a position to perform any statistical analysis.

Shapiro (1959) also estimates the effect on the zonal wind. His data was for all times of the year and to consider the westerlies at this time we must use the polar westerly index. Shapiro's study for the Western Hemisphere indicates that the maximum speed of the westerlies ($Z1_p$) should be September 3 and it occurred September 4 (see Figure 4). He indicates that the minimum should be September 11 and it occurred September 10.

We have several other wind indices:

Δlat in Figure 4 which takes in lower latitudes over about 1/2 the hemisphere (it is not wind but a rough measure of it) shows strong westerlies September 6 and the weakest westerlies for a long period around September 13.

W-E covers a whole ring around the earth and it indicates a maximum difference between westerlies and easterlies near the pole on September 4 and a sustained minimum centered on September 13. This minimum corresponds to the longer time lag for weakening the westerlies that Shapiro* noted for Europe.

---

* Shapiro attempted to link the high persistence and weak westerlies with the statement that high persistence and strong westerlies go with large pressure systems and that low persistence and weak westerlies go with small pressure systems. We found this statement confusing until we recalled that he filters ordinary troughs and ridges; and by large systems, he means a polar low cell with two or three subtropical highs and by small systems, he means blocks and cut-off lows and highs.

With this noteworthy confirmation of a result that was found statistically significant on previous data, we are encouraged to study the rest of the two month period.

Study of the lag flags in Figure 4 indicates the following predictions and confirmations:

Predicted Westerlies		Observed Westerlies
August 1-9	High values	High values began July 29 and lasted until August 5.
August 10-18	Confused	Many peaks and valleys slowly rising.
August 19-25	Low values	Low values August 22 to 27.
August 26-31	No prediction	Rise begins on August 29.
September 1-6	High values	Peak on September 4.
September 7-11	No prediction	Low values.
September 12-17	Low values	Low values; rise begins on September 15.
September 18-22	High values	High values.
September 23-30	Confused	High values until September 27; then rapid decrease.

There are five unequivocal predictions possible during the two month period and all of them are correct.

Calculation of linear correlation coefficients between indices provided additional information to assist in evaluating the August-September 1961 weather. The entire series of daily data was used in calculating 5-day mean values. The 5-day means were identified by the ending date of the period for which the mean was being calculated.

The latitude difference between the 18, 200 feet and 19, 200 feet contour on the 500 mb chart showed a correlation coefficient of -0. 6 with the 700 mb temperate zonal index for the westerlies. Since larger latitude differences are associated with slower westerlies, the results are in the expected direction.

The 5-day mean K_p (daily sum) index had a +0. 1 linear correlation with the 700 mb zonal westerlies for the western quadrisphere. An attempt was also made to check the lag relationships between K_p and the zonal index for the 700 mb temperate westerlies with these results:

Lag:	0 day	2 day	4 day	5 day	6 day	13 day	14 day
	+0. 1	-0. 2	-0. 4	-0. 5	-0. 6	-0. 2	-0. 3

Note that in common with most of the studies of geomagnetism and winds or pressure data, more happens between days 4 and 6 than at other times. When you recognize that during this period the polar westerlies and the temperate westerlies at 500 mb had a very high negative correlation, then this report becomes a fair confirmation of Shapiro's and Ward's findings and even indicates there is some possible profit in day to day correlation of K_p and the maximum westerlies.

The weather maps for August 30, September 3 and September 11 which we have chosen to be of particular interest are in Figure 7 (contained in the pocket in back of this report).

Surface maps show a striking difference between August 30 and September 11, especially in the low latitudes where hurricanes

predominate on September 11. The map for September 3 perhaps has the seeds of the hurricane but they have not formed. The increased polar westerlies between August 30 and September 3 are noteworthy in Europe and the Pacific Ocean. The 500 mb chart shows an increase in blocking and meridional flow between August 30 and September 11, and the westerlies have significant jet streams far to the south on September 11. The 500 mb chart for September 3 shows the westerlies contracted into the pole but otherwise is much like the chart for August 30.

The 100 mb charts are all pretty much the same for all three days.

The 30 mb chart shows a very significant difference between August 30 and September 11 in that there is a polar low and a ring of high pressure on August 30 and a two cell non-polar pattern on September 11. It is also significant that the map for September 3 looks very much like the two cell 10 mb chart for September 11 except that a migration of the high cell from the magnetic pole to the west during the period has occurred.

The comparison of TIROS III data for the two periods August 29, 30 in Figure 5, and September 2, 3 in Figure 6 shows little difference that can be considered as significant. There is a tendency for increased cloudiness in high cells and near the poles and decreased cloudiness in low cells. This analysis has been hampered by time limitations as has been indicated before. There was not enough area photographed by TIROS III on September 9, 10, 11 and on August 28, 29, 30 to see if

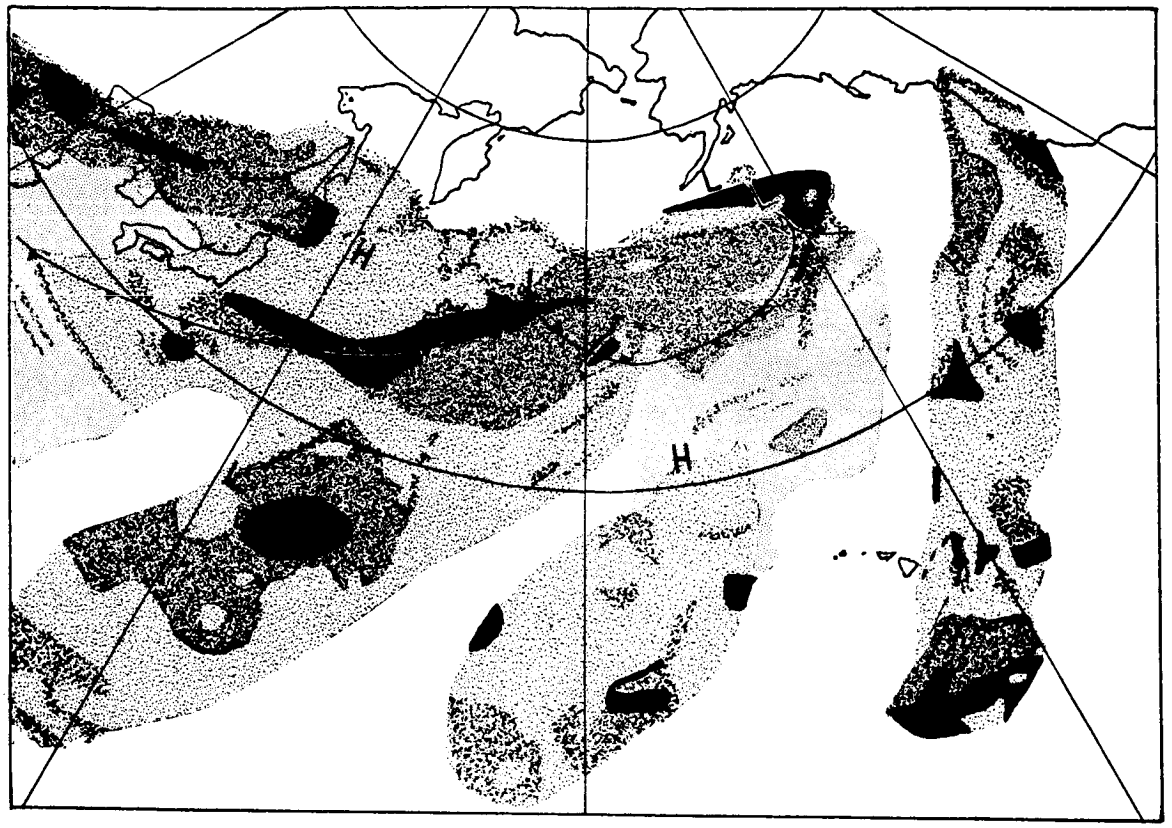

LEGEND :

CLEAR
BROKEN
WARM FRONT
SCATTERED
OVERCAST
COLD FRONT
NO TIROS DATA
L H SURFACE PRESSURE CENTERS

FIGURE 5
CLOUD ANALYSIS AFTER TIROS III AND WEATHER ANALYSIS,
30 AUGUST 1961 (SUPPLEMENTED BY THE 29th)

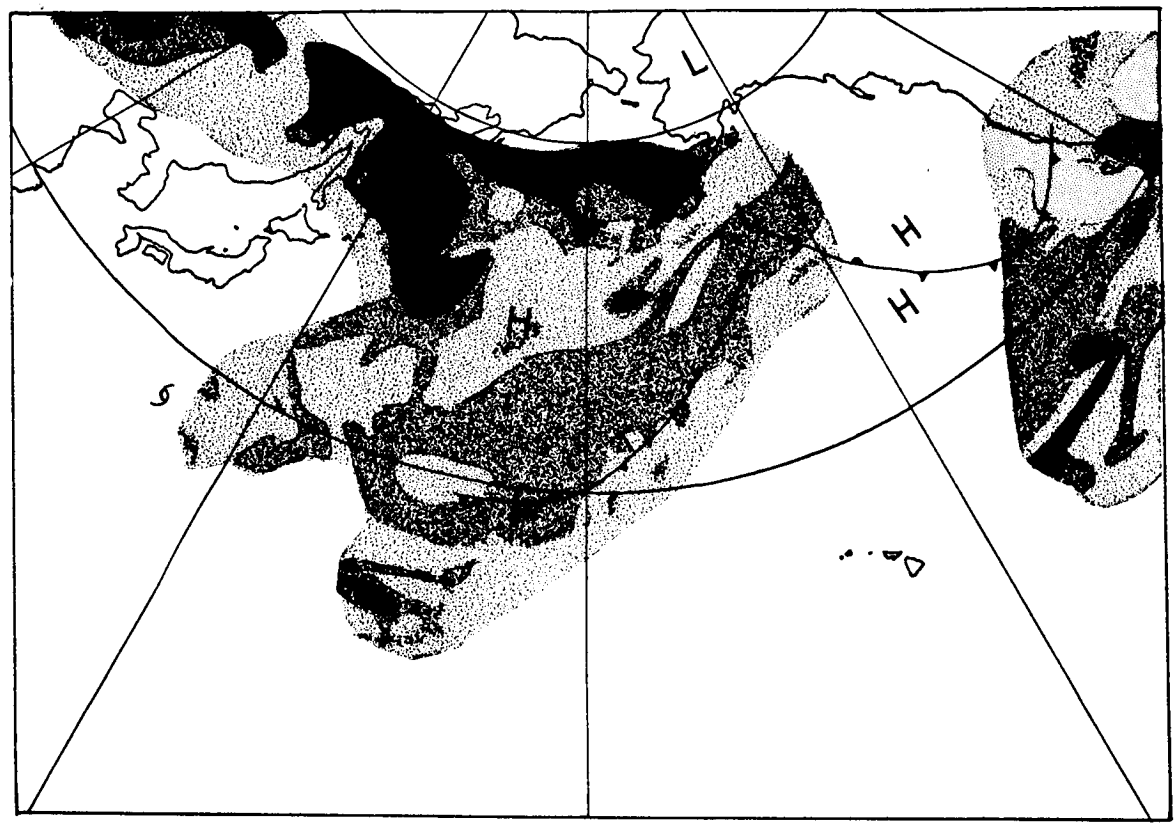

LEGEND :

CLEAR
BROKEN
WARM FRONT
SCATTERED
OVERCAST
COLD FRONT
NO TIROS DATA
L H SURFACE PRESSURE CENTERS

FIGURE 6
CLOUD ANALYSIS AFTER TIROS III AND WEATHER ANALYSIS,
2 SEPT. 1961 (SUPPLEMENTED BY THE 3rd)

there was a significant difference between the appearance of the earth's clouds from above. Obviously, the hurricanes will have circular overcast spots associated with them and there was a marked increase in the number of hurricanes. On September 11 the Atlantic and Gulf were filled with hurricanes from Mexico to Africa.

Our first analysis indicates that the difference between the appearance of clouds and cloud patterns are much more strongly related to synoptic weather patterns than to world wide weather changes. Also for 1961 the time density of TIROS photographs is not sufficient to allow any other criterion than that of availability of photographs to dictate the choice of days to be studied.

REFERENCES

Akasofu, S.-I., and S. Chapman, 1960: The sudden commencement of geomagnetic storms. Vrania, 250, 1-35.

Bartels, Julius, 1962: Collection of geomagnetic planetary indices K_p and derived daily indices, A_p and C_p for the years 1932 to 1961. IAGA Bulletin No. 18, Amsterdam, North-Holland Publishing Co., 188 pp.

Blum, Ronald, 1963: The interaction between the geomagnetic field and the solar corpuscular radiation. Icarus, 1, 459-488.

Dessler, A. J., 1959: Ionospheric heating by hydromagnetic waves. J. Geophys. Res., 64, 397-401.

Dessler, A. J., 1962: Further comments on stability of interface between solar wind and geomagnetic field. J. Geophys. Res., 67, 4892-4894.

Dessler, A. J., and E. N. Parker, 1959: Hydromagnetic theory of geomagnetic storms. J. Geophys. Res., 64, 2239-2252.

Freeman, Jr., J. C., 1963a: On the thickness of a shock wave in the solar wind (See Appendix I).

Freeman, Jr., J. C., 1963b: A possible oscillation of the wind in the equatorial stratosphere with a period of 24 to 27 months (see Appendix II).

Freeman, Jr., J. C., 1963c: A possible inertial oscillation of the equatorial stratosphere (see Appendix III).

Freeman, J. W., 1963: The morphology of the electron distribution in the outer radiation zone and near the magnetospheric boundary as observed by Explorer XII. Doctorate dissertation, State University of Iowa, Iowa City, Iowa.

Harris, I. and W. Priester, 1962: Time-dependent structure of the upper atmosphere. J. Atmos. Sci., 19, 286-301.

Jacchia, L. G., 1963: Electromagnetic and corpuscular heating of the upper atmosphere. Space Res. III, Amsterdam, North-Holland Publishing Co., 3-18.

Johnson, F. S., 1961: Structure of the upper atmosphere. Satellite Environment Handbook, Stanford, California, Stanford University Press, 9-24.

King-Hele, D. G., 1963: Upper-atmosphere scale height and its variation with solar activity. Space Res. III, Amsterdam, North-Holland Publishing Co., p. 27.

Lincoln, J. Virginia, 1961: Geomagnetic and solar data. J. Geophys. Res., 66, 3949 and 4302.

Lincoln, J. Virginia, 1962: Geomagnetic and solar data. J. Geophys. Res., 67, 387 and 887.

Macdonald, N. J., and W. O. Roberts, 1960: Further evidence of a solar corpuscular influence on large-scale circulation at 300 mb J. Geophys. Res., 65, 529-534.

Macdonald, N. J. and W. O. Roberts, 1961: The effect of solar corpuscular emission on the development of large troughs in the troposphere. J. Meteor., 18, 116-118.

Miers, B. T., 1963: Zonal wind reversal between 30 and 80 km over the southwestern United States. J. Atmos. Sci., 20, 87-93.

Shapiro, Ralph, 1958: Some observations of the persistence of the surface pressure distribution. J. Meteor., 15, 435-439.

Shapiro, Ralph, 1959: A comparison of the response of the North American and European surface pressure distributions to large geomagnetic disturbances. J. Meteor., 16, 569-572.

Shapiro, Ralph and Fred Ward, 1962a: The harmonic persistence correlation and geomagnetic disturbance. J. Atmos. Sci., 19, 60-65.

Shapiro, Ralph and Fred Ward, 1962b: A neglected cycle in sunspot numbers, J. Atmos. Sci., 19, 506-508.

Snyder, C. W., Marcia Neugebauer and U. R. Rao, 1963: Preliminary results on interplanetary plasma from Mariner II (to be published).

Warwick, James W., 1959: Some remarks on the interaction of solar plasma and the geomagnetic field. J. Geophys. Res., 64, 389-396.

Willett, H. C., 1961: Research directed toward study of stmospheric reactions to changing conditions of solar activity. Final Report, Contract No. AF19(604)-3056.

Woodbridge, D. D., N. J. Macdonald and T. W. Pohrte, 1958: A possible relationship of geomagnetic disturbances to 300 mb trough development. J. Meteor., 15, 247-248.

SOURCES OF WEATHER ANALYSES

U. S. Weather Bureau copies of NWAC Northern Hemisphere working maps.

Die Grosswetterlagen Mitteleuropas, Amtsblatt des Deutschen Wetterdienstes.

Institut für Meteorologie und Geophysik der Freien Universität Berlin, "Preliminary Daily Northern Hemisphere 10-Millibar Synoptic Weather Maps of the Year 1961," Meteorologische Abhandlungen, Band XX.

Institut für Meteorologie und Geophysik der Freien Universität Berlin, "Preliminary Daily Northern Hemisphere 30-Millibar Synoptic Weather Maps of the Year 1961," Meteorologische Abhandlungen, Band XIX.

U. S. S. R. TSentral 'nyi institut prognozov. Ezhednevnyi biulletin' pogody.

LIST OF SYMBOLS

A_p	planetary magnetic A index from Bartels.
C_p	planetary magnetic character index from Bartels.
D_{ST}	special magnetic index used as a measure of the intensity of individual magnetic storms.
F_{10}	flux of 10.7 cm wave length radio waves.
F_{20}	flux of 20 cm wave length radio waves.
K_p	planetary magnetic K index from Bartels.
L	indication of the dates on which certain events are expected according to Shapiro.
$\dot{P}_R$	radiation pressure drag.
$\dot{P}_R - \dot{P}$	radiation pressure drag minus measured drag on a satellite.
R_M	Radius of the magnetopause
S_pL	electron energy spectrometer channel with pass band 90 kev to 50 kev.
SSN	sun spot number.
T	temperature in the high ionosphere in ^{o}K.
T'_{100}	Jacchia's standardized temperature.
W-E	maximum westerlies minus the maximum easterlies.
$Z1_p$	polar zonal index of westerly wind speeds.
$\Delta_{lat.}$	difference between the mean latitude of the 18,200 feet height contour at 500 mb and the 19,200 feet height contour at 500 mb.

PART B

A MODEL OF THE ATMOSPHERE FOR INVESTIGATING THE INTERACTION WITH THE SUN THROUGH THE SOLAR WIND

by

John C. Freeman, Jr. and Leon F. Graves

A MODEL OF THE ATMOSPHERE FOR INVESTIGATING THE INTERACTION WITH THE SUN THROUGH THE SOLAR WIND

One of the fondest gambits of the scientist, critical of the influence of the sun on the weather, is "how does the energy get from the very low density ionosphere to the troposphere?" This question has not been answered by even the most enthusiastic supporters of solar influence (see, for example, Macdonald and Roberts, 1961).

Theoretical discussions have resulted in the conclusion that very little energy can propagate from the ionosphere to the troposphere. (Charney and Drazin, 1961; Ooyama, 1958.) We submit that the question of downward energy transport has been settled once and for all by the work of McCreary (1959), Reed, et al (1961), Ebdon and Veryard (1961) for the equatorial latitudes and by Miers (1963), Batten (1961, Reed and Rogers (1962) for the middle latitudes, with their observations of downward propagation wind changes. These waves that carry the significant energy are not likely to be gravity waves and have a period of 12 months to 26 months. We can assume that Charney and Ooyama failed to include physical phenomena of this time scale in their analysis so their conclusions do not apply. Freeman (1963b) has shown that an oscillation that can carry the energy and that has periods of the proper magnitude are possible in stable atmospheres. Furthermore, a wave with a one year period near 45^{o} is likely to have a longer than two year period near the equator.

Since the time honored barrier of a method of energy transmission has now been overcome by data and to a certain extent by theory and we can look forward with confidence that it is likely that changes in the state of the ionosphere bring about ultimate changes in tropospheric weather, let us review the current theory of solar-ionosphere relationships.

The influence of the sun on the ionosphere begins with the concept of the "solar wind." (Dessler and Parker, 1959, Blum, 1963) The solar wind occurs in the corona of the sun which is now postulated to extend (Figure 8) beyond the known planets and to form an "atmosphere" of the solar system. This flow of (very low density, collisionless) plasma streams radially out from the sun and is ruled by the laws of hydromagnetics. The magnetic field is so weak that it is carried by the particles and does not affect the flow. The speed of the flow is "always" greater than that of Alfven waves. This condition results in flow very much like supersonic gas flow and a shock wave is expected in front of an obstacle. (e.g. see Freeman, 1963a.)

The solar wind varies by several hundred percent of the minimum value on time scales significant to meteorology and climatology. Because of this variation the solar wind is one of the most likely energy transport media in the solar system to carry the results of variations on the surface of the sun to the earth. It is now generally accepted that the aurora, motions of ionospheric reflecting layers, ring currents and many magnetic variations are related to the sun through the solar wind.

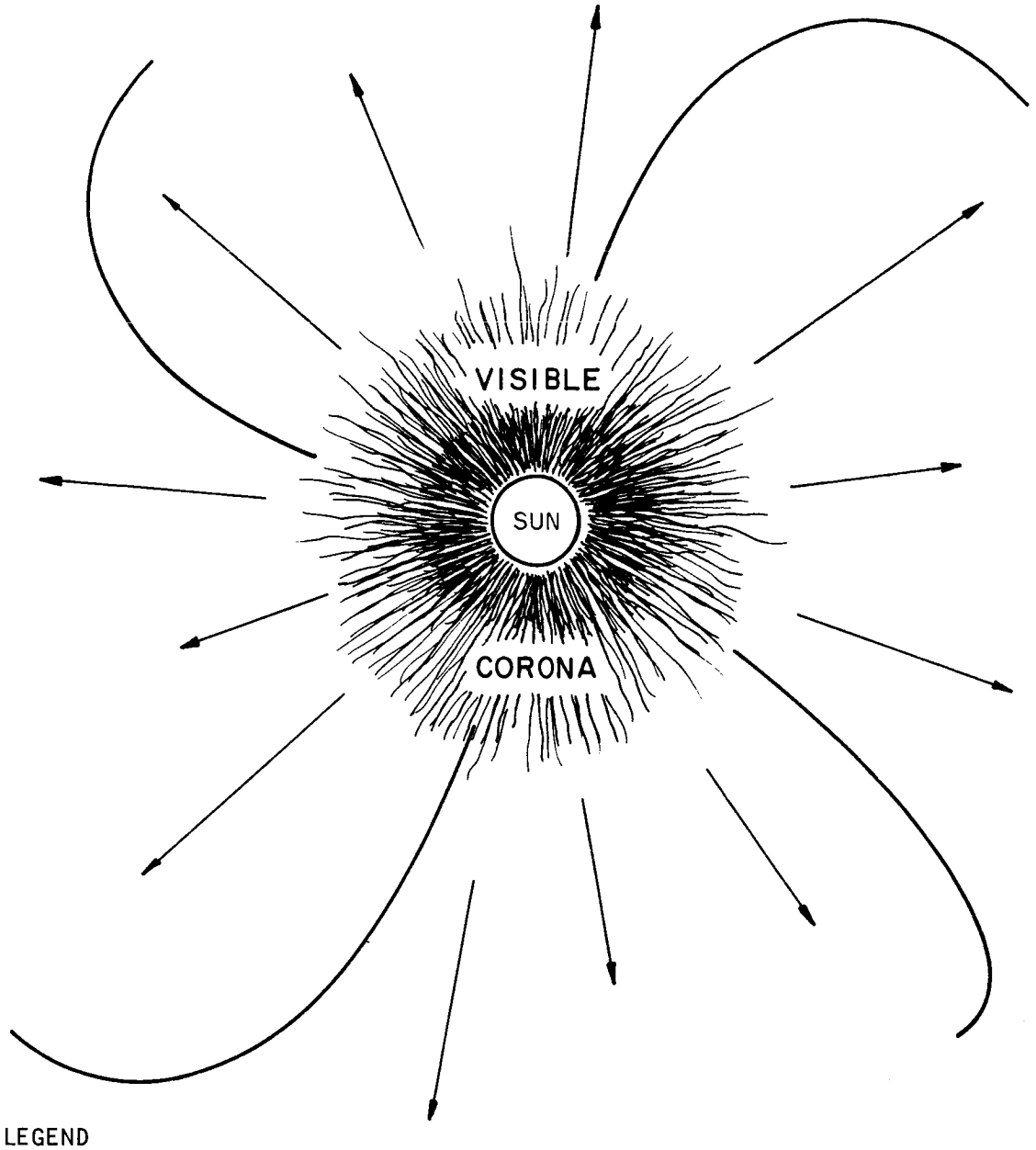

LEGEND

Protons and other particles are heated near the sun and, probably, in the visible corona they and the electrons stream out as a collisionless plasma with neutral average charge. This solar wind carries the sun's magnetic field lines bodily into the solar system. This coupled with the rotation of the sun results in spiral field lines in the plane of the ecliptic.

FIGURE 8

VISIBLE CORONA AND SOLAR WIND

It is possible for a plasma flow to be formed and diverted by a magnetic field. This is exactly what is postulated to happen in the vase of the magnetic field of the earth. The "pressure force" of the solar wind pushes against the earth's magnetic dipole and distorts it from the dipole shape extending to infinity into a compressed tear drop shape similar to the way a doublet solution of the hydrodynamic equation is distorted by constant fluid flow (see Johnson, 1961, p. 139).

The boundary between the earth's magnetic field and the solar wind is called the magnetopause and it has the shape of a tear drop as shown in Figure 9. The magnetopause is the trap that holds the Van Allen radiation to the earth. Study of Van Allen radiation may ultimately be one way to gain indirect information about the magnetopause on a regular basis.

The magnetopause is a new and most significant geophysical and space science discovery. It has been probed by several satellites which led to its discovery but it has not yet been studied in a manner satisfactory to geophysicists. Our present work indicates that study of it will be a necessary step to complete understanding of solar-weather relationships.

At the present time there is a debate among space scientists as to whether the magnetopause is a stable or unstable boundary (Dessler, 1961b and 1962). In any event there is evidence that increased solar wind creates more disturbances of the magnetopause. If the boundary is unstable this motion could be similar to that of wind ripples in a flag. If the boundary is stable, this possibly would indicate that

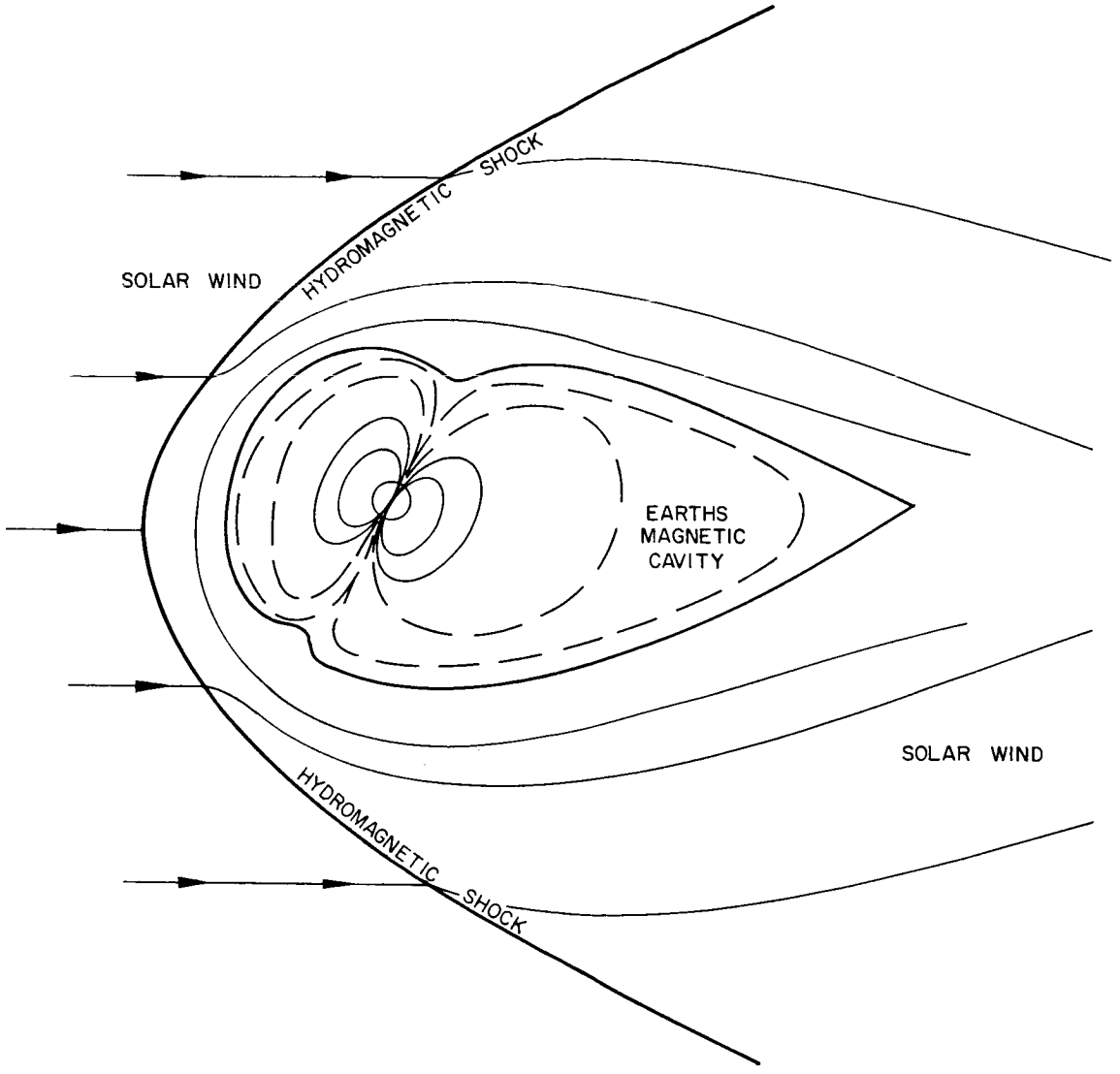

LEGEND

The solar wind streaming out from the sun creates a force that compresses and confines the earth's magnetic field into a teardrop cavity. The solar wind flows around it forcing a streamlined shape. Van Allen radiation is trapped inside the cavity. Since the solar wind is flowing at "superalfvenic" velocity or has an Alfven number (similar to mach number) greater than 1, there is a shock in the solar wind ahead of the cavity.

FIGURE 9

EARTH'S MAGNETIC CAVITY

variability of the solar wind increases with the solar wind. (Our best and most accepted observations are that increased solar activity brings about increased ionospheric disturbances. The effect of solar disturbances on the solar wind could possibly be only to increase the variability and not the speed of the solar wind. However, the Mariner data (Snyder, et al, 1963) indicates a disturbance-speed of the solar wind relationship.)

Dessler (1959a, 1959b) has advanced the theory that the fluctuations of the magnetopause cause hydromagnetic shock waves in the earth's magnetic field that dissipate in the ionosphere. (His papers accompany this report.) These shock waves heat the ionosphere in the auroral zone by a two stage process. The hydromagnetic shock waves impart a high speed to the charged particles in the ionosphere and cause them to move along the magnetic line of force. These collide with the neutral particles, especially when they reach the lower and more dense layers of the ionosphere. The heated particles form a "corona" of the earth at 150 km and above. Snyder, et al (1963) indicate that a magnetic index, the K_p index, is a measure of the solar wind. We use this measure but recognize that it and solar influence must be affected by the shock wave in front of the magnetopause.

The important result to weather is that a solar storm brings about heating of the lower ionosphere in the auroral zones of the earth. Some idea of the importance of this heating can be gained from a comparison of the temperature of the ionosphere in sun spot minimum and sun spot maximum periods in Figure 10 adapted from Johnson (1961)

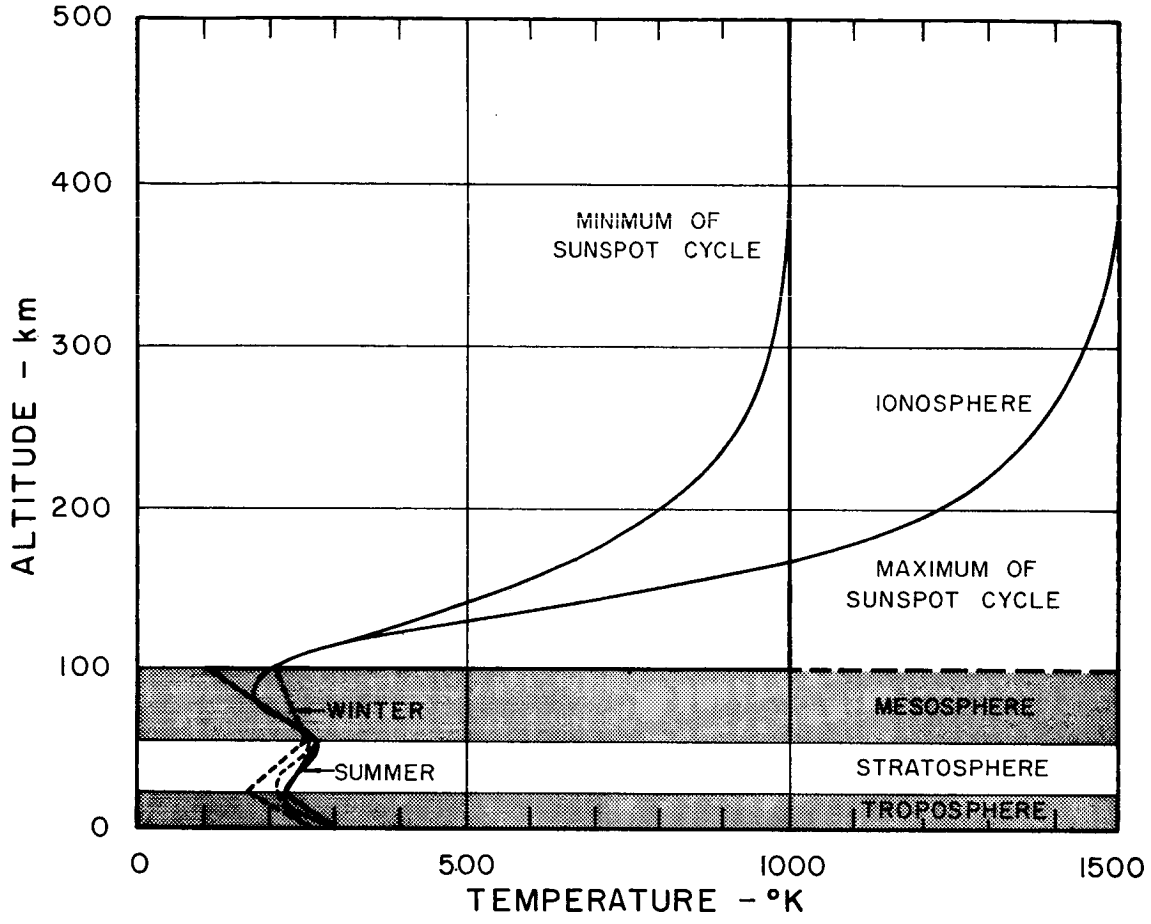

LEGEND

The model of the atmosphere discussed in this report superimposed on F. S. Johnson's model of the atmosphere.

FIGURE 10
ATMOSPHERIC MODEL

and from its consideration by Harris and Priester (1962). Harris and Priester discuss waves that are probably sound or gravity waves since they have a small period. Freeman (1963b) has considered inertial waves and in (1963c) has considered centrifugal waves caused by hydromagnetic heating.

The work of Wexler (1950) considers the motion of a lower layer of fluid when there are density and height changes in an upper layer. He draws the conclusion that a large wind change in a layer of very low mass will not lead to a significant change in wind or pressure in a lower layer of large mass. The difference between Wexler's and this work is that we consider the ionosphere heated and the density "increased" while Wexler considers it heated and the pressure decreased.

It is common to upper air studies to assume that low energy supply and small pressure changes must result from high layers. If we consider adiabatic layers then we have a paradox. The top of an adiabatic layer near zero pressure has a much smaller density than the bottom. A sustained pressure gradient above the surface results in a height gradient of a constant pressure surface. This height gradient is the same throughout the fluid and the change in wind will be the same at every level. Thus a very small pressure gradient at upper levels can result in a very large pressure gradient in the lower levels in an adiabatic (barotropic) layer.

The usual argument against adiabatic layers in the atmopshere is based on the fact that they reach zero density and pressure at too low a level (about 10 km) if you start from temperatures between -50°

and 50°C at any tropospheric level. However, if we investigate the atmosphere starting from the top we do not meet the same paradox.

We begin with a strongly distorted atmosphere of two adiabatic layers, one with the potential temperature representative of 100 km and one with the potential temperature representative of the surface layer.

This model results in a potential temperature difference of 900° at the interface with the air in the lower layer at 200° (Figure 11).

Thus a pressure gradient in the upper fluid at this interface would be reduced by a factor of $\frac{200}{1100}$. This is a significant decrease in the pressure gradient but it is not small enough to back claims that there is no effect of a very small pressure change in the upper levels.

The unreality of the model can be modified extensively by consideration of many layers.

If we had three layers (for instance) we could have a 450° temperature change at the middle of the upper layer. Then we would have*

$$\frac{\partial h}{\partial x}_{\text{middle}} = \frac{650}{1100} \frac{\partial h}{\partial x}_{\text{upper}}$$

Then at the bottom of the middle layer we would have

$$\frac{\partial h}{\partial x}_{\text{lower}} = \frac{200}{650} \frac{\partial h}{\partial x}_{\text{middle}} = \frac{200}{1100} \frac{\partial h}{\partial x}_{\text{upper}}$$

Thus there would still be the same 17% of the 100 km height change at the troposphere. During solar disturbance contour height changes of several thousand feet in a few hours are not uncommon at

---

* $\frac{\partial h}{\partial x}$ is the slope of a surface of constant pressure.

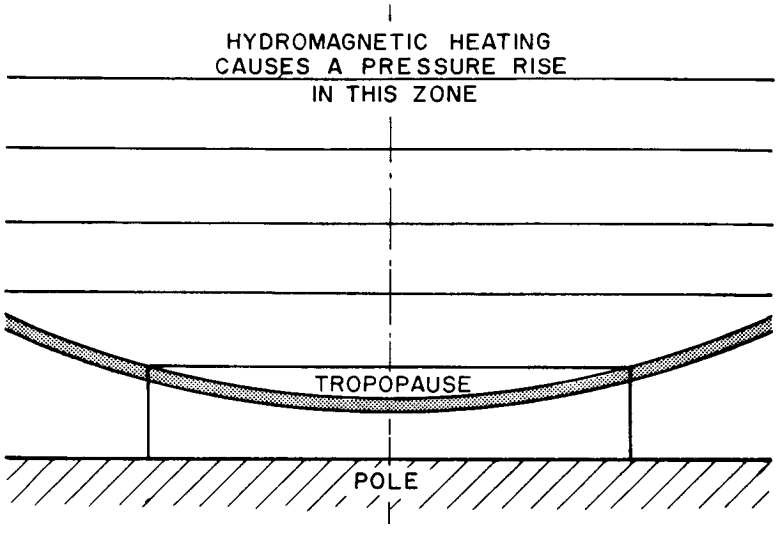

LEGEND

Level stable layers over a polar tropopause with east wind at the surface and a cold pole. Hydromagnetic heating due to an increase in solar wind causes a pressure rise.

FIGURE 11
RESPONSE OF THE POLAR TROPOPAUSE TO HEATING

100 km; thus we can expect significant height changes in the stratosphere as a result of solar disturbances.

This is a statement of sweeping generality similar to those previous statements that you cannot expect effects in lower levels as a result of solar disturbances. Here, however, we have a theoretical development that predicts very large changes and two sets of observations of downward energy transport. We now have a problem of discovering why the changes are as small as they are.

The idea of horizontal dissipation of energy through vertically propagating sound or gravity waves must be viewed in light of the large geographic distribution of the disturbances being considered. Any dissipation mechanism could be in itself a significant source of solar effects on weather.

Since we now have an accepted mechanism for heating the atmosphere near 100 km as a result of solar disturbances, it is time to devise a model of that atmosphere that bears some semblance to reality and can respond to this heating. We base the model of the atmosphere on Johnson's temperature diagram shown in Figure 10.

First let us consider the summer and equatorial atmosphere and consider its structure in the vertical. We assume that the ionosphere is very stable and ends in a discontinuity (called the mesopause) at approximately 100 km with density above 1/8 to 1/5 of that of the mesosphere below. This should be a very flat surface because of gravitational stability.

There is a layer about 50 km thick just below the ionosphere in

which the temperature increases with descent. It is called the mesosphere by upper atmosphere meteorologists. Since it is a region that is heated below and is capable of chemical reaction among gaseous components we would expect weather phenomena similar to those encountered in the troposphere.

The stratopause occurs at about 50 km. This is the top of the stratosphere and the bottom of the mesosphere. Because of the overwhelming stability, any change in thickness of the mesosphere is not likely to result from changing the height of the stratopause. However, the mesopause is even more stable so that the mesosphere may be expected to be a relatively constant thickness.

The stratosphere goes down to the tropopause below which accepted atmospheric models are quite adequate for the purpose of energy transmission. The temperature and wind are reasonably well known for all seasons in the stratosphere except near the equator, as indicated by Batten (1961). As indicated in the beginning of this paper we are gaining insight concerning equatorial winds.

The winter mesosphere starts at the slightly (about 20°) colder tropopause and with its very stable lapse rate is about 100° warmer at the mesopause. The model does not have a winter stratopause.

The flow above the mesosphere (or the pressure at the top of the mesosphere) is controlled by the temperature density relationship. Above the top of the mesosphere high temperature and high density go together resulting in high pressure. The winter hemisphere has a high temperature and high pressure at the top of the mesosphere. Some of

the temperature effect leaks over into the summer hemisphere near the equator resulting in a cold pole and a warm equator on top of the mesosphere in the summer hemisphere. As soon as the year advances far enough that both magnetic poles are in darkness then we have two warm poles at the top of the mesosphere and east winds predominate over most of the earth at this level.

This is an adaptation of Dessler's theory of heating by hydromagnetic shock waves. They heat more near the poles of the earth so the heating occurs under the following conditions:

1. When there is greater solar wind.
2. At the poles.
3. Possibly at night. (Warwick, 1959 and Harris and Priester, 1962)

Any combination of 1, 2 and 3 will give increased heating. The most effective combination occurs in deep winter at the poles during high solar activity. This should result in stronger east winds in the winter hemisphere and stronger west winds in the summer hemisphere.

When there is a summer hemisphere the magnetic pole spends most of the day lighted and it would be expected that heating would be less effective at the top of the mesosphere. Near the equinox both poles are experiencing night and the heating is effective at both poles. This results in high pressure at the poles and low pressure at the equator. This situation is outlined graphically in Figure 11.

The heating by the electromagnetic waves from the sun affects

the ground layers and the center of the mesosphere. The usually accepted constancy of the short wave radiation from the sun leads us to assume that this forcing function is effective in the lower layers and creates most of the well known atmospheric disturbances and phenomena. The heating of the mesosphere will be considered a disturbance of a basic "well known" hemisphere flow. The seasonal aspects of even the mesosphere flow will be taken as "given" and the effects of changing solar winds will be considered.

We assume the wind distribution as illustrated by Batten (1961) and the temperature distribution in the Handbook of Geophysics (1961) with additions and modifications as indicated by the thermal wind equation. Freeman (1963b) indicates that the waves that move down at the equator are waves of the centrifugal type that are moving with the period of about 26 months. This discussion is occupied with long term variation at the equator but similar reasoning will apply at any latitude.

The alternating westerly and easterly winds of the equator as reported by Reed and Rogers (1962) are obviously a downward moving impulse in the atmosphere. These winds are an obvious physical occurrence similar to the seasons and cry for a theoretical explanation.

The two natural questions are:

1. Is there a phenomenon that affects the earth with the same period as the winds? Conjunction of the Earth and Mars has the same period but there is no accepted way that Mars can affect the Earth.

2. Is there a natural period inherent in this wind system? If there is a natural period, must the waves always move down? If not, we have a good clue that there is a strong disturbing influence in the upper atmosphere.

The study of the response of conservation of potential vorticity to heating on a flat earth is outlined by Freeman (1963c), a paper which accompanies this report.

We define the following quantities:

D is the vertical distance between isentropes.

L is the horizontal distance between isentropes.

H is the vertical distance between isotach.

W is the horizontal distance between isotachs.

There is a special vorticity equation at the north and south pole, namely $\frac{\partial}{\partial t}\left(\frac{\Omega+\omega}{D}\right)=0$, where ω is the relative angular velocity.

If we start with a ribbon of fluid $S_{mn}\ D_{mn}$ in the area on the cross section centered at latitude ϕ_{mn} then the relation $S_{mn}\ D_{mn}\ R \cos\ \phi_{mn}$ = const. is true. (R is the radius of the earth in the equation.)

In the usual vorticity equation, $\frac{\zeta+f}{D}$ = const., where $f = 2\ \Omega \sin\ \phi$, there is a hidden assumption that SD = const. In other words, the assumption is really $S(\zeta+f)$ = const. In our case, therefore, we have $\frac{\zeta+f}{D\cos\phi}$ = const. is the vorticity equation.

We need to refine the thermal wind equation somewhat to the form

$$\frac{\partial u}{\partial Z} = - \frac{g}{2\Omega \sin\phi \, T(\theta, z)} \frac{\partial \theta}{\partial y}$$

$T(\theta)$ is the temperature corresponding to θ at this given pressure altitude.

In our accompanying paper, Freeman (1963c) has given wave solutions in highly restricted models related to our present discussion. We are investigating slowly changing flows with meridional velocity $v << w$ and most of them very stable so that $\frac{\partial w}{\partial t} << fu$, where w is the vertical velocity.

We write the wind in the form $U_g + \Delta U$ where U_g is the geostrophic wind and U is the deviation from geostrophic.

The primary dynamic equation of our system is

$$\frac{d^2 a}{dt^2} = 2\Omega \sin\phi \Delta U \qquad (1)$$

$a = R\phi$ is the y coordinate (in degrees of latitude of the boundary of a ribbon of known potential vorticity. Inside of the ribbon we have

$$\frac{d}{dt} \left(\frac{\frac{\partial (U + \Delta U)}{\partial y} + 2w \sin\phi}{D \cos\phi} \right) = 0$$

where ϕ is the latitude and D is the thickness of the layer. This can be re-expressed as

$$\frac{-\partial \left(\frac{U + \Delta U}{\partial y} \right) + 2w \sin\phi}{D \cos\phi} = - \frac{\frac{\partial (U + \Delta U)}{\partial y}\Big|_0 + 2w \sin\phi}{D_0 \cos\phi_0} \qquad (2)$$

Continuity of mass is also expected to be true so that we have

$$\frac{d}{dt}(\Delta\phi R^2 D \cos\phi) = 0$$

This can be written as

$$\Delta\phi R^2 D \cos\phi = R^2(\Delta\phi)_0 \cos\phi_0 \tag{3}$$

where $\Delta\phi$ is the latitude covered by a ribbon of constant vorticity or a material surface and D is the thickness of the material ribbon.

We can find $U + \Delta U$, $R\phi$, and D for each point from Eqs. (1), (2) and (3).

Now if we are given U at some level we can use the thermal wind equation

$$\frac{\partial U}{\partial Z} = \frac{-g}{2\Omega \sin\phi T(\theta,Z)} \frac{\partial\theta}{\partial y} \tag{4}$$

to find U at all other levels.

We now subtract

$$U + \Delta U - U = \Delta U \tag{5}$$

and substitute in Eq. (1) and continue the computation. From (1) we get ϕ and from ϕ we get U and D. This gives $(\frac{\partial\theta}{\partial y}, T)$ which gives ΔU. This computation is continued until $U = 0$ or a new impulse arrives.

Before we obtain some quantitative results, we will indulge in a physical description.

The model in Figure 11 is acted upon by an addition of high pressure at the pole at 100 km. This pressure is not in geostrophic balance. The first reaction is that the layers get thinner and move poleward and geostrophic balance is attained. Since the upper layer moves fastest (because of stability) the balance is probably attained there first and there is certainly a greater response.

An intermediate state would be indicated in Figure 12, in which the upper layers have moved far out from the pole and get thinner and the faster moving troposphere will be required to compensate. Since the troposphere gets thicker, its west winds are increased. Thus we are left with an increased west wind in the troposphere and a decreased west wind in the stratosphere and a decreased west wind in the stratosphere and a tropopause shape that does not give the proper thermal wind.

The prime mover of the stratospheric layer has now been neutralized by geostrophic balance so that any changes that take place must be expected in the troposphere.

The troposphere would now "relax" to the pressure distribution imposed by the stratospheric winds and the shape of the tropopause.

The pressure distribution still calls for outflow in the lower layers; this outflow will cause the tropopause to sink and the westerlies to decrease until a geostrophic balance is attained. This should be the balance for the new stratospheric winds, as indicated in Figure 13.

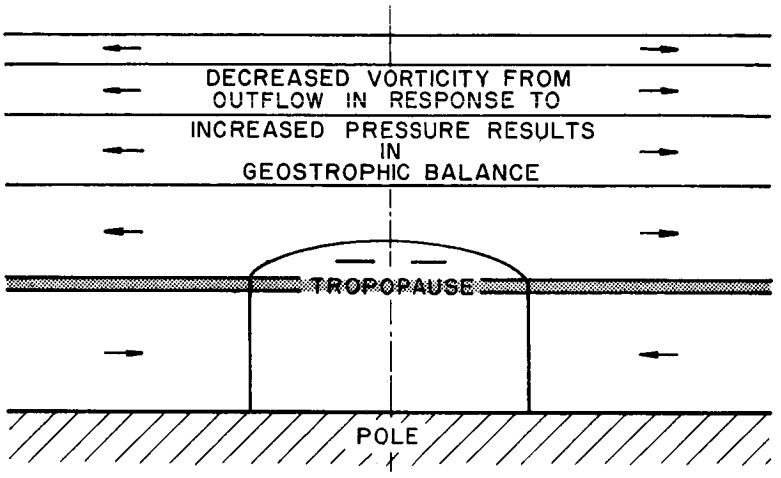

LEGEND

The stability is so great that the response is greater at 100 km by a factor of 4 to 8 so that layer reaches geostrophic balance quickly and is grossly affected. The balance is attained with decreased vorticity as indicated by the thin layer. This pulling up of the stratosphere layers results in the tropopause rising and air moving into the pole at the tropopause and in increased west winds. This condition does not satisfy the geostrophic balance condition in the troposphere.

FIGURE 12

RESPONSE OF THE POLAR TROPOPAUSE TO HEATING

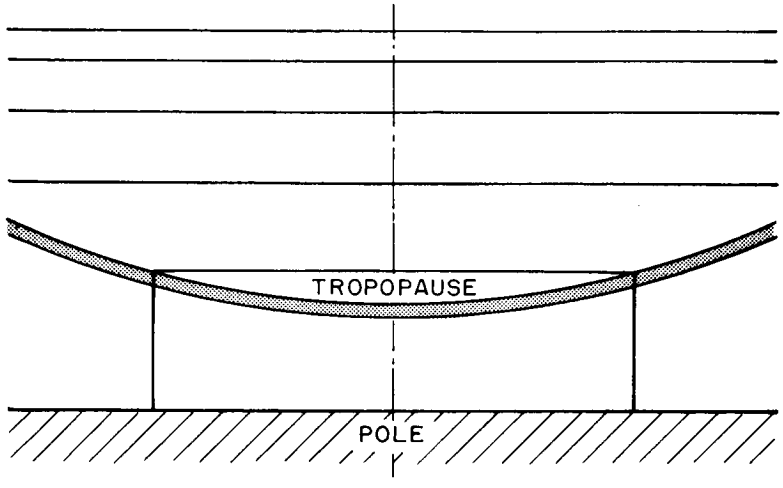

LEGEND

When geostrophic balance is attained with the higher tropopause and with weaker winds aloft, the thermal wind equation calls for much lower west winds (or stronger east winds) at the surface.

FIGURE 13

RESPONSE OF THE POLAR TROPOPAUSE TO HEATING

REFERENCES

Batten, E. S., 1961: Wind systems in the mesosphere and lower ionosphere. J. Meteor., 18, 283-291.

Blum, Ronald, 1963: The interaction between the geomagnetic field and the solar corpuscular radiation. Icarus, 1, 459-488.

Charney, J. G.and P. G. Drazin, 1961: Propagation of planetary-scale disturbances from the lower into the upper atmosphere. J. Geophys. Res., 66, 83-109.

Dessler, A. J., 1959a: Ionospheric heating by hydromagnetic waves. J. Geophys. Res., 64, 397-401.

Dessler, A. J., 1959b: Upper atmosphere density variations due to hydromagnetic heating. Nature, 184, 261-262.

Dessler, A. J., 1961a: Geomagnetism. Satellite Environment Handbook, edited by F. S. Johnson, Stanford, California, Stanford University Press, 110-144.

Dessler, A. J., 1961b: The stability of the interface between the solar wind and the geomagnetic field. J. Geophys. Res., 66, 3587-3590.

Dessler, A. J., 1962: Further comments on stability of interface between solar wind and geomagnetic field. J. Geophys. Res., 67, 4892-4894.

Dessler, A. J. and E. N. Parker, 1959: Hydromagnetic theory of geomagnetic storms. J. Geophys. Res., 64, 2239-2252.

Ebdon, R. A. and R. G. Veryard, 1961: Fluctuations in equatorial stratospheric winds. Nature, 189, 791-793.

Freeman, Jr., J. C., 1963a: On the thickness of a shock wave in the solar wind (see Appendix I).

Freeman, Jr., J. C., 1963b: A possible oscillation of the wind in the equatorial stratosphere with a period of 24 to 27 months (see Appendix II).

Freeman, Jr., J. C., 1963c: A possible inertial oscillation of the equatorial stratosphere (see Appendix III).

Handbook of Geophysics, 1961: Revised edition. Air Research and Development Command, Air Force Research Division, Geophysics Research Directorate, New York, The Macmillan Company, 656 pp.

Johnson, F. S., 1961: Structure of the upper atmosphere. Satellite Environment Handbook, Stanford, California, Stanford University Press, 9-24.

Macdonald, N. J., and W. O. Roberts, 1961: The effect of solar corpuscular emission on the development of large troughs in the troposphere. J. Meteor., 18, 116-118.

McCreary, F. E., 1959: Stratospheric winds over the tropical Pacific Ocean. Conference on Stratospheric Meteorology, Minneapolis, Minnesota.

Miers, B. T., 1963: Zonal wind reversal between 30 and 80 km over the Southwestern United States. J. Atmos. Sci., 20, 87-93.

Ooyama, K., 1958: On the vertical propagation of a disturbance through the mesosphere. (Unpublished report) Department of Meteorology and Oceanography, New York University, 69 pp.

Reed, R. J., W. J. Campbell, L. A. Rasmussen and D. G. Rogers, 1961: Evidence of a downward propagating, annual wind reversal in the equatorial stratosphere. J. Geophys. Res., 66, 813-818.

Reed, R. J. and D. G. Rogers, 1962: The circulation of the tropical stratosphere in the years 1954-1960. J. Atmos. Sci., 19, 127-135.

Snyder, C. W., Marcia Neugebauer and U. R. Rao, 1963: Preliminary results on interplanetary plasma from Mariner II (to be published).

Warwick, J. W., 1959: Some remarks on the interaction of solar plasma and the geomagnetic field. J. Geophys. Res., 64, 389-396.

Wexler, Harry, 1950: Possible effects of ozonosphere heating on sea level pressure, J. Meteor., 7, p. 370.

LIST OF SYMBOLS

a	horizontal distance from a standard latitude.
D	vertical distance between isentropes.
D_{mn}	vertical distance between material surfaces for ribbon m, n.
f	earth's vorticity.
g	acceleration of gravity
H	vertical distance between isotachs.
L	horizontal distance between isentropes.
R	radius of the earth.
S_{mn}	horizontal distance between material surfaces for ribbon m, n.
u	zonal velocity.
U_g	geostrophic zonal wind.
ΔU	deviation from geostrophic wind.
v	meridional velocity.
w	vertical velocity.
W	horizontal distance between isotachs.
$\frac{\partial h}{\partial x}$	slope of a surface of constant pressure.
ζ	relative vorticity.
θ	potential temperature.
ϕ	latitude.
ϕ_{mn}	latitude of ribbon m, n.
ω	relative angular velocity.
Ω	angular velocity of the earth about its axis.

APPENDIX I

THICKNESS OF A SHOCK WAVE IN THE SOLAR WIND

by

John C. Freeman, Jr.

N64-11720

ON THE THICKNESS OF A SHOCK WAVE IN THE SOLAR WIND

The solar wind seems to be continuous and to be moving with speed of 350 to 750 km per second as verified by the Mariner flights (Snyder, et al, 1962). The solar wind seems to be one of the most variable features of the continuous emissions of the sun toward the earth and the rest of the solar system. The solar wind varies with a time scale that leads directly to the speculation that it is related to the weather. The variability of the solar wind also corresponds to that of weather phenomena. It has already been postulated (Axford, 1962; Kellogg, 1962) that the solar wind moves faster than Alfven waves and that there is a shock wave in front of the magnetopause (or magnetosphere).

There seems to be no accepted theory (Johnson, 1963) for the nature and the thickness of this shock other than that it has to do with ion flow or plasma dynamics and that a thin shock occurs in plasma shock tubes even with mean free path longer than the experimental apparatus.

It is the purpose of this note to point out that the text book Ion Flow Dynamics by Demetrios G. Samaras predicts the thin shock wave in the laboratory as being limited by the Larmor radius. The estimate for the Larmor radius for the solar plasma is 600 km.

According to Samaras (p. 485) it has been shown by Rose (1956) that the shock wave in a very high temperature (very long mean free

path) plasma is smaller than the Larmor radius (but almost equal to it).

Samaras (p. 480) predicts that there will be shock waves of the order of the Larmor radius in shock tubes. Since the original surmise of a shock ahead of the magnetopause was based on the observation of this shock, we will assume that the shock in front of the earth's magnetopause is about the thickness of the Larmor radius. Using the Mariner and Pioneer (Snyder, et al, 1962) data and Dessler's (1959) method of averaging and Parker's (1962) estimate of temperature based on the solar wind we obtain an estimate of a Larmor radius of 400 - 600 km (Table I) at the earth. This is based on magnetic induction 5 γ and solar wind 350 - 750 km/sec. Thus the temperature would be 1-1/2 to 2-1/2 million degrees K.

If we accept that the Larmor radius is the thickness of the shock and that it is a mechanical shock resulting from the streamlines flowing around the magnetpause of the earth, then (because of its small thickness) we are forced with the distinct possibility that there is a shock caused by the moon. The moon shock would be one place to look for the link between the moon and the earth's rainfall (see Bradley, Woodbury, and Brier, 1962).

The shock associated with the moon would be in its wake similar to the disturbance discussed by Bowly, et al (1962) in the wake of an island under an inversion.

The possibility that there is a shock wave between the Galactic magnetic field and the solar wind at about 100 A. U. has been postulated

by Johnson (1963). Since he assumes an isothermal solar atmosphere and a constant thermal wind speed the shock he postulates must also be about the same thickness. It would seem that a sharp moving conducting surface in a sphere around the solar system would generate electromagnetic waves of detectable amplitude or would be observable by some kind of reflection.

TABLE I

Solar Wind	Temperature	$R_L \times B$	R_L
350 km/sec	1-1/2 million deg. K	2×10^{-3} weber/m	400 km
750 km/sec	2-1/2 million deg. K	3×10^{-3} weber/m	600 km

$B = 5\gamma = 5 \times 10^{-5}$ gauss $= 5 \times 10^{-9}$ weber.

REFERENCES

Axford, W. I., 1962: The interaction between the solar wind and the earth's magnetosphere. J. Geophys. Res., 67, 3791-3796.

Bowly, Clinton J., A. H. Glaser, R. J. Newcomb, and R. Webster, 1962: Satellite observation of wake formation beneath air inversion. J. Atmos. Sci., 19, 52-55.

Bradley, D. A., M. A. Woodbury, G. M. Brier, 1962: Lunar synodical period and widespread precipitation. Science, 137, p.748.

Dessler, A. J. and E. N. Parker, 1959: Hydromagnetic theory of geomagnetic storms. J. Geophys. Res., 64, 2239-2252.

Johnson, F. S., May 24, 1963: Personal Communication, Dallas, Texas.

Kellogg, P. J., 1962: Flow of plasma around the earth. J. Geophys. Res., 67, 3805-3811.

Parker, E. N., 1962: Dynamics of the geomagnetic storm. Space Sci. Rev., 1.

Rose, M. H., 1956: On the structure of a steady hydromagnetic shock: One fluid theory. USAEC Computing Facility Nyo-7693.

Samaras, D. G., 1962: Ion flow dynamics. Englewood, N.J., Prentice-Hall Space Technology Series, p. 480 and p. 485.

Snyder, Conway, J. R. Anderson, M. Neugebauer and E. J. Smith, 1962: Interplanetary space physics. Lunar and planetary sciences in space exploration, NASA SP-14

LIST OF SYMBOLS

R_L	Larmor radius or cyclotron radius.
B	Magnetic induction
γ	10^{-5} gauss = 5×10^{-9} weber

APPENDIX II

A POSSIBLE OSCILLATION OF THE WINDS IN THE EQUATORIAL STRATOSPHERE WITH A PERIOD OF 24 TO 27 MONTHS

by

John C. Freeman, Jr.

A POSSIBLE OSCILLATION OF THE WINDS IN THE EQUATORIAL STRATOSPHERE WITH A PERIOD OF 24 TO 27 MONTHS

The alternating, descending westerlies and easterlies at the equator have been discovered by McCreary and discussed, their longitudinal extension verified by Ebdon and Veryard[1] and by Reed, Campbell, Rasmussen and Rogers[2]. These winds are a striking physical phenomenon and cry for a theoretical explanation as simple as the relation between the tilt of the earth's axis and the annual temperature cycle in middle latitudes. However, the theoretical evidence in this paper points to an explanation bearing a family resemblance to that for the semi-diurnal pressure wave in the tropics.

Near the equator (within about 10^{o}) and all around the earth there is a region in which alternating bands of westerlies and easterlies overlie each other and move down. Each band is about 200 km wide and 10 km thick. They form descending waves with a period of 24 to 27 months. At the present time (and based on 56 months of data) 26 months is the accepted period.

There has been some difficulty in devising a physical mechanism that can bring about these bands or anything similar to them and most of the efforts toward explanation have centered on searches for forcing functions of 24 to 27 months period.

The present paper presents a model of the equatorial winds in which alternating easterlies and westerlies are possible. The model

is very dependent on the equatorial environment and as a bonus the period of the oscillation between easterlies and westerlies is of the right order of magnitude.

We postulate a very stable and therefore nearly flat layer of the atmosphere at the equator. The stability is approximated by discontinuities in the potential temperature with differences $\Delta\theta$ above and below the layer of thickness 2D. We will make the gross (and probably unnecessary) assumption that the middle of this layer remains level.

All of the air of this layer has absolute vorticity $\zeta + \beta y = 0$ where $\beta = \frac{2\Omega}{R_E}$. In our case $\zeta = -\frac{\partial u}{\partial y}$. Thus the potential vorticity equation becomes $\frac{-\frac{\partial u}{\partial y} + \beta y}{2D} = 0$. In other words, convergence and divergence will not change the vorticity.

We can write

$$\frac{\partial}{\partial y}\left(-u + \frac{\beta y^2}{2}\right) = 0$$

or

$$-u + \frac{\beta y^2}{2} = \text{const.} = -u(a) + \frac{\beta a^2}{2}$$

where $u(a)$ is the wind velocity at $y = a$.

If we assume there is a moving boundary at $y = a(t)$ (and $y = -a(t)$) of our layer and that $u(a) = \text{const.} > 0$ (or is a west wind) then we have

$$u(y) = u(a) - \frac{\beta a^2}{2} + \frac{\beta y^2}{2}$$

In particular we are interested in u when $y = 0$ or at the equator.

$$u(o) = u(a) - \frac{\beta a^2}{2}$$

We can see from this equation when a is small then $u(o) \approx u(a)$ (a west wind) and when a is large then $\frac{\beta a^2}{2}$ is large and $u(o) < 0$ (or we have east winds).

The "physical" appearance of the bands in east winds and west winds is symbolized in Figure II-1.

A "map" of the winds is given in Figure II-2.

The stability is important in this discussion as a restoring force. This can be seen roughly by the high values of D at the equator. Actually, the stability is more important as a link between the pressure and the height of a potential temperature surface. Thus we have a mechanism for alternating west winds and east winds. We also can see that there is some reason to think it will oscillate.

In order to investigate the period of oscillation we need a little previous philosophical and mathematical discussion.

The theoreticians in oceanography have had a distinct advantage over their counterparts in meteorology. The only significant measure they have had of deep ocean currents has been a result of density measurement and the geostrophic approximation. Thus in oceanography

$$fu = -\frac{1}{\rho}\frac{\partial P}{\partial y} \qquad \text{and} \qquad fv = +\frac{1}{\rho}\frac{\partial P}{\partial x}$$

have always been acceptable approximations. The numerical weather prediction group led by Charney has also given the geostrophic

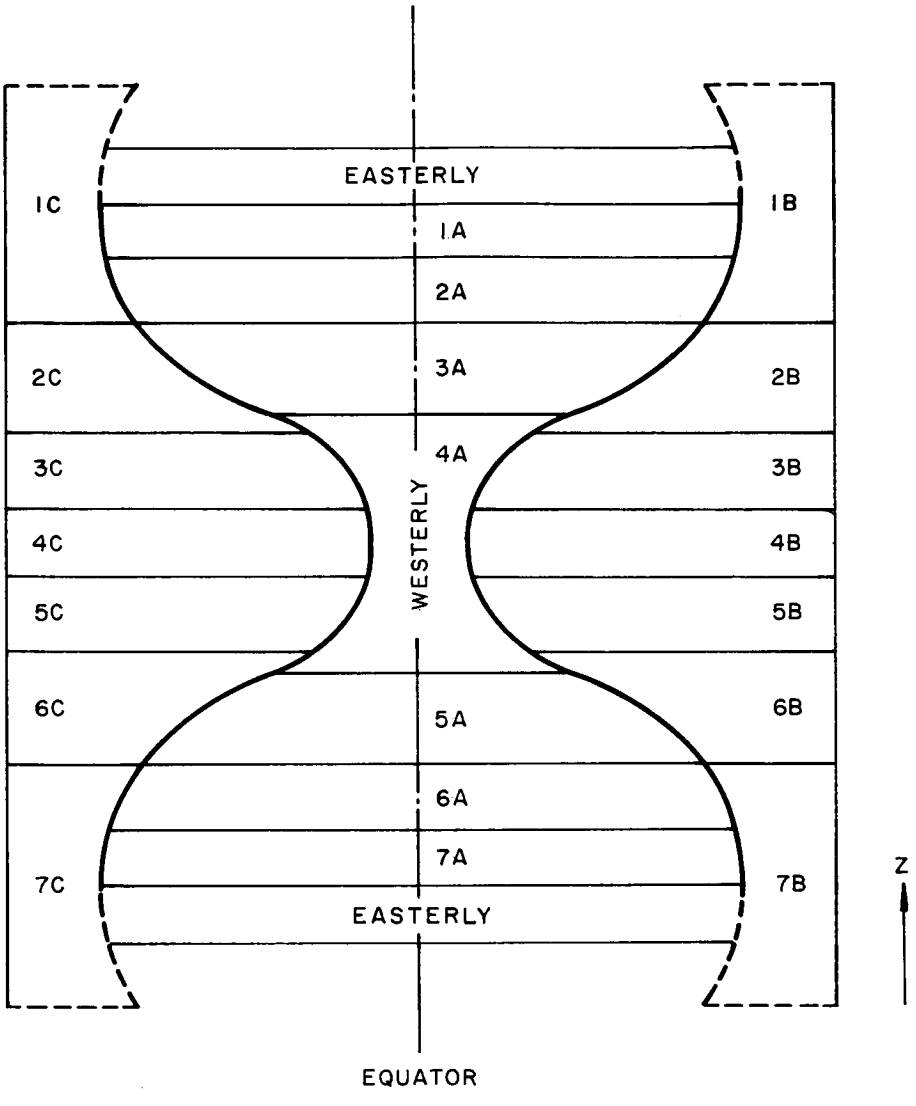

LEGEND

The bands or ribbons of stable air that undulate in width and thickness with the frequencies discussed in the model.

FIGURE II-1

VERTICAL WAVE MODEL

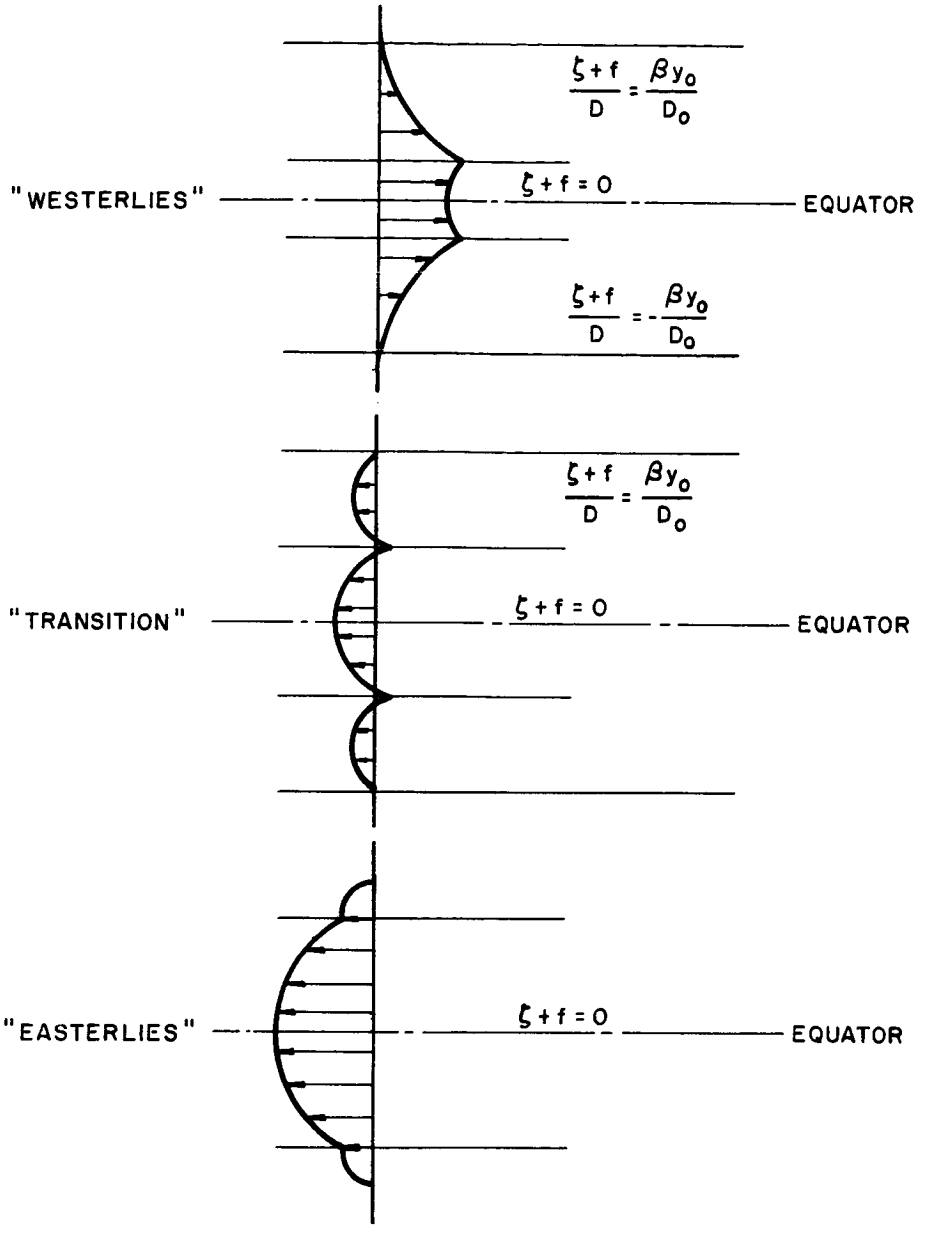

LEGEND

Horizontal drawings of the wind profiles in the model discussed in this paper. The boundary bands of $\frac{\zeta + f}{D} = \frac{\beta y_0}{D_0}$ are important in defining the westerlies, and the central band of $\zeta + f = 0$ is important in defining the easterlies.

FIGURE II-2

BANDS OF VORTICITY

approximation an aura of respectability in meteorology. Freeman, Baer and Jung[3] have shown that flow becomes nearly geostrophic rapidly when it is free to do so. We are going to study a problem in which we can find u when the boundary a is known. Thus it will be to our advantage to use the approximation in the sense, "given the wind we use the geostrophic approximation to find the pressure."

Exactly on the equator this results in the statement

$$\frac{\partial p}{\partial z} = -2\Omega\rho g \qquad \text{(II-1)}$$

This is a modification of the hydrostatic equation. This statement should also be true for several degrees of latitude away from the equator.

Near the equator we have

$$\frac{1}{\rho}\frac{\partial \rho}{\partial y} = -\beta y u \qquad \text{(II-2)}$$

We are going to be considering a system in which alternating values of positive and negative u overlie each other so the best geostrophic approximation in the horizontal is

$$\frac{1}{\rho}\frac{\partial p \text{ hydrostatic}}{\partial y} = -\beta y u$$

In order to follow the north south motion of the boundary a we write

$$\frac{\partial a}{\partial t} = \nu$$

and

$$\frac{d}{dt}\frac{\partial a}{\partial t} = \frac{\partial^2 a}{\partial t^2} = -\frac{1}{\rho}\frac{\partial p}{\partial y} - \beta y u \qquad \text{(II-3)}$$

Now we want to use a changed value of g.

$$gu = g + 2\Omega u$$

With our stable layer and no value of u we had

$$-\frac{1}{\rho}\frac{\partial p}{\partial y} = -\gamma\frac{\partial D}{\partial y} = -g\frac{\Delta\rho}{\rho}\frac{\partial D}{\partial y} = \text{hydrostatic pressure gradient}$$

Now with u having a value we can say

$$-\frac{1}{\rho}\frac{\partial p}{\partial y} = \gamma u\frac{\partial D}{\partial y} = -g\frac{\Delta\rho}{\rho}\frac{\partial D}{\partial y} - 2\Omega u\frac{\Delta\rho}{\rho}\frac{\partial D}{\partial y}$$

$$= -\frac{1}{\rho}\frac{\partial p\ \text{hydrostatic}}{\partial y} - 2\Omega u\frac{\Delta\rho}{\rho}\frac{\partial D}{\partial y}$$

$$= \beta yu - 2\Omega u\frac{\beta yu}{g}$$

Substituting this in Eq. (II-3) and putting a for y we get

$$\frac{\partial^2 a}{\partial t^2} = -\frac{2\Omega\beta u^2}{g}a$$

If we set

$$a = a_o \sin.\frac{2\pi t}{T}$$

$$\frac{\partial u}{\partial t} = \frac{2\pi a_o}{T}\cos\frac{2\pi t}{T}$$

$$\frac{\partial^2 a}{\partial t^2} = -\frac{4\pi^2 a_o}{T}\sin\frac{2\pi t}{T}$$

and we get

$$\frac{4\pi^2}{T^2} = -\frac{2\Omega\beta u^2}{g}$$

this gives

$$T^2 = \frac{4\pi^2 g}{2\Omega\beta u^2} \qquad T = \frac{2\pi}{|u|}\sqrt{\frac{g}{2\Omega\beta}}$$

Let us evaluate these terms:

$$1 \text{ day} = 8.64 \times 10^4 \text{ sec.}$$

$$1 \text{ yr.} = 3.153 \times 10^7 \text{ sec.}$$

$$\Omega = \frac{2\pi}{8.64} \times 10^{-4}/\text{sec.}$$

$$\beta = \frac{2\pi}{8.64 \times 3} \times 10^{-10}/\text{m.sec.}$$

$$g = 10 \text{ m/sec}^2$$

$$T = \frac{2\pi}{|u|}\sqrt{\frac{10 \times 10^{14}}{\frac{2 \times 2\pi \times 2\pi}{3 \times 8.64 \times 8.64}}}$$

$$= \frac{8.64}{|u|} \times 10^7 \sqrt{\frac{10 \times 3}{2}}$$

$$3.15 \times 2.16 = \frac{3.9 \times 8.64}{|u|}$$

$$|u| = \frac{3.9 \times 8.64}{3.15 \times 2.16} = \frac{33.69}{6.80} = 4.95$$

$$|u| = 5 \text{ m/sec. when } T = 26 \text{ mos.}$$

Our previous analysis has resulted in a reasonable frequency of vibration for the atmosphere and a mode of vibration that will allow alternate easterly and westerly winds at the equator.

The frequency was found to be in the range of interest resulting from the observed 24 to 27 month period of vibration of the equatorial

winds.

We now need some way of arriving at a vertical wave length for the waves. The first analysis (for the period) has assumed that the stability is so great that no vertical motion is possible. Since we have an organized vertical motion resulting from the expansion and contraction of ribbons of fluid it is not surprising that in order to find the vertical motion of the waves we must give some vertical motion to the fluid.

We assume $w = \frac{\partial(h-h_o)}{\partial t}$ where h_o is the fixed height for a fluid ribbon at which some variable has a fixed value. Now h_{o2} and h_{o1} can be subtracted to give D_o and $h_2 - h_1 = D$. This can be expressed in differential form as $D \frac{\partial w}{\partial z} = D \frac{\partial^2 h}{\partial z \partial t} = \frac{\partial D}{\partial t}$. The continuity equation for narrow levels is already sufficient to give us

$$\frac{\partial aD}{\partial t} = 0$$

The geostrophic approximation and previous considerations in the first equation of motion is sufficient to give us

$$\frac{\partial u}{\partial t} = -\left(2\Omega + \frac{\partial u}{\partial z}\right) w$$

We differentiate with respect z and get

$$\frac{\partial}{\partial z}\frac{\partial u}{\partial t} = -\left(2\Omega + \frac{\partial u}{\partial z}\right)\frac{\partial w}{\partial z} = -\left(2\Omega + \frac{\partial u}{\partial z}\right)\frac{1}{D}\frac{\partial D}{\partial t}$$

We know from continuity that $\frac{1}{a}\frac{\partial u}{\partial t} = -\frac{1}{D}\frac{\partial D}{\partial t}$ so we can write

$$\frac{\partial}{\partial t}\frac{\partial u}{\partial z} = +\frac{\left(2\Omega + \frac{\partial u}{\partial z}\right)}{a}\frac{\partial a}{\partial t}$$

We assume max $\frac{\partial u}{\partial z} >> 2\Omega$ so we can say $\frac{\frac{\partial}{\partial t}\frac{\partial u}{\partial z}}{\frac{\partial u}{\partial z}} = \frac{\frac{\partial a}{\partial t}}{a}$

This tells us that $\log \frac{\partial u}{\partial z} - \log a = \text{const.}$ in time

or $\frac{\partial}{\partial t} \log \frac{\partial u}{\partial z} \Big/ a = \text{const.}$

or $\frac{\partial u}{\partial z} \Big/ a = \text{const.} = \frac{\frac{\partial u}{\partial z} \Big/ \text{max.}}{a_{\text{max.}}}$

This equation can be written

$$\frac{\partial u}{\partial z} = \frac{\frac{\partial u}{\partial z\ \text{min.}}}{a_{\text{max.}}}\, a$$

If $u = u_0 \cos\left(\frac{2\pi z}{2} - \frac{2\pi z}{T}\right)$, $a = a_0 \sin\left(\frac{2\pi z}{2} - \frac{2\pi t}{T}\right)$.

We find that this condition is compatible with any set of waves moving near the equator. In other words the vertical waves can have any apeed depending on max $\frac{\partial u}{\partial z}$. Apparently the condition on $\frac{\partial u}{\partial z}$ is inherent in the driving function.

REFERENCES

1. Ebdon, R. A., and R. G. Veryard, 1961: Fluctuations in equatorial stratospheric winds. Nature, 189, 791-793.

2. Reed, R. J., W. J. Campbell, L. A. Rasmussen and D. G. Rogers, 1961: Evidence of a downward propagating, annual wind r4versal in the equatorial stratosphere. J. Geophys. Res., 66, 813-818.

3. Freeman, Jr., J. C., L. Baer, and G. H. Jung, 1957: The bathystropic storm tide. J. Marine Res., 16, 12-22.

LIST OF SYMBOLS

a	horizontal distance from a base latitude
a_o	fixed value of a
D	vertical distance between material surfaces
D_o	vertical distance (fixed) between material surfaces
f	earth's vorticity (coriolis parameter)
g	acceleration of gravity
h	height of a material surface
h_o	fixed height for a fluid ribbon at which some variable has a fixed value
p	pressure
R_E	radius of the earth
t	time
T	absolute temperature
u	zonal velocity
v	north-south velocity
w	vertical velocity
x	east-west distance
y	north-south distance
z	vertical distance
β	horizontal rate of change of earth's vorticity
ζ	relative vorticity
$\Delta\theta$	vertical difference of potential temperature

ρ	density
$\Delta\rho$	vertical density difference
Ω	earth's angular velocity

APPENDIX III

A POSSIBLE INERTIAL OSCILLATION OF THE EQUATORIAL STRATOSPHERE

by

John C. Freeman, Jr.

A POSSIBLE INERTIAL OSCILLATION OF THE EQUATORIAL STRATOSPHERE

The descending waves of alternating easterly and westerly winds at the equator were the subject of a previous paper. During the attempt to find the very long period mode of vibration of the atmosphere related to these waves we have found an unusual way for the atmosphere to oscillate with the inertial frequency.

This type of oscillation is very likely much more important at higher latitudes than at the equator but we will discuss it at the equator for ease of theoretical discussion and for comparison with the waves of 25 month period discussed previously.

A gross picture of the model is given in Figures III-1 and III-2. The oscillating boundary a with constant wind speed u allows alternate east and west winds as it moves from and to the equator.

Ebdon and Veryard (1961) make a point that the long term east and west changes in the wind have some brief breaks in them. It is our purpose here to show that there is a much shorter vibration of the same type possible and that it is probably a mechanism for a two to fifteen day lag in the response of the tropospheric circulation to solar and geomagnetic disturbances.

We assume stable flat layers of the atmosphere with absolute vorticity $\zeta + \beta y = 0 \cdot \left(\beta = \frac{2\Omega}{R_E}\right)$. We only have a zonal wind so $\zeta = -\frac{\partial u}{\partial y}$. We integrate this equation as outlined in the paper

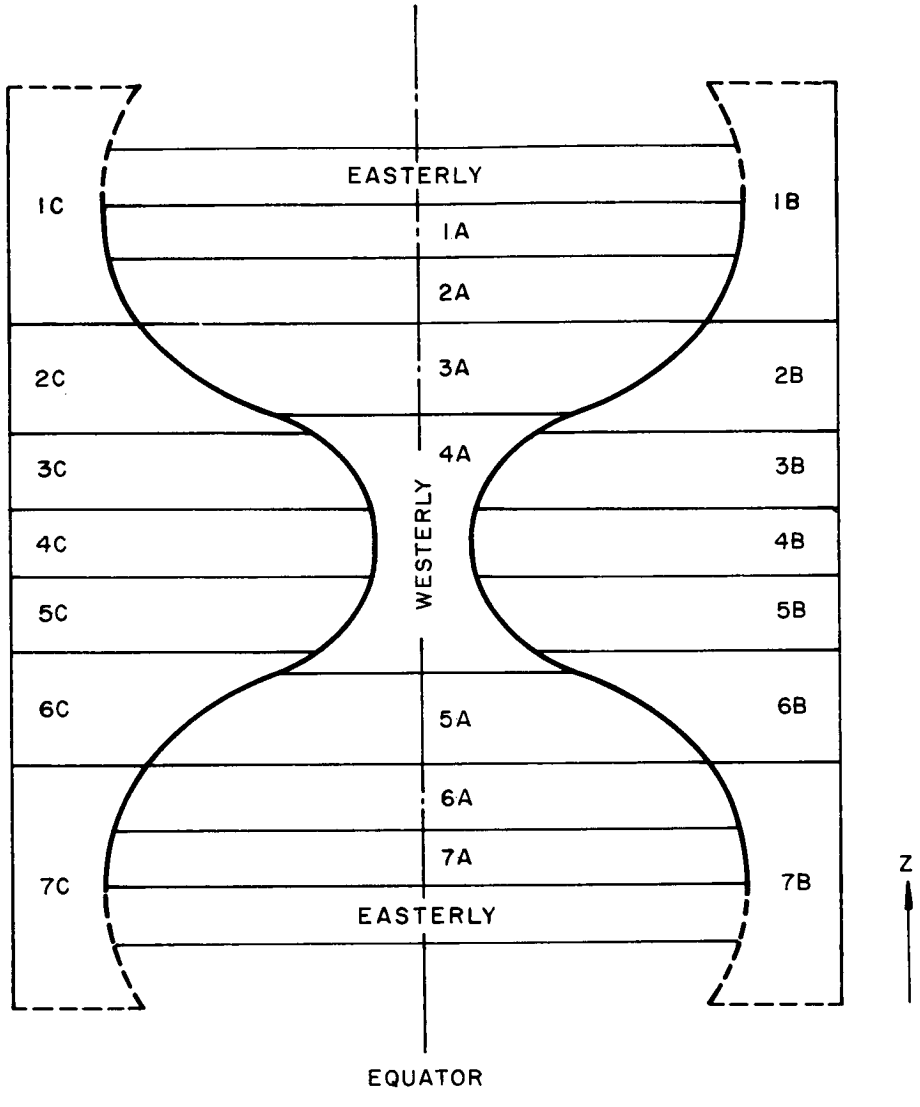

LEGEND

The bands or ribbons of stable air that undulate in width and thickness with the frequencies discussed in the model.

FIGURE III-1

VERTICAL WAVE MODEL

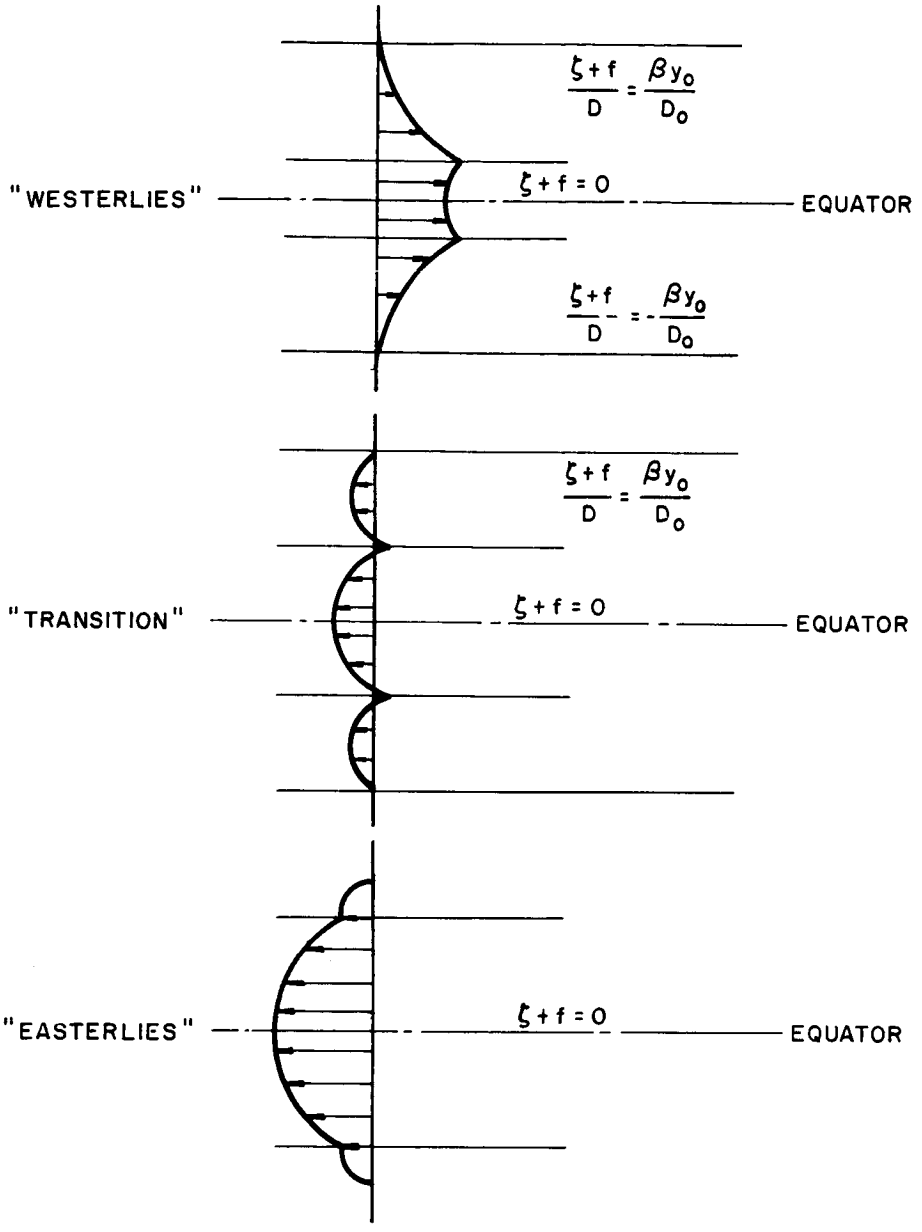

LEGEND

Horizontal drawings of the wind profiles in the model discussed in this paper. The boundary bands of $\frac{\zeta+f}{D} = \frac{\beta y_o}{D_o}$ are important in defining the westerlies, and the central band of $\zeta + f = 0$ is important in defining the easterlies.

FIGURE III-2

BANDS OF VORTICITY

"A Possible Oscillation of the Winds in the Equatorial Stratosphere with a Period of 24 to 27 Months" (Freeman, 1963), and we get

$$u(y) = u(a) - \frac{\beta a^2}{2} + \frac{\beta y^2}{2}$$

Thus with $u(o) = u(a) - \frac{\beta a^2}{2}$ we can get alternating winds $u(o)$ at the equator with sufficient variation in the distance, a, to the place where the velocity is constant.

We assume that the stability is so great that there is little, if any, value of $\frac{\partial h}{\partial y}$ (where h is the height of a stable layer) and that whatever slope there is in the surface h is balanced by

$$\frac{\Delta\theta g}{\theta} \quad \frac{\partial h}{\partial y} = -\beta y U$$

The boundary of the band of constant vorticity, a, is given by $\frac{\partial a}{\partial t} = v(a)$ and we also know

$$\frac{d}{dt} \quad \frac{\partial a}{\partial t} = \frac{\partial^2 a}{\partial t^2} = -\frac{\Delta\theta g}{\theta} \quad \frac{\partial h}{\partial y} - \beta a U \qquad \text{(III-1)}$$

This is a result of the second equation of motion.

Our previous paper concerned oscillation of the atmosphere that was only about 10 - 20 km in vertical wave length and we took advantage of that small wave length in the theoretical discussion.

We now concern ourselves with waves that are so deep that $-\frac{g\Delta\theta}{\theta} \quad \frac{\partial h}{\partial y}$ cannot be changed significantly because it would have to be changed through so deep a stable layer that a very large amount of energy would be required. If we now assume that the zonal wind on

the boundary U is changed by an amount ΔU then we have

$$\frac{\partial^2 a}{\partial t^2} = -\frac{\Delta\theta g}{\theta}\frac{\partial h}{\partial y} - \beta a (U + \Delta U) \qquad \text{(III-2)}$$

We have already said

$$-\frac{\Delta\theta g}{\theta}\frac{\partial h}{\partial y} - \beta a U = 0 \qquad \text{(III-3)}$$

so from (III-2) and (III-3) we are left with

$$\frac{\partial^2 a}{\partial t^2} + \beta a \Delta U = 0 \qquad \text{(III-4)}$$

The sine wave solution of (III-4) tells us that such large scale vertical waves have a period

$$T = \frac{2\pi}{\sqrt{\beta \Delta U}}$$

which is about 2 to 15 days for reasonable values of ΔU.

REFERENCES

Ebdon, R. A. and R. G. Veryard, 1961: Fluctuations in equatorial stratospheric winds. Nature, 189, 791-793.

Freeman, Jr., J. C., 1963: A possible oscillation of the winds in the equatorial stratosphere with a period of 24 to 27 months. (See Appendix II.)

LIST OF SYMBOLS

a	oscillating boundary measured from a fixed latitude
D	vertical thickness between material surfaces
D_o	chosen fixed vertical distance between material surfaces
f	earth's vorticity (coriolis parameter)
g	acceleration of gravity
h	height of a stable layer
R_E	earth's radius
t	time
T	absolute temperature
u	zonal wind speed
U	special value of zonal wind
ΔU	vertical change in zonal velocity
v	north-south velocity
y	north-south distance
y_o	chosen fixed horizontal distance
β	horizontal change in earth's vorticity
ζ	relative vorticity
θ	potential temperature
$\Delta\theta$	vertical difference of potential temperature
Ω	angular velocity of the earth

APPENDIX IV

A THEORY FOR ATMOSPHERIC CROSS SECTIONS

by

John C. Freeman, Jr.

A THEORY FOR ATMOSPHERIC CROSS SECTIONS

Objectives and Conclusions

It is our purpose here to describe the flow in the upper troposphere by means of a simple mechanism. We postulate that the upper troposphere acts in accord with two very basic principles - the conservation of vorticity and the thermal wind approximation - which permit explanation of the gross features.

The concept to be developed here will show that: (1) a concentration of isentropes and isotachs results as a natural process of the atmosphere responding to the vorticity conservation and the thermal wind relationship when a disturbance in the initial flow arises from an outside cause; (2) on cross sections, the process in (1) can continue until a complete discontinuity is obtained in the isentropic and isotach fields; this discontinuity appears in the middle of a region of increasing anticyclonic vorticity in accord with the vorticity conservation law.

The discontinuity itself, appearing as a line on weather charts and cross sections, represents an actual finite zone within the atmosphere where strong gradients of potential temperature are developed and continued as long as the flow concentrates isentropes and isotachs in the region.

Mixing across the concentration region then transforms the cyclonic wind shear across the discontinuity (usually situated in a zone of anticyclonic vorticity) into large cyclonic relative vorticities

which results in much larger values of potential vorticity than had previously existed in the system.[1] This vorticity creation involves the generation of new values of $\frac{\zeta + f}{D}$, a process which violates the potential vorticity conservation law. Thus the conservation law holds completely within the regions adjacent to the discontinuity and, indeed, up to the discontinuity itself. It does not hold, however, in the discontinuity and it is suggested that, here, large values of the potential vorticity are actually created.

Meridional cross sections showing the vertical distribution of potential temperature and wind speed are used as analysis tools throughout the discussion. Various cross sections from earlier studies as well as model diagrams are used to illustrate the mechanism described here.

The premise that the upper troposphere follows vorticity conservation and the thermal wind relation is not new; the appearance of new high values of potential vorticity in the jet stream vicinity has been noted as well (Reed, 1955).

Having stated the conclusions which will be shown, let us now develop the argument in detail.

---

1. The term $\frac{\zeta + f}{D}$, represents the vertical component of the potential vorticity of a fluid particle; ζ represents the relative vertical vorticity component (expressed as $\frac{\delta v}{\delta x} - \frac{\delta u}{\delta y}$ in rectangular coordinates), f is the vorticity due to the earth's motion, and D is the vertical distance between material surfaces. The conservation equation for this component may be written $\frac{d}{dt}\left(\frac{\zeta + f}{D}\right) = 0$. Thus when D changes, the quantity $(\zeta + f)$ changes in the same sense in accord with the conservation law. Potential vorticity thus is distinguished from absolute vorticity, $(\zeta + f)$, representing the sum of relative and earth-derived vorticities.

Cross Sections and a Paradox

In upper level shear zones where isentropic surfaces are closely spaced in the vertical (D is small), potential vorticity conservation requires that absolute vorticity, ($\zeta + f$), also be small. However, very large values of ζ or ($\zeta + f$) are observed on cross sections within these zones. Several detailed synoptic studies within recent years have demonstrated this last statement. Hsieh (1950) notes that ζ increases within such zones, while a study by Reed and Sanders (1953) shows that ($\zeta + f$) is generated within a mid-tropospheric frontal zone; Petterssen (1955) shows a similar, more pronounced, generation of absolute vorticity.

In an outstanding case of shear line formation in the upper atmosphere, Hsieh (1950) illustrates the hypothesis that upper troposphere shear lines can be extensions of surface frontal surfaces. In the example, there is pronounced downward motion of isentropic surfaces below 350 mb during the entire study, which leads to a packing of isentropes between 600 and 700 mb. Hsieh notes this observed so-called "direct" solenoidal circulation is a necessary, but not sufficient, condition for formation of a shear line in the upper atmosphere. Hsieh also remarks on the observed (horizontal) divergence below about 400 mb, recalling that the vorticity equation requires a <u>decrease</u> of originally-existing relative cyclonic vorticity, ζ, in the absence of meridional motion (f remains constant). Then, he goes on, the <u>observed increase</u> of ζ near the trough line at the 500 and 700 mb surfaces must be due to downward transport of ζ

from upper levels, in excess of the decrease accompanying the lower-level divergence.

We note that Reed and Sanders (1953) do not agree with Hsieh in regard to the origin of the relative cyclonic vorticity present here. Reed and Sanders describe the generation of absolute vorticity ($\zeta + f$) in a mid-tropospheric frontal zone, and demonstrate that the observed increase of cyclonic ($\zeta + f$) is primarily <u>generated</u> locally, rather than being pre-existing cyclonic vorticity that is transported downward into the shear line region.

Austin (1954) states, in a case of strong upper level trough development, that a large amount of absolute vorticity is created in the upper troposphere, and that this arises from subsidence in the vicinity of the upper trough where horizontal divergence is small. He notes that the shear vorticity varies rapidly in the horizontal, requiring a close network of values to portray the actual relative vorticity distribution.

Petterssen (1955) illustrates the same view with a case history showing a situation where ($\zeta + f$), from the surface to 200 mb, increases more than fourfold in a 24-hour period; he shows that vast amounts of ζ were created and dispersed over large areas surrounding a developing cyclone center. He further shows that ζ was created in a subsiding region to the west of an approaching upper trough; thus when this newly-created mid-troposphere moved over a surface disturbance, very rapid cyclogenesis was initiated. The storm developed was then made self-perpetuating by the thermal

advection. Newton (1954) also illustrates these points with a different synoptic study.

The paradox is recognized by Reed (1955) leading to these statements regarding the validity of vorticity conservation within certain tropospheric zones: p. 233: "...the equation expressing the conservation of partial potential vorticity[2], which has provided the basis of numerous studies, including recent work on numerical prediction ... does not adequately describe developments within a highly baroclinic region." p. 236: "...The potential vorticity on pressure surfaces (partial potential vorticity) is poorly conserved in strong baroclinic zones."

Reed notes as well that the observed increase of horizontal temperature gradient (on isentropic surfaces in upper-level frontogenetic regions) is due to a steepening of the slope of isentropic surfaces as a result of an "indirect"[3] solenoidal circulation. He finds the upper-level frontal zone is a dynamically-produced phenomenon which intensifies as the storm intensifies, and the circulation within it is the reverse of that required for energy release in the classical sense. Further, the frontal zone does not separate air of immediate polar and tropical origin.

---

2. Reed defines this as $(\zeta_p + f)_p/\partial\theta$, where $\zeta_p = \left(\frac{\partial u}{\partial x} - \frac{\partial u}{\partial y}\right)_p$ is measured on a constant pressure surface.

3. Murray and Daniels (1953) show cross stream velocities in a jet which indicate a direct thermal circulation above or below the jet at the jet "entrance" (looking downstream) and an indirect thermal circulation at a jet "exit." Newton (1955) discusses this also.

A Model that Resolves the Paradox

A basic tool for this discussion will be the meridional cross section showing the vertical distribution (z-direction) of wind speed and potential temperature with latitude. It is assumed that such a section, oriented perpendicular to the latitude circles (y-direction) is also perpendicular to the jet stream flowing in the westerlies belt of winds at mid-latitudes (in the x-direction). Having assumed the flow is essentially west-east, it follows that v, the north-south wind velocity, is much smaller than u, the west-east velocity. We also assume $\frac{\partial u}{\partial x}$ is much smaller than $\frac{\partial u}{\partial y}$. The cross sections studied here will be a time series occurring along a single meridian. The flow is assumed to be isentropic, so that surfaces of constant potential temperature (isentropes in cross section) will be material surfaces. Thus in the vorticity equation

$$\frac{d}{dt}\left(\frac{\zeta + f}{D}\right) = 0 \qquad \text{(IV-1)}$$

D refers to the normal distance between two adjacent surfaces of potential temperature. In the equation above, the relative vorticity is given by

$$\zeta = -\frac{\partial u}{\partial y} \qquad \text{(IV-2)}$$

and f is the Coriolis parameter which is assumed constant. The derivative in (IV-1) is the material derivative.

We also assume that the thermal wind equation holds[4]

$$\frac{\partial u}{\partial z} = -K(z)\frac{\partial T}{\partial y} \qquad \text{(IV-3)}$$

where T represents temperature and z represents height.

For simplicity we assume

$$\frac{\partial u}{\partial z} = -K\left(\frac{\partial \theta}{\partial y}\right) \qquad \text{(IV-4)}$$

where K is a constant and θ is potential temperature. As an initial assumption, when $D = D_o$, $\zeta = 0$. This is equivalent to an initial or boundary condition where all isentropes are a distance D_o apart in the vertical, and the velocity is constant in the horizontal at a particular level. Thus Eq. (IV-1) becomes

$$\frac{\zeta + f}{D} = \frac{f}{Do} \qquad \text{(IV-5)}$$

The following quantities will be used in the further development:

H	vertical distance between isotachs, lines of constant wind speed.
W	horizontal distance between isotachs.
L	horizontal distance between isentropes.
Δu	constant increment between isotachs.
$\Delta \theta$	constant increment between isentropes.

4. This is essentially the geostrophic approximation. The paper, "The Bathystrophic Storm Tide," by Freeman, Baer, and Jung (1957) shows that fluid systems seek geostrophic flow. Experience in meteorology shows the same thing.

Eq. (IV-5) becomes

$$\frac{\frac{-\Delta u}{W} + f}{D} = \frac{f}{D_o} \qquad \text{(IV-6)}$$

and Eq. (IV-4) becomes

$$\frac{\Delta u}{H} = -K \frac{\Delta \theta}{L} \qquad \text{(IV-7)}$$

Rewriting (IV-6) and (IV-7),

$$D = D_o \left(1 - \frac{\Delta u}{f W}\right) \qquad \text{(IV-8)}$$

$$H = -\frac{1}{K} \frac{\Delta u}{\theta} L \qquad \text{(IV-9)}$$

Eqs. (IV-8) and (IV-9) indicate that when the horizontal gradients of wind and potential temperature (W and L) are known in a plane, then it is possible to determine the vertical gradients of wind and potential temperature (D and H) across the plane. Thus additional horizontal surfaces, above and below the original, can be drawn, and the horizontal distribution of wind and potential temperature can be determined for the new surfaces. The "chain" can be continued indefinitely, as long as it is valid to assume the vorticity equation and the thermal wind relationship.

To demonstrate this relationship, the initial conditions of the air are shown in Figure IV-1. Figure IV-5 has been prepared by use of a nomogram, shown in Figures IV-3 and IV-4, which is based on Eqs. (IV-8) and (IV-9). The values in Figure IV-2 represent the bouncary conditions, while the remaining values in Figure IV-5 are

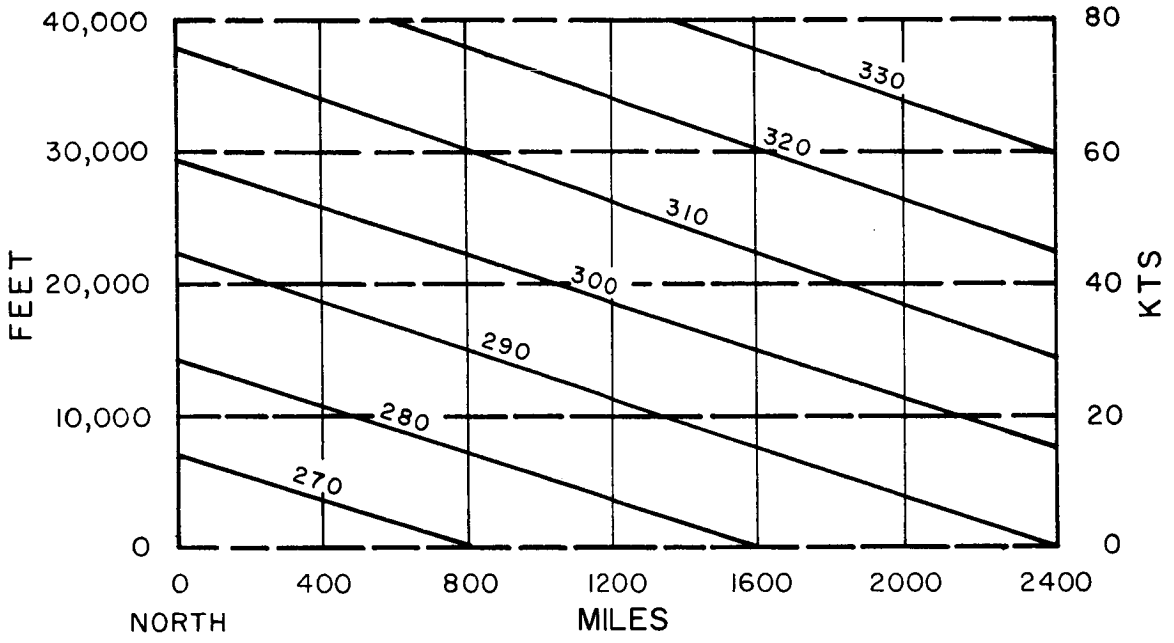

LEGEND

Isentropes and isotachs in a cross section in middle latitudes. The horizontal scale is in miles.

FIGURE IV-1

ISOTACHS AND ISENTROPES

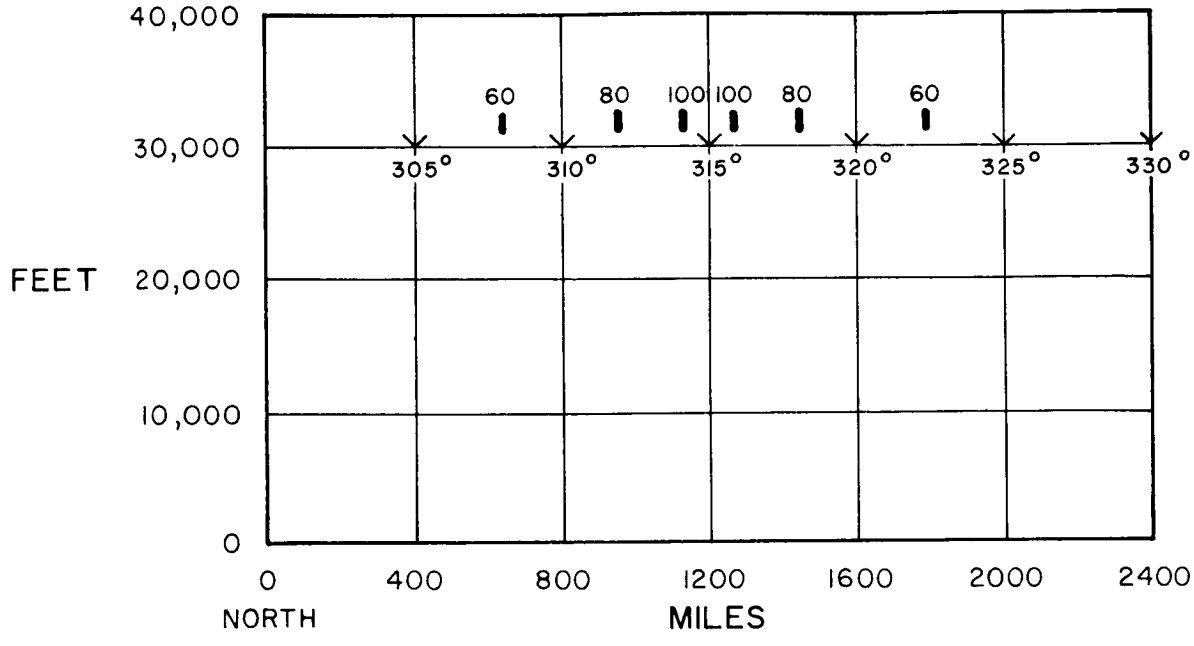

LEGEND

The winds and temperatures at one level are given and it is assumed that the same air as the original is at that level.

FIGURE IV-2

THE DISTURBED WIND FIELD

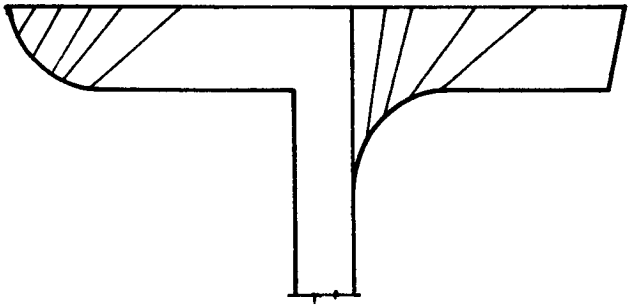

LEGEND

The scale for relating vertical distance of isentropic surfaces to horizontal wind gradients.

FIGURE IV-3

THE GRAPHICAL COMPUTER

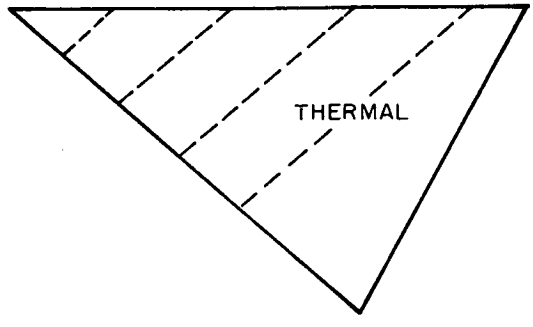

LEGEND

The scale for relating horizontal temperature gradients to vertical wind gradients.

FIGURE IV-4

THE GRAPHICAL COMPUTER

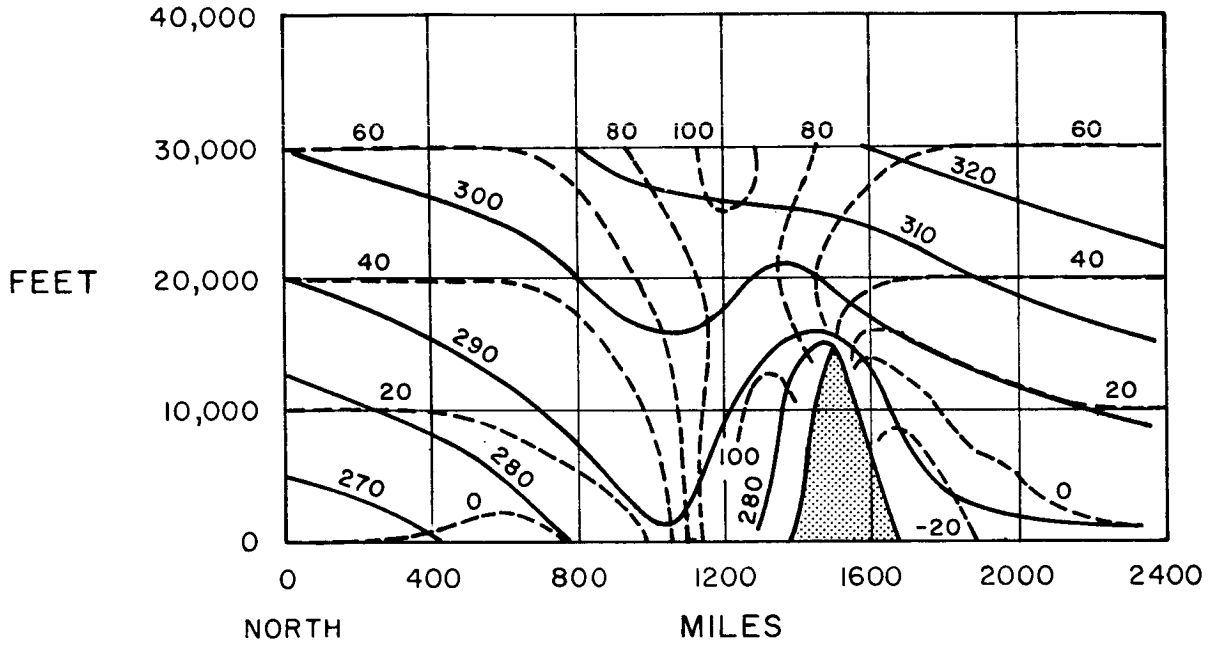

LEGEND

The results of the computation indicated in Figure 2. Note bulges in the isentropic surfaces and the shaded are where the computation must be adjusted with a new physical assumption. The discontinuities can be avoided by limiting the study to the upper 15,000 feet.

FIGURE IV-5

THE NEW STEADY STATE

computed values.

The initial and boundary conditions in Figure IV-1 were carefully selected to avoid discontinuities in the flow. However, the wind speed increase has resulted in cold air moving to a position under the axis of the jet stream. This indicates that, in actual synoptic examples, one can expect limited southward motion of cold air at the surface to be related to increased wind speeds aloft. In Figure IV-5, there is even a hint of a cut-off dome of cold air to the right of the jet stream axis.

The discontinuity of Figures IV-6, IV-10 and IV-11 may be explained through the following considerations. The thermal wind equation requires, for the normal tropospheric temperature gradient across mid-latitudes, that the wind speeds increase with height. Such a localized increase in wind speeds result in an anticyclonic wind speed shear and a decrease in cyclonic vorticity. Correspondingly, a decrease in spacing between isentropic surfaces must occur, thus strengthening the potential temperature gradient (horizontally as well as vertically); a stronger temperature gradient requires an increase in the vertical wind shear so that the process is self-perpetuating. Eventually, the thickness, D, between isentropes becomes zero so that a discontinuity in potential temperature has been formed which corresponds to the shear line formation process of Hsieh, or the mid-trospheric frontal zones described by Reed and Sanders. This could be the vortex sheet formation process which, in a theory of Rossby, must somehow be a source of new potential vorticity[5].

5. Verbal communication, 1952.

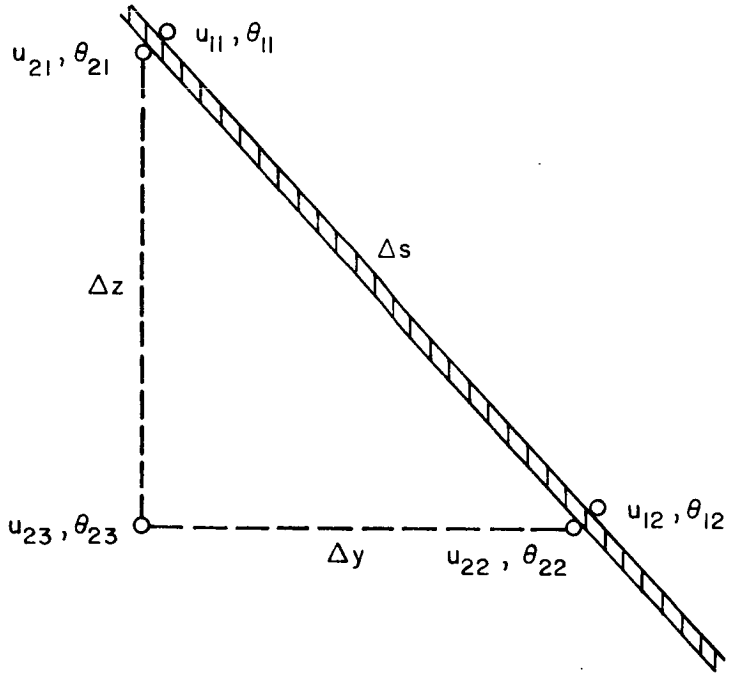

LEGEND

The new physical assumption is that an interface is created which is a vortex sheet and a temperature discontinuity.

FIGURE IV-6
INTERFACE CONDITIONS

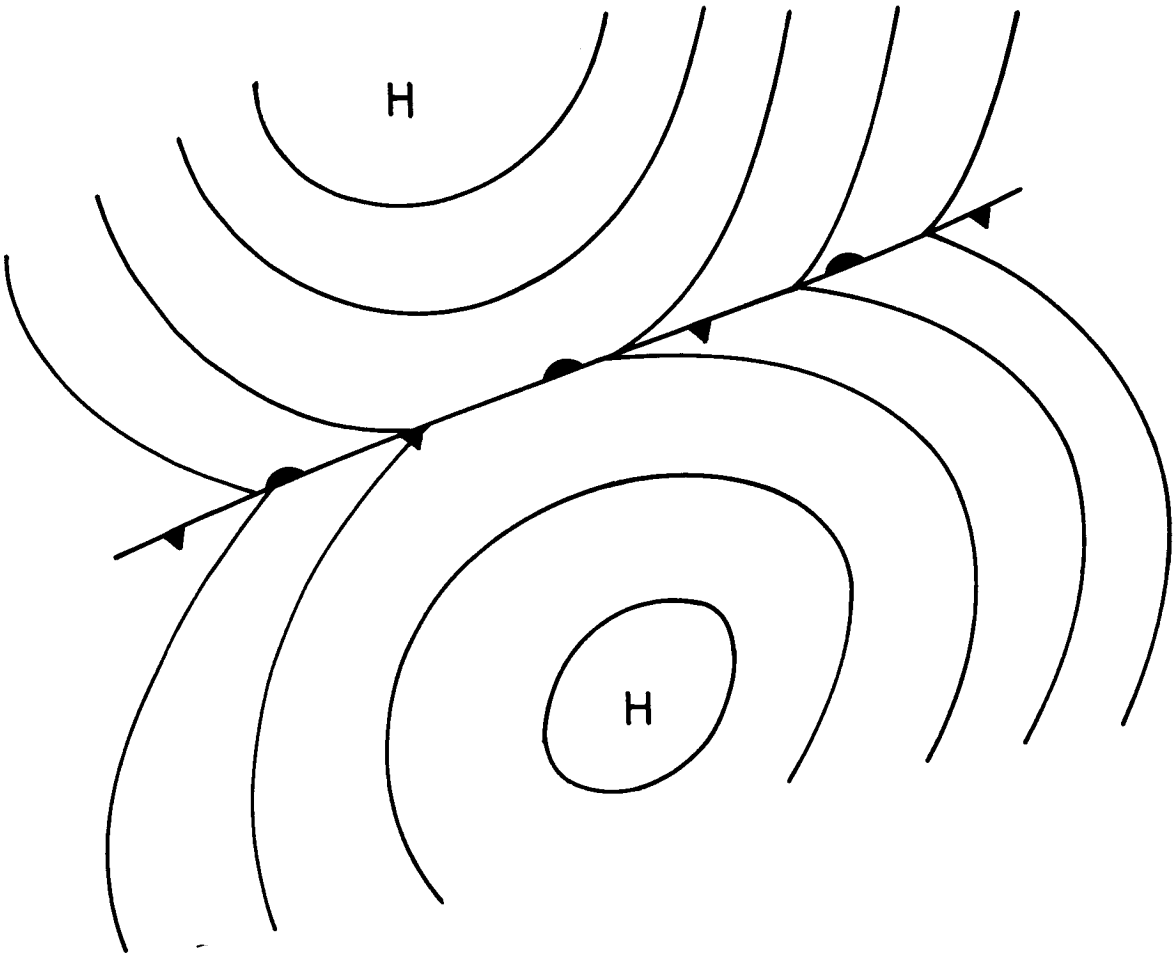

LEGEND

Temperature and wind discontinuities in regions of maximum anticyclonic vorticity in two fluids is not really a new meteorological concept. This is typical of a very common analysis of surface pressure.

FIGURE IV-7

FRONT IN ANTICYCLONIC VORTICITY

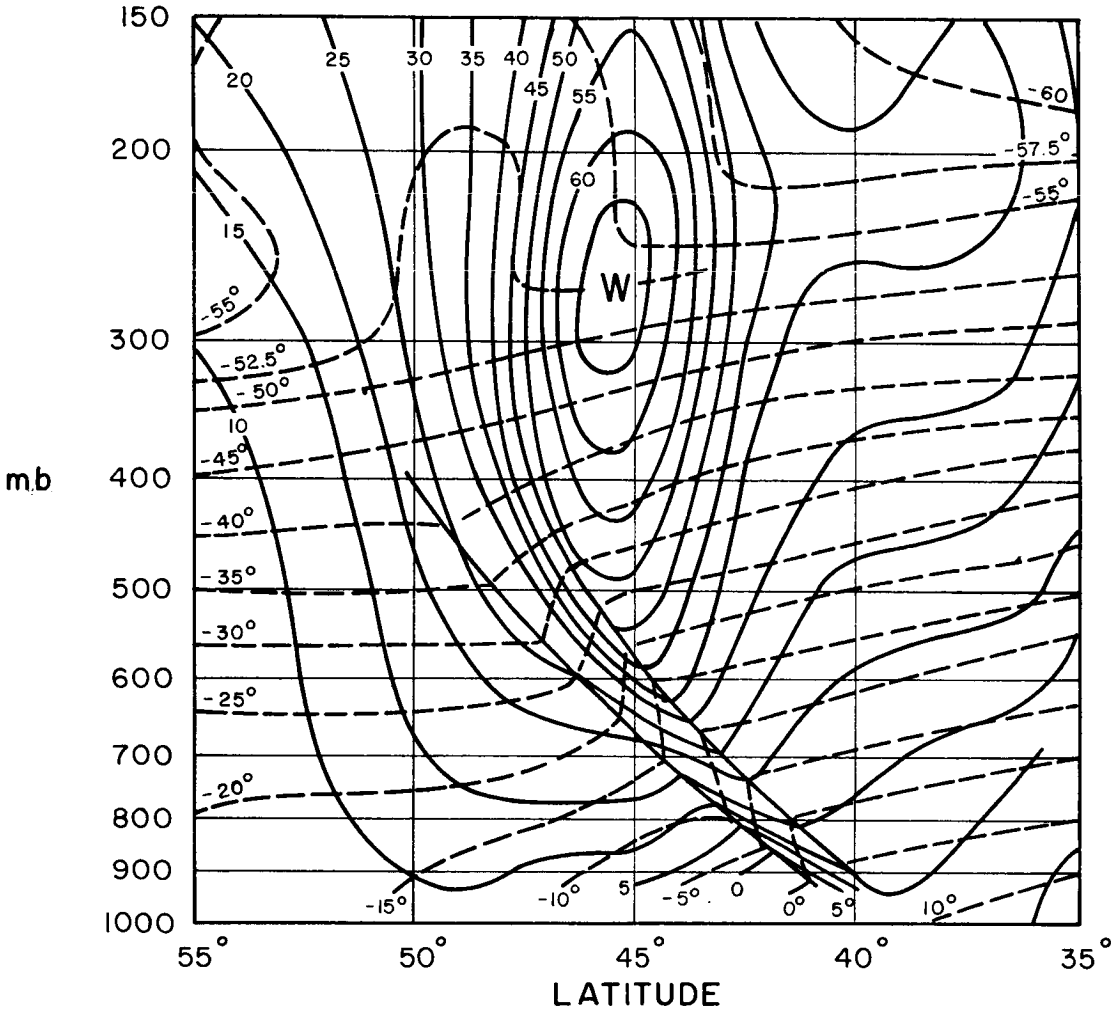

LEGEND

Bjerknes (1951) analysis of a frontal surface. Note that the maximum discontinuity is in a region of anti-cyclonic wind shear.

FIGURE IV-8

JET STREAM AND FRONT

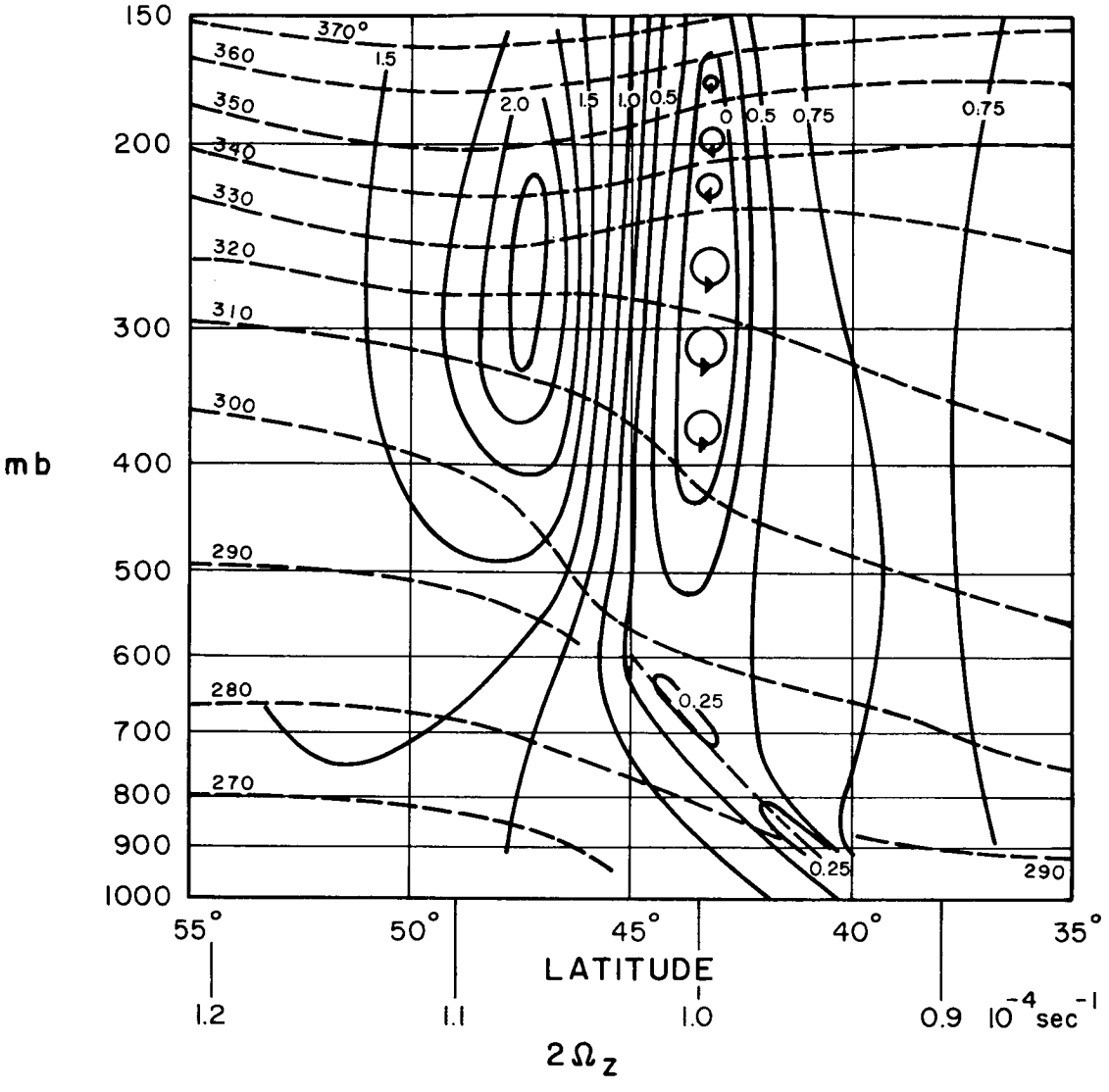

LEGEND

Absolute vorticity chart for Figure 8, also from Bjerknes (1951), confirming that anticyclonic (i.e., values less than value plotted on bottom) vorticity is found near the front.

FIGURE IV-9

VORTICITY DISTRIBUTION

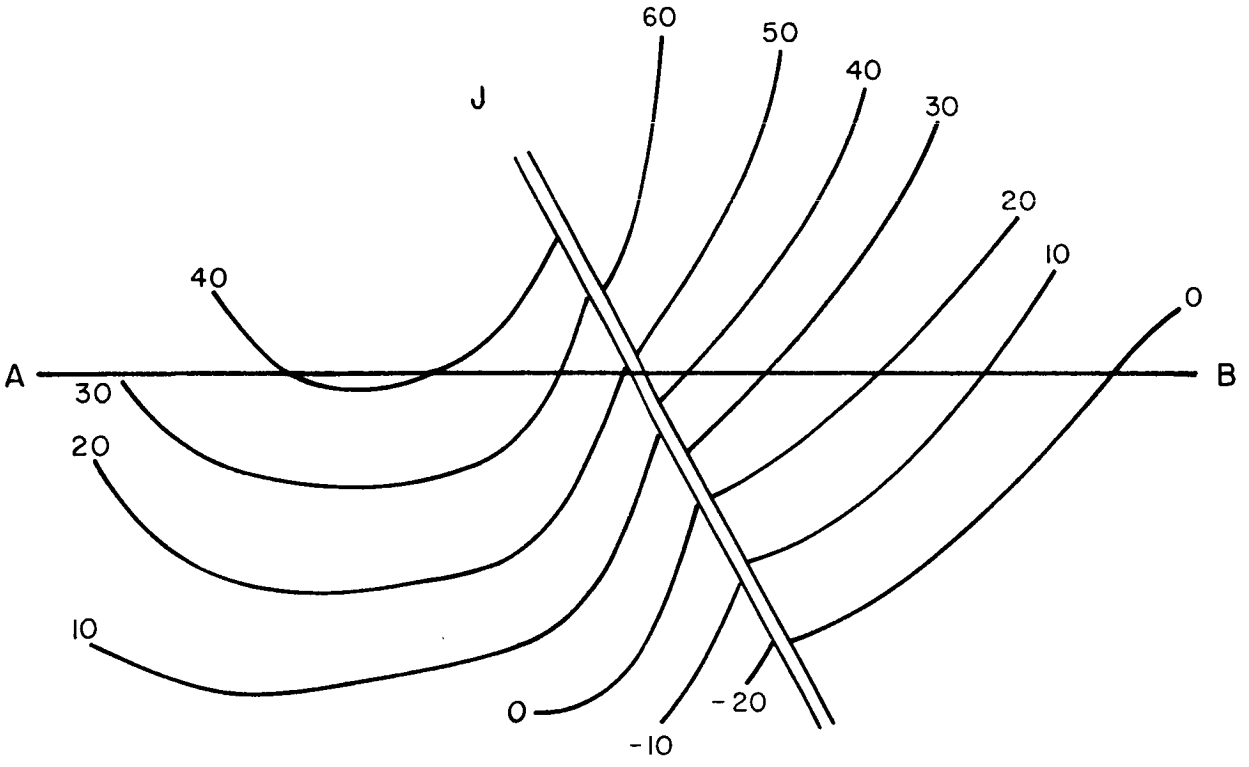

LEGEND

A model of a front similar to the actual case outlined in Figure 8.

FIGURE IV-10
MODEL JET STREAM AND FRONT

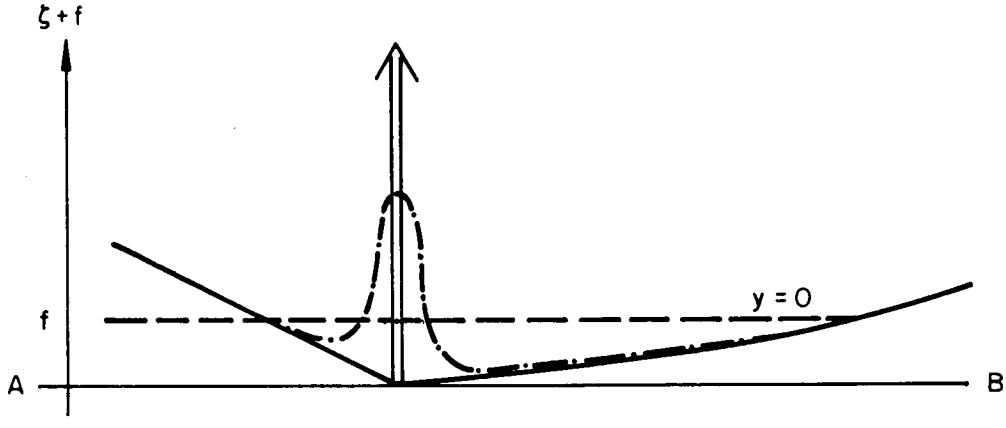

LEGEND

The delta-function type vorticity distribution at the discontinuity with an indication of the result of diffusion of vorticity from the finite circulation per unit length.

FIGURE IV-11

DIFFUSION OF VORTICITY

Through the mutual interaction of vorticity conservation and the thermal wind relationship it has been demonstrated that vortex sheets are forced by the pinching out of isentropic layers, and that the velocity distribution thus becomes discontinuous. This discontinuity region is surrounded by closely-spaced isentropic surfaces, and is imbedded in a region of anticyclonic vorticity. There can be cyclonic wind shear across the discontinuity, but no cyclonic vorticity.

The nature of this discontinuous wind velocity distribution should be considered. The magnitude of the discontinuity depends on the scale of the chart or cross section on which data are entered. Thus very sharp discontinuities drawn on weather charts or sections of usual scale become less sharp when drawn to larger scale. These discontinuities, when considered in the actual atmosphere represent zones of finite thickness over which the given change in wind occurs. The same applies for temperature discontinuities. Figure IV-7 serves as a reminder that fronts in regions of maximum anti-cyclonic vorticity are not complete physical paradoxes.

Intense mixing within these zones of discontinuity is commonly observed; it is postulated here that this mixing represents the agency whose action creates cyclonic potential vorticity within the zone. In the gross picture then, potential vorticity is essentially conserved while the model developed here explains the observed generation of new cyclonic vorticity in regions of discontinuous wind and temperature, which represent small finite portions of the gross picture. The final conditions will be much like those shown in Figures IV-8 and IV-9

which were taken from Bjerknes (1951).

The Model and the Atmosphere

This model can be shown in actual operation in the atmosphere by referring to actual synoptic situations which have been investigated in detail and the results published by various authors as cited below.

Let us examine the basic premises of the model in the light of previous investigations:

(1) The atmosphere must satisfy both the conservation of vorticity and the thermal wind relation:

The success of current numerical weather prediction techniques is evidence that the atmosphere behaves roughly in accord with the absolute vorticity conservation principles advocated by Rossby and adopted as the basis for the NWP models.

There is need for considering the thermal wind relation along with the vorticity conservation principle; however, as shown by Sawyer and Bushby (1953), for example, who point out that a baroclinic model of the atmosphere which includes the thermal wind (restricted, however, to a single direction) appears to remedy prediction discrepancies of NWP barotropic models without thermal wind considerations.

Another example of the approach to the atmosphere from a dynamic point of view is given by Newton, et al (1951). They describe pressure trough deepening which was accompanied by baroclinicity in the upper troposphere increased with time in the shear line region,

indicating the thermal wind relation was in operation.

Reed and Sanders (1953) describe vertical shear terms in their dynamic analysis of a synoptic situation. These terms act to transform vorticity about a horizontal axis to vorticity about a vertical axis. Thus they illustrate a horizontal gradient of vertical velocity (i.e. sinking motion) that gives rise to a changing (intensified) horizontal temperature gradient leading to a marked change (increase) in vorticity, as in our model.

Austin (1954) notes that upper trough development, such as described by Reed and Sanders (1953), is accompanied by the creation of an upper-level zone (400 - 600 mb) of strong temperature contrast just upstream from the developing trough or shear line. The thermal gradient decreases markedly toward the earth's surface.

Petterssen (1955), concerned only indirectly with upper troposphere development, considers both dynamic and thermal aspects in his analysis of cyclogenesis.

Reed (1955) notes that air particles acquired greater thermal stability in order to conserve potential vorticity during development of an upper-level region of frontogenesis. Reed clearly calls for the simultaneous operation of vorticity conservation and the thermal wind relation.

In starting from purely thermodynamic considerations, on the other hand, McIntyre (1953) takes up the problem of converting potential into kinetic energy in the atmosphere originally investigated by Margules and Normand, and concludes that dynamic, as well as

thermodynamic factors must be taken into account. Because of the earth's rotation, final equilibrium will not be attained when the enthalpy is at a minimum, but rather when the newly-created kinetic energy has organized itself in such a way that the thermal wind equation is satisfied.

(2) The compaction of isentropic layers underneath and to the left of the jet stream (facing downstream) during development of upper tropospheric shear line:

Rossby (1951) has shown that in order to achieve the observed vertical concentration of momentum in oceanic and atmospheric jet streams, currents tend to approach the "critical" velocity which leads to a minimum transfer of momentum and in many cases must shrink vertically to develop a sharp velocity maximum at or below the free surface (in this case the tropopause), for the general case of a continuous fluid density distribution. Reed and Sanders (1953) demonstrate that the underlying mechanism for their case of intense frontogenesis at 500 mb involves a cross stream gradient of sinking motion with strongest subsidence at the warm edge of the frontal zone. Austin (1954) calls attention to the importance of this region in which subsiding motion initiates the frontogenesis. Reed (1955) presents an outstanding example of subsidence in such a region. Pothecary (1956) provides evidence for descending motion of air as it approaches the jet stream from the left (looking downstream) in the form of moisture records on flights in this region. The extremely dry air here indicates subsidence is occurring. Newton (1954), p. 458-459, discusses other evidence of this feature as well. His Figure 13a, when adopted for

frontogenesis conditions, illustrates this condition, as does Figure 10 of Reed (1955).

(3) The "self-perpetuating" feature brought about through interaction of vorticity-conservation and the thermal wind effect:

Petterssen (1955) considers upper tropospheric processes affecting surface cyclogenesis. He suggests that advection of vorticity over an incipient system initiates the development; at this time the thermal advection is very small. However, once initiated, the developing cyclone distorts the temperature field so that temperature advection becomes a prominent factor in the cyclogenesis, and "in Sutcliffe's terminology, the system has become self-developing." Since the upper tropospheric process we are describing is connected with surface frontogenesis or cyclogenesis (see Austin, 1954; Reed, 1955), Petterssen's observations support the self-perpetuating feature of our proposed model. The confluence mechanism of Namias and Clapp, which accounts partly for concentrating the temperature field in the middle troposphere, is necessary for frontogenesis according to Newton (1954). This is an essential feature linked with vertical as well as horizontal variations in the wind field. It acts in addition to those factors which are significant in bringing about changes in vertical shear and stability.

(4) The weather chart or cross section discontinuity is actually a finite zone where wind and temperature have very large, although finite, gradients:

Hurst (1952, 1953) describes the microstructure of winds across

a strong jet stream at 300 mb. The winds shown here present a continuous distribution when drawn in large-scale; in weather-chart scale, however, this would have been a pronounced discontinuity.

(5) Mixing occurs across the zones of high wind shear:

In the papers presented at the February 20, 1952 meeting of the Royal Meteorological Society, the topic of "Meteorology and the Operation of Jet Aircraft" was discussed. The remarks by several authors concerning the occurrence of clear air turbulence, as well as observations given relating place of occurrence to the jet stream axis, lends support to the hypothesis that clear air turbulence is the sensible manifestation of the mixing process across wind shear zones as postulated in our model. An article by Bannon (1952) illustrates that observed clear air turbulence occurs in the regions anticipated by our model's mixing region. The second of two possible mechanisms to explain clear air turbulence proposed by Scorer (1952) involves folding of stratospheric air beneath tropospheric air, producing static instability causing the turbulence. This folding process is similar to the process postulated by Reed (1955) in explaining upper level frontogenesis. Scorer continues that this "folding process" may continue for a long time so that new instability is continuously generated.

Arakawa (1953) notes the work of Bannon in clear air turbulence, who concluded that clear air turbulence is associated with wind shear in the vertical. Arakawa notes that cases of clear air turbulence also occur with wind shear in the horizontal, and sets up an equation for critical cyclonic shear to produce such turbulence. Values of critical

shear which Arakawa thus determines compare favorably with those of Bannon's diagram, where the tropopause is discontinuous near the jet stream. In almost every case of observed turbulence the isentropic shear or horizontal (wind) shear was large, occurring mostly on the low-pressure side of the jet stream where the shear is cyclonic in sense and excessive. He concludes, like Scorer, that such turbulence can occur in mixing of tropospheric and stratospheric air across "breaks" in the tropopause.

We do not concur with the view that the stratosphere is folded down into the troposphere; we maintain that the continued self-perpetuation of our model leads to vortex sheet formation which resembles the situation described by Scorer and Reed. We postulate that clear air turbulence is the mixing which occurs in the process of vorticity creation observed in the several cases described and permitted in our model.

In a brief discussion to be submitted in the near future, the effects of non-adiabatic heating on the model behavior will be illustrated and discussed. It will be shown that the model is capable of incorporating these effects while retaining its basic approach. Thus the model permits such outside influences to enter into consideration, which adds a very desirable feature to the model in its application to the actual atmospheric behavior.

Including Heating Effects in the Model

Up to this point the discussion has centered on how a cross section of atmospheric particles can change in response to basic

physical laws. The hypothesized mechanics are shown to fit results of detailed synoptic studies published previously.

Now let us consider why the changes occur; if this can be answered to satisfaction, a potentially powerful forecasting technique has been developed.

From this point on in our discussion one previous assumption is dropped. Non-adiabatic effects are now considered, so that the resulting motion is no longer adiabatic. It will be necessary, then to follow the motion of material surfaces which may initially coincide with particular isentropic surfaces; however, these material surfaces later move through the isentropic surfaces and become deformed as the result of the non-adiabatic disturbing effects. The only such effects to be considered here will be those arising from non-adiabatic heating of the atmosphere.

If we think of the atmosphere as a dynamic system, non-adiabatic heating then resembles a forcing function. It is fairly well established in the study of dynamic systems that the long-term changes are closely related to the forcing function - more than to the details of the system dynamics. For example, in mechanical vibrations the particular phase of free vibration that was in effect at the initial time is less important than the history of the forcing function in determining future vibration behavior.

In the atmosphere, the long waves in the westerlies correspond to the free vibrations of the mechanical system. The analogy suggests that the initial phase or longitudinal positioning of the particular set of

long waves enters into future long-term behavior only incidentally as is the case with initial phase of mechanical vibrations. Thus a mean atmospheric cross section in a sense filters out such incidental initial detail over an interval of time, in which many long waves have passed through the section. Heat added to the atmosphere during this time should exercise control over the changes in the cross section. In order to facilitate discussion of heating we need some new definition of layers.

The Mixed Layer

The model proposed here is a multilayered model of the atmosphere. In order to approximate known conditions in the atmosphere and various theories of local winds, it seems desirable to describe another distinct type of layer.

Mixing is the primary property of this layer and the temperature and momentum are functions of the height of the bottom and top of the layer, of the boundary conditions and of the vertical transport function of the layer. The whole layer must be considered as an entity. The upper and lower boundaries of the layer are easy to follow but the surfaces of constant potential temperature show very little organization.

Except in special cases a vertical description of the atmosphere will include both types of layer, usually more than one of each. Mixed layers are to be expected near the ground and in wind shear zones, and isentropic layers in the stratosphere.

The writer is quite aware of some of the troubles inherent in the

study of mixed layers with a stable lid (as illustrated in "The Solution of Nonlinear Meteorological Problems by the Method of Characteristics," Freeman, 1951) and in geostrophic isentropic layers, as indicated in the contents of this paper. The jumps and roll waves behind a mountain and the vortex sheets formed when a jet is squeezed are very real physical phenomena.

The boundary between stable and mixed layers can be of several types and we consider two of them here.

(1) A lower layer of height $H(x, y, t)$ with $\Theta(x, y, t)$, $C_m(x, y, t)$ forms a boundary as shown in Figure IV-12. On this kind of boundary we have:

$$\frac{du_m}{dt} = -\frac{1}{\rho}\frac{\partial p}{\partial x} + fv + K\frac{\partial}{\partial z}u_m\left|u_m^2 + v_m^2\right| - \frac{g(h_{m+1} - h_m)\frac{\partial \theta}{\partial z}}{\theta}\frac{\partial H}{\partial x}$$

$$\frac{dv_m}{dt} = -\frac{1}{\rho}\frac{\partial p}{\partial y} + fv + K\frac{\partial}{\partial z}v_m\left|u_m^2 + v_m^2\right| - \frac{g(h_{m+1} - h_m)\frac{\partial}{\partial z}}{\theta}\frac{\partial H}{\partial y}$$

(2) Several isentropic layers meet a mixed layer, or two mixed layers meet (see Figure IV-13). This type of coundary results in mutual determination of boundary conditions and the mixed layer may possibly grow at the expense of the isentropic layers and occasionally vice versa (especially near discontinuities).

In dealing with a mixed layer from h_m to h_{m+1} we consider the following:

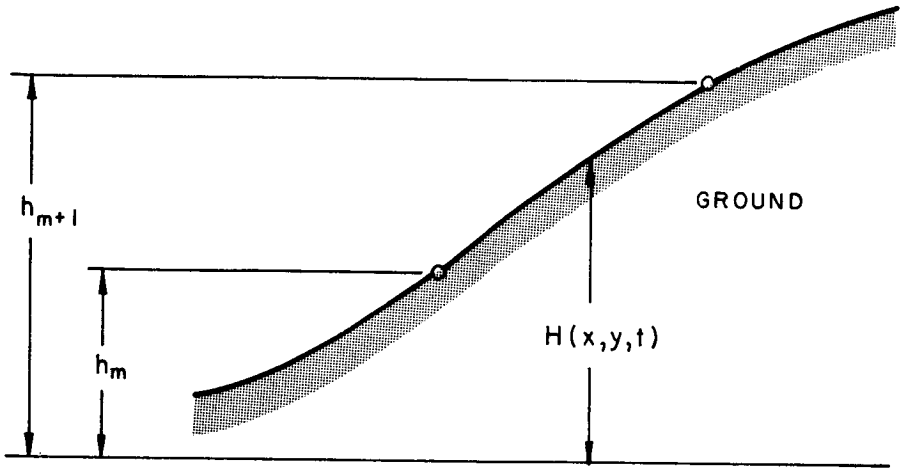

LEGEND

Isentropic layers meeting the ground.

FIGURE IV-12
LAYERS ON A SLOPING GROUND

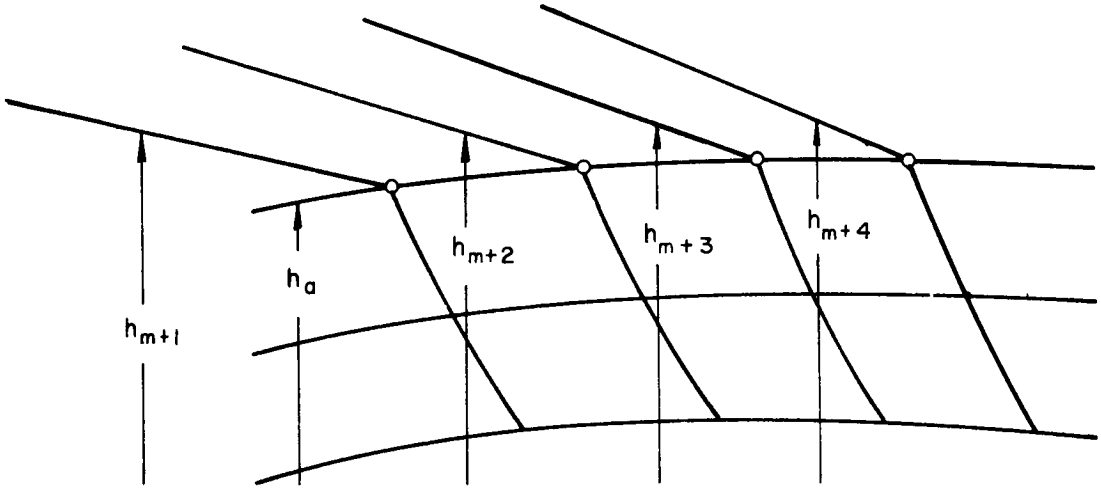

LEGEND

Different kinds of layers meeting. A mixed layer of height h_m and stable layers h_{m+1} to h_{m+4}.

FIGURE IV-13
STABLE AND ADIABATIC LAYERS

$$\theta(Z) = H\ (h_m, h_{m+1}, \theta_m, \theta_{m+1},\ \text{flux}_m\theta, \text{flux}_{m+1}\theta, u_m, u_{m+1}, v_m, v_{m+1})$$

$$u(Z) = U\ (h_m, h_{m+1}, \theta_m, \theta_{m+1}, \text{flux}_m u,\ \text{flux}_{m+1}u, u_m, u_{m+1}, v_m, v_{m+1})$$

$$v(Z) = V\ (\text{similar function})$$

Of course, this will usually be a relatively simple function like a linear or exponential θ and an Ekman spiral for u and v.

In this case we use integrated momentum and temperature equations as well as integrated continuity equations to find u_m, h_m, θ_m, etc. and to compute the needed Θ, U, V.

For example, the problems in the paper by Freeman (1951) are degenerate forms of these equations in which $h_m = 0$, $h_m = h$, $u_m = u_{m+1} = u$, $v_m = v_{m+1} = v$, and $\Theta = \theta_1 = \theta_m$.

In order to work with mixed layers and with thick stable layers it is handy to have an analytic form of the solution of the equation we have been discussing.

We rewrite the equations:

$$\frac{\partial \theta}{\partial y} = -K_1 \frac{\partial u}{\partial z} \qquad \text{(Thermal Wind)}$$

$$\frac{\partial \theta}{\partial z}\left(-\frac{\partial u}{\partial y} + f\right) = K_2 \qquad \text{(Vorticity Equation)}$$

If we differentiate the first equation with respect to y and the second with respect to x we get

$$\frac{\partial^2 \theta}{\partial y^2} = -K_1 \frac{\partial^2 u}{\partial z \partial y}$$

$$-\frac{\partial^2 u}{\partial z \partial y} = \frac{K_2 \Big/ \dfrac{\partial^2}{\partial z^2}}{\left(\dfrac{\partial \theta}{\partial z}\right)^2}$$

$$\frac{\partial^2 \theta}{\partial y^2} = \frac{K_1 K_2 \dfrac{\partial^2 \theta}{\partial z^2}}{\left(\dfrac{\partial \theta}{\partial z}\right)^2}$$

If we set

$$\theta = F(y)\,G(z) + K_3 y + K_4$$

$$\frac{\partial^2 \theta}{\partial^2} = F''G, \quad \frac{\partial \theta}{\partial} = FG', \quad \frac{\partial^2 \theta}{\partial^2} = FG''$$

and our equation becomes

$$F''G = K_1 K_2 \frac{FG''}{(FG')^2}$$

$$F''F = \frac{K_1 K_2 G''}{GG'^2} = K_5$$

We have now succeeded in separating the variables in this equation and we can say

$$F''(y)\,F(y) = K_5$$

Or, if we multiply by F'

$$F''F' = \frac{K_5 F}{F}$$

$$\frac{F'^2}{2} = K_5 \log F + \frac{K_6}{2}$$

$$F' = \sqrt{2K_5 \log F + K_6}$$

We make a simple substitution

$$\log F = \bar{H}$$

$$\frac{F'}{F} = \bar{H}'$$

$$H' C^{H} = \sqrt{2K_5 \bar{H} + K_6}$$

Now we set $w = \sqrt{2K_6 \bar{H} + K_6}$ and find

$$\bar{H} = \frac{w^2 - K_6}{2K_5}$$

$$\bar{H}' = \frac{2ww' - K_6}{2K_6}$$

$$\frac{2ww'}{2K_5} C \frac{w^2 - K_6}{2K_5} = w$$

The solution of this equation is the probability integral.

$$\int_{w_0}^{w} C \frac{w^2 - K_6}{2K_5} = K_5 (y - y_0)$$

Returning to the equation in z we find

$$\frac{K_1 K_2 G''}{G'} = K_5 G G'$$

Or integrating we get

$$K_1 K_2 \log G' = \frac{K_5}{2} G^2 \log K_6$$

Simple transformation gives

$$\frac{G' K_1 K_2}{K_6} = C \frac{K_5}{2} G^2 \quad \text{and} \quad G' = K \frac{1}{K_1 K_2} C \frac{K_5}{2 K_1 K_2} G^2$$

The solution to the equation is then:

$$\int_{G_o}^{G} C \frac{K_5}{2 K_1 K_2} \eta^2 \, d\eta = z - z_o$$

Thus we have closed form equations giving the values of z and y for certain values of θ from these equations.

REFERENCES

Arakawa, H., 1953: Clear air turbulence near the jet stream. Quart. J. R. Meteor. Soc., 79, 162-163.

Austin, J. M., 1954: The forecasting significance of the Reed-Sanders article. J. Meteor., 11, 253-254.

Bannon, J. K., 1952: Weather systems associated with some occasions of severe turbulence at high altitude. Meteor. Magazine, London, 81, 97-101. (His Figure 3 appears in Quart. J. R. Meteor. Soc., 78, 441.)

Bjerknes, J., 1951: Extratropical cyclones. Compendium of Meteorology, Boston, American Meteorological Society, 577-598.

Freeman, Jr., J. C., 1951: The solution of nonlinear meteorological problems by the method of characteristics. Compendium of Meteorology, Boston, American Meteorological Society, 421-433.

Freeman, Jr., J. C., L. Baer, and G. H. Jung, 1957: The bathystrophic storm tide. J. Marine Res., 16, 12-22.

Hsieh, U., 1950: On the formation of shear lines in the upper atmosphere. J. Meteor., 7, 382-387.

Hurst, G. W., 1952: The profile of a jet stream observed 18 January 1952. Quart. J. R. Meteor. Soc., 78, 613-615.

Hurst, G. W., 1953: The profile of a jet stream observed 1 September 1952. Quart. J. R. Meteor. Soc., 79, 407-411.

McIntyre, D. P., 1955: On the baroclinic structure of the westerlies. J. Meteor., 12, 201-210.

Murray, R., and S. M. Daniels, 1953: Transverse flow at entrance and exit to jet streams. Quart. J. R. Meteor. Soc., 79, 236-241.

Newton, C. W., 1954: Frontogenesis and frontolysis as a three-dimensional process. J. Meteor., 11, 449-461.

Newton, C. W., 1955: An investigation of cyclone development. Storm No. 5. University of Chicago Technical Report 5, Contract AF 19(604)-1293, 45 pp.

Newton, C. W., N. A. Phillips, J. E. Carson and D. L. Bradbury, 1951: Structure of shear lines near the tropopause in summer. Tellus, 3, 154-171.

Newton, C. W., and J. E. Carson, 1953: Structure of wind field and variations of vorticity in a summer situation. Tellus, 5, 321-339.

Petterssen, S., 1955: A general survey of factors influencing development at sea level. J. Meteor., 12, 36-42.

Pothecary, I. J. W., 1956: Comments on "A study of characteristic type of upper-level frontogenesis." J. Meteor., 13, 316-317.

Reed, R. J., 1955: A study of a characteristic type of upper-level frontogenesis. J. Meteor., 12, 226-237.

Reed, R. J., and F. Sanders, 1953: An investigation of the development of a mid-tropospheric frontal zone and its associated vorticity field. J. Meteor., 10, 338-349.

Roberts, G. S., et al, 1952: Meteorology and the operation of jet aircraft. Quart. J. R. Meteor. Soc., 78, 427-456.

Rossby, C.G., 1951: On the vertical and horizontal concentration of momentum in air and ocean currents. 1. Introductory comments and basic principles with particular reference to the vertical concentration of momentum in ocean currents. Tellus, 3, 15-27.

Sawyer, J. S., and F. H. Bushby, 1953: A baroclinic model atmosphere suitable for numerical integration. J. Meteor., 10, 54-59.

Scorer, R. S., 1952: Comments on two possible explanations of clear-air turbulence. Quart. J. R. Meteor. Soc., 78, 449-450.

University of Chicago, Staff Members, Department of Meteorology, 1947: On the general circulation of the atmosphere in middle latitudes. Bull. Amer. Meteor. Soc., 28, 255-280.

LIST OF SYMBOLS

D	vertical distance between material surfaces
D_o	original vertical distance between potential temperature surfaces
f	vorticity due to the earth's motion
F	function of y
g	acceleration of gravity
G	function of altitude
H	vertical distance between isotachs
$\bar{H}^1$	function of F
$H(x, y, t)$	height of a mixed layer
K	"constant" in a condensed thermal wind equation
K_i	constants of integration in the solution of an equation
L	horizontal distance between isentropes
p	pressure
t	time
T	absolute temperature
u	zonal velocity
u_n	zonal velocity
Δu	constant increment between isotachs
U	integrated zonal velocity
v	north-south velocity
V	integrated north-south velocity
w	function of H

W	horizontal distance between isotachs
x	east-west distance
y	north-south distance
z	height
ζ	relative vertical vorticity component
ζ_p	relative vorticity on a constant pressure surface
η	variable of integration
θ	potential temperature
θ_1	potential temperature
$\Delta\theta$	constant increment between isentropes
$\textcircled{H}(x,y,t)$	value of potential temperature for a mixed layer
ρ	density

APPENDIX V

SELECTION OF KEY DAYS

by

Leon F. Graves

SELECTION OF KEY DAYS

An analysis by Shapiro (1956) of 3-day mean values of sea level pressure distribution over North America shows a pronounced decrease in a persistence correlation two weeks after large increases in geomagnetic activity. Shapiro used adjacent non-overlapping 3-day means and identified the time periods by giving the first day of the earlier 3-day mean. He picked as zero days those days when the value of C_i had increased by 1.0 or more from its value on the preceding day.

Shapiro (1956) also found the largest persistence correlation values from day zero through day 8 were very close to the corresponding values for North America.

Shapiro (1959) used standardized coefficients of Tschebycheff polynomials to represent the pressure patterns. He reports that the Z_7 coefficient represents the average North-South pressure gradient throughout the region and is therefore a type of zonal index. Over the North American region Z_7 reached a maximum about 5 days and in the European region about 7 days after the key day.

The North American data show a low value of Z_7 at day 13, but the European data indicate that the value decreased until day 19, the last day for which data was given.

Shapiro (1958) points out that surface pressure persistence correlations have maximum in winter and summer and minimum in spring and fall. The pressure distribution over Europe is considerably more

persistent than that over North America. The persistence correlation value is high when the speed and development of pressure system is small and the scale is larger.

Shapiro (1954) using 5-day running sums had previously found a tendency for a decrease in persistence at the 500 mb level about 10 days after a rapid rise in K_p.

As reported by Woodbridge, Macdonald and Pohrte (1958) and Macdonald and Woodbridge (1959), a comparison of winter troughs in the Alaska-Aleutian area, showed that those that first appeared three to four days after a geomagnetic disturbance were more likely to become larger deep troughs.

In selecting criteria to identify moderate to high solar activity, Willett (1961) found radio flux, A_p solar flares and auroral activity to be the four observables of primary importance.

Prohaska (1954) confirms that the geomagnetic indexes A_p, K_p, and C_i are highly related and may be used interchangeably for meteorological studies.

According to Bartels (1962) the daily planetary character figure C_p is quite similar to the old C_i. We, therefore, examined daily increases in C_p as this seemed to be an acceptable procedure for selecting key days of increased geomagnetic activity. During the period July 15 - September 30, 1961 there were thirteen daily increases of 0.5 or more in C_p. Increases of 0.7 or more occurred seven times and were therefore selected for further study (Table I).

Utilizing these dates and the reported relationships, we can

TABLE I

Zero-day	C_p	ΔC_p	3-9 Days (high)		14-19 Days (low)	
July 27	1.9	0.8	July 30	Aug. 5	Aug. 10	Aug. 15
Aug. 2	1.5	1.1	Aug. 5	Aug. 11	Aug. 16	Aug. 21
Aug. 8	0.9	0.8	Aug. 11	Aug. 17	Aug. 22	Aug. 27
Aug. 29	0.9	0.7	Sept. 1	Sept. 7	Sept. 12	Sept. 17
Sept. 14	1.2	0.8	Sept. 17	Sept. 23	Sept. 28	Oct. 3
Sept. 24	1.5	1.5	Sept. 27	Oct. 3	Oct. 8	Oct. 13
Sept. 30	1.4	1.1	Oct. 3	Oct. 9	Oct. 14	Oct. 19

draw a few conclusions about what should have happened in August and September, 1961, if Shapiro and Ward's results apply. The periods indicated by the dates in the 3-9 day column should be days of low speed, large scale systems.

The Z_7 "zonal index" should have a high value, relatively, and therefore the westerlies should be somewhat stronger at this time.

The 14-19 day column should represent days of higher speed, smaller scale pressure systems. These conditions are somewhat inconsistent in themselves, and we see by an examination of Table I that the two columns overlap in time because the zero days are not usually at least three weeks apart. The only zero-day which gives a clear cut non-overlapping period for study is August 29. We should therefore expect the period September 1-7 to be one of slow moving large scale pressure systems. We should also expect September 12-17 to exhibit low persistence characteristics, namely, faster moving smaller pressure systems. The "Z_7 zonal index" should be high September 1-7 and low September 12-17.

If a trough appeared in the Alaska-Aleutian region about September 2 or 3, this trough might be expected to develop into a strong trough.

With lesser confidence, one might also consider the periods August 16-24 and August 22-27 to illustrate periods of low persistence. Likewise, the period September 17-23 could be considered a period of high persistence following the low persistence period September 12-17.

It must be noted here that we have arbitrarily selected a daily

increase of 0.7 or more in C_p to obtain these days.

It is indeed fortunate that in our arbitrary method of selecting what seemed to be a reasonable "break" in the ΔC_p distribution, we arrived at a single key day. There were no changes of 0.6 in daily C_p and dropping the limit to 0.5 would have added six dates to the 2-1/2 month C_p period under consideration.

REFERENCES

Macdonald, N. J. and D. D. Woodbridge, 1959: Relation of geomagnetic disturbances to circulation changes at 30,000-foot level. Science, 129, 638-639

Shapiro, Ralph, 1954: A possible solar-weather effect. J. Meteor., 11, 424-425.

Shapiro, Ralph, 1956: Further evidence of a solar-weather effect. J. Meteor., 13, 335-340.

Shapiro, Ralph, 1958: Some observations of the persistence of the surface pressure distribution. J. Meteor., 15, 435-439.

Shapiro, Ralph, 1959: A comparison of the response of the North American and European surface pressure distributions to large geomagnetic disturbances. J. Meteor., 16, 569-572.

Willett, H. C., 1961: Research directed toward study of atmospheric reactions to changing conditions of solar activity. Final Report, Contract No. AF 19(604)-3056.

Woodbridge, D. D., N. J. Macdonald and T. W. Pohrte, 1958: A possible relationship of geomagnetic disturbances to 300 mb trough development. J. Meteor., 15, 247-248.

LIST OF SYMBOLS

A_p	planetary magnetic A index
C_i	international magnetic character index similar to C_p
C_p	planetary magnetic character index
ΔC_p	change in C_p per day
K_p	planetary magnetic K index
Z_7	coefficient of a polynomial representation of the pressure field that gives a measure of the zonal wind

APPENDIX VI

INDICES OF SOLAR ACTIVITY

by

Leon F. Graves

INDICES OF SOLAR ACTIVITY

"Indices of Solar Activity" by Athay and Warwick (1961) is an excellent review of the various indices of solar and geomagnetic activity. The article also presents an explanatory tabulation of indices of solar radiation, an extensive list of sources of data on solar and geomagnetic indices, and gives 141 references to other papers and publications.

We quote from page 65:

"The amplitude of actual variation of the earth's field, dependent as it is on latitude and local time, is not a convenient index for statistical studies. Several indices have been devised that combine data from various stations to give a world-wide description of magnetic conditions.

The international character figure C_i is a mean of character figures from different stations. These are based on the daily range (the difference between the highest and lowest values of a given magnetic component during a Greenwich day) and on the general character of the variability during the day. Being somewhat subjective, this estimate may change systematically over the sunspot cycle. An attempt to attain greater long-term uniformity is represented by the K index, which measures the range of variation over each 3-hour period. The K values for each station are scaled according to the usual values at that station and their average represented by K_p,

the planetary index. The indices a_p (3-hour) are related to K_p in an approximately exponential way, and the daily index A_p is the sum of the eight a_p values. The A_p changes more drastically for large disturbances than does K_p."

"Magnetism of the Earth" by Nelson, Hurwitz and Knapp (1962) summarizes existing knowledge of the earth's magnetic field and its variation in time and space. Sixty-six references provide excellent leads to relevant sources of information.

We quote from page 27:

"Quiet-day daily variation is normal and should not be classed as disturbance. However, from time to time the records show disturbance in great variety, from moderate fluctuations to those which can be completely recorded only by insensitive instruments. Any marked degree of natural disturbance is classed as a magnetic storm.

Though the name comes from analogy with the meteorological storm, the magnetic storm is not perceptible to the senses and has no established correlation with the weather. Obviously no direct association is possible between magnetic storms, which are widespread phenomena, and detailed weather conditions, which depend so much on local effects."

J. W. Freeman (1963) used Akasofu's values of D_{st} for San Juan and Honolulu. Akasofu and Chapmen (1960) define D_{st} as one part of the average variation in field during a magnetic storm. "The additional D-field, present during a storm, is a function of storm time and of position. In each element, at each instant of time, D_{st}

denotes the mean value of the storm field round a parallel of geomagnetic latitudes; thus D_{st} is a function of time and geomagnetic latitude. It represents the part of the field that is symmetrical around the geomagnetic axis."

The magnetic equator is an imaginary line passing through the points of the earth's surface at which the field is horizontal. A magnetic pole of the earth is a point at which the field is vertical.

REFERENCES

Akasofu, S. I. and S. Chapman, 1960: The sudden commencement of geomagnetic storms. Vrania, 250, 1-35.

Athay, R. G. and Constance S. Warwick, 1961: Indices of solar activity. Advances in Geophysics, Vol. 8, New York, Academic Press, p. 1-83.

Freeman, J. W., 1963: The morphology of the electron distribution in the outer radiation zone and near the magnetospheric boundary as observed by Explorer XII. Doctorate dissertation, State University, Iowa City, Iowa.

Nelson, J. H.,L. Hurwitz, and D. G. Knapp, 1962: Magnetism of the earth. Publication 40-1, U. S. Dept. of Commerce, Coast and Geodetic Survey, Washington, D. C., 79 pp.

LIST OF SYMBOLS

A_p	planetary magnetic A index
C_i	international magnetic character index similar to C_p
D_{ST}	special magnetic index that measures the intensity of a chosen magnetic storm
K_p	planetary magnetic K index

APPENDIX VII

A MODEL OF EQUATORIAL FLOW

by

John C. Freeman, Jr.

A MODEL OF EQUATORIAL FLOW

The motion of bands of fluid with constant vorticity has always lagged behind wave motions in a constant flow as a method of study of fluid flow. The present application of this technique to the flow in the tropics is in the same tradition.

We consider a band of fluid that reaches from the horse latitudes to the equator and all with the same absolute vorticity, namely, that of the earth at some "latitude" y_o with coriolis parameter f_o and with no flow across y_o .

The east wind is 0 at y = a and $-\frac{\partial u}{\partial y} + f_o + \beta(y-y_o) = f_o$ expressed the conservation of vorticity. We integrate and find

$$u(a) - u(y) = +\int_y^a \beta(y-y_o) = +\frac{\beta(a-y_o)^2}{2} - \frac{\beta(y-y_o)^2}{2}$$

We are assuming $u(a) = 0$ so we have

$$u(y) = -\frac{\beta(a-y_o)^2}{2} + \frac{\beta(y-y_o)^2}{2}$$

The continuity equation for this motion is

$$\frac{\partial a}{\partial t} = -\frac{\partial}{\partial x}\int_{y_o}^a u\,dy = -u(a)\frac{\partial u}{\partial x} - \int_{y_o}^a \frac{\partial u}{\partial x}$$

$$= +\int_{y_o}^a \beta(a-y_o)\frac{\partial a}{\partial x}\,dy$$

$$= +\beta(a-y_o)(a-y_o)\frac{\partial a}{\partial x}$$

This can be written as

$$\frac{\partial a}{\partial t} - \beta(a-y_0)\frac{2\partial a}{\partial x} = 0 \qquad \text{(VII-1)}$$

Eq. (VII-1) tells us that the boundary of the easterlies, a, keeps a constant value along a line that moves from the east at a speed $(a - y_o)^2$. If y_o is about 15^o latitude and $a = 25^o$ latitude, which would be a case of extensive easterlies, we use the approximation $\beta = \frac{1/6 \text{ per day}}{\text{per degree of latitude}}$. This speed is about 16^o per day or 40 miles per hour from the east. If we keep $y_o = 15^o$ and further investigate more restricted easterlies, we find that if $a = 20^o$ then $\beta (a - y_o)^2 = 4\text{-}1/4^o$ latitude per day which is a very common speed for "normal" waves in the easterlies.

These waves can be "modified" by taking the curvature of the boundary into account and a steady state wave can be found. We will not do that in this paper but will investigate the more interesting problem of the jump or block in the easterly flow.

Eq. (VII-1) gives the result that a far north extension of the easterlies moves westward faster than weak easterlies that do not extend far northward. This is illustrated in Figure VII-1.

In a situation as illustrated in Figure VII-1 the ultimate flow must contain a jump or a block in the easterlies very similar to a breaker on a beach. (The "breaker" occurs in the horizontal rather than the vertical frame of reference.)

The block results when the fast easterlies catch up with the slow

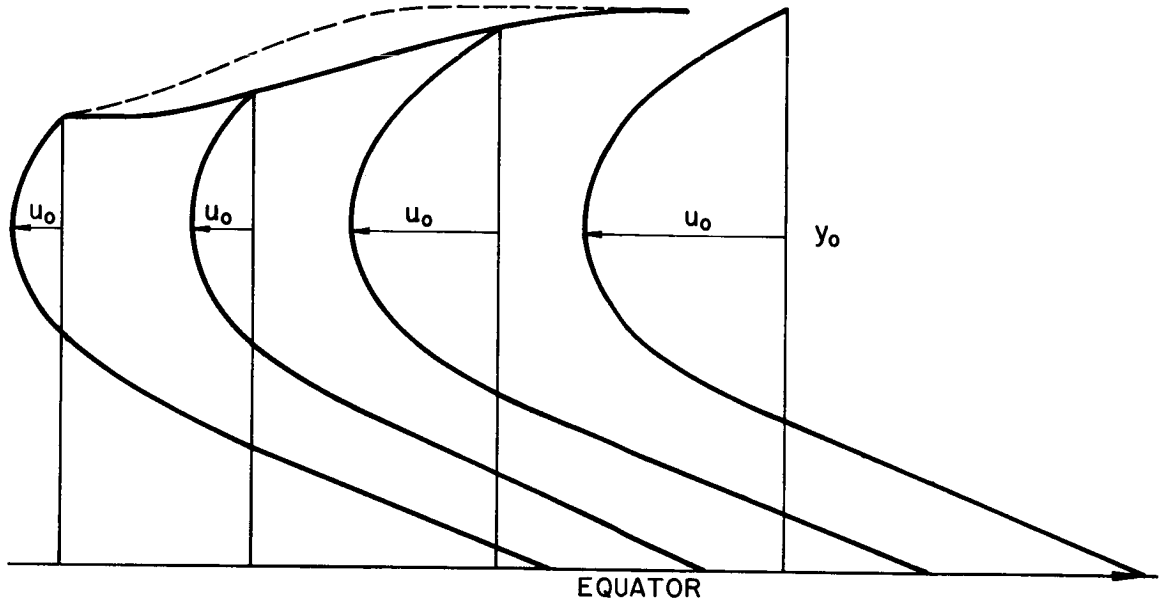

LEGEND

The strong easterlies with large values of a move from east to west faster than the weak easterlies. (Weak easterlies lead to westerlies near the equator).

FIGURE VII-1

TROPICAL VORTICITY BANDS

easterlies and try to pass them. The result is an abrupt change in the wind speed and the northward extension of the easterlies.

The idealized block is shown in Figure VII-2.

We can compute the speed of such a block if we assume that it is moving at a constant speed and that we have continuity of mass. We assume the block moves at a constant speed V and we find that

$$\int_{y_0}^{a_1} (u - V)\, dy = \int_{y_0}^{a_2} (u - V)\, dy$$

Substitution for u gives

$$\int_{y_0}^{a_1} \left[-\beta \frac{(a_1 - y_0)^2}{2} + \beta \frac{(y - y_0)^2}{2} - V \right] dy = \int_{y_0}^{a_2} \left[-\beta \frac{(a_2 - y_0)^2}{2} + \beta \frac{(y - y_0)^2}{2} - V \right] dy$$

$$-\beta \frac{(a_1 - y_0)^3}{2} + \beta \frac{(a_1 - y_0)^3}{6} - V(a_1 - y_0) = -\beta \frac{(a_2 - y_0)}{2} \beta \frac{(a_2 - y_0)}{6} - V(a_2 - y_0)$$

$$-\frac{\beta (a_1 - y_0)^3}{3} - V (a_1 - y_0) = -\frac{\beta (a_2 - y_0)^3}{3} - V (a_2 - y_0) \qquad \text{(VII-2)}$$

$$V (a_2 - a_1) = \frac{-\beta}{3} \left[(a_2 - y_0)^3 - (a_1 - y_0)^3 \right]$$

$$V = \frac{-\beta}{3} \left[(a_2 - y_0)^2 + (a_2 - y_0)(a_1 - y_0) + (a_1 - y_0)^2 \right]$$

Eq. (VII-2) gives the speed of a block.

An interesting value of V is provided by assuming that easterlies are moving into westerlies; namely, that $a_1 = y_0$. In that case the east wind of maximum value $u = -\frac{\beta (a_2 - y_0)^2}{2}$ would

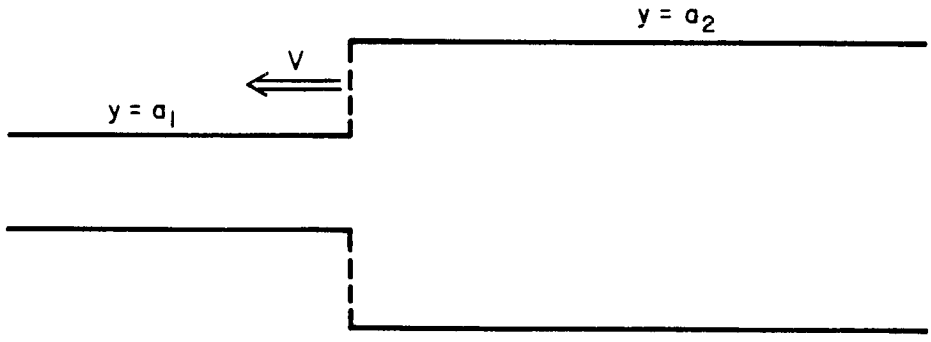

LEGEND

The idealized block in the easterlies. The block moves with speed V .

FIGURE VII-2

OUTLINE OF A BLOCK

move into the westerlies as speed $V = -\frac{\beta(a_2 - y_o)^2}{2}$. Or if $a_2 = 25^o$ and $y_o = 15^o$ we would have lost winds of 20 miles per hour moving westward at 13 miles per hour.

Of course, this wave cannot have a complete discontinuity in the wind as illustrated in Figure VII-2. We should investigate a possible transition in the wind systems that will take us from a_1 to a_2 over a small area and maintaining constant vorticity. For one thing it is obvious that $v \approx 0$ and $\frac{\partial v}{\partial x} = 0$ must be dropped as approximations in this area. We do have that

$$\frac{\partial u}{\partial t} + V\frac{\partial u}{\partial x} = 0, \qquad \frac{\partial a}{\partial t} + V\frac{\partial a}{\partial x} = 0, \qquad \frac{\partial v}{\partial t} + V\frac{\partial v}{\partial x} = 0,$$

We know from incompressibility of the barotropic fluid that $\frac{\partial u}{\partial x} + \frac{\partial v}{\partial y} = 0$. We know from the vorticity equation that in the block

$$\frac{\partial z}{\partial x} = z\sqrt{\frac{1}{z^2} - \frac{1}{z_1^2} + \frac{1}{z_1^2}\left(\frac{\partial z}{\partial x}\right)_1 + \frac{2\beta}{V}\log\frac{z}{z_1}}$$

must be true where $z = a - y_o$.* If we assume that every block has the shape such that the strong easterly flow performs a gradual transition then we have

$$\frac{\partial z}{\partial x} = z\sqrt{\frac{1}{z^2} - \frac{1}{z_2^2} + \frac{2\beta}{V}\log\frac{z}{z_2}}$$

---

* This derivation and that of the pressure distribution are found on pages VII-11, VII-12, VII-13 and VII-14 of this appendix.

Suppose $Z = K(x)\, Z_2$

$$z_2 \frac{\partial K}{\partial X} = K z_2 \sqrt{\frac{1}{K - z_2^2} - \frac{1}{z_2^2} + \frac{2\beta z_2^2}{V} \log K}$$

$$\frac{\partial K}{\partial x} = \frac{K}{z_2} \sqrt{\frac{1}{K^2} - 1 + \frac{2\beta z_2^2}{V} \log K}$$

$$0 \leq K \leq 1$$

β = 1/6 per day per degree of latitude.

We set $Z = K Z_2$, $\frac{Z_1}{Z_2} \leq K \leq 1$

and note $V = -\frac{\beta}{3} (Z_1^2 + Z_1 Z_2 + Z_2^2)$

$$\frac{\partial K}{\partial x} = \frac{G(K, \alpha)}{z_2}$$

Integrate from $K = \frac{Z_1}{Z_2}$ to $K = 1$. To find x for various K and the shape of the block:

$$G(K, \alpha) = K \sqrt{\frac{1}{K^2} - 1 + \alpha \log K} = \sqrt{1 - K^2 + \alpha K^2 \log K}$$

where

$$\alpha = \frac{2\beta z_2^2}{V}$$

We include a table of $G(K, \alpha)$ for estimating shapes of jumps which can be found on the following page.

If we take K_o where $Z_1 = K_o Z_2 = 0.49\, Z_2$ and $Z_2 = 10^o$ we

get $\alpha = 80$. Under these conditions, using $\beta = 1/6$,

$$V = \frac{100}{18}\ (K_o^2 + K_o + 1) = 0.24 + 0.49 + 1 = \frac{163}{18}\ 100$$

$$V = 9.05^\circ \text{ per day.}$$

Using the $y_o = 15^\circ$, the steady state block would go from 19.9° N to 25°N and would be moving from east to west at 9.05° per day. The slope $G(K, \alpha)$ would be about 1° latitude per degree longitude so the block would take effect in about 5 degrees.

The north-south speed v is given by $v = - Z \frac{\partial u_0}{\partial x}$. The nature of a steady state block is such that

$$\frac{\partial u_0}{\partial x} = \frac{V}{z} \frac{\partial z}{\partial} = \frac{V}{Kz_2} \frac{\partial z}{\partial x}$$

Thus, we can write

$$v = - z \frac{V}{Kz_2} \frac{\partial z}{\partial x} = \frac{zV}{z_2} \frac{G(K, \alpha)}{K}$$

In our case $\frac{V}{Z_2} = \frac{9.05}{10} = .905$ and we have the following table:

K	.50	.60	.80	.90
$\frac{G(K,\alpha)}{K}$	2.32	1.90	1.18	.80
$G(K,\alpha)$	1.16	1.15	.94	.70

Thus, for each value of K we can plot $\frac{\partial u_0}{\partial x}$ and v(y). See Figure VII-3. Since we know all winds and acceleration it is possible to draw the isobars for this disturbance. They are shown in Figure VII-4.

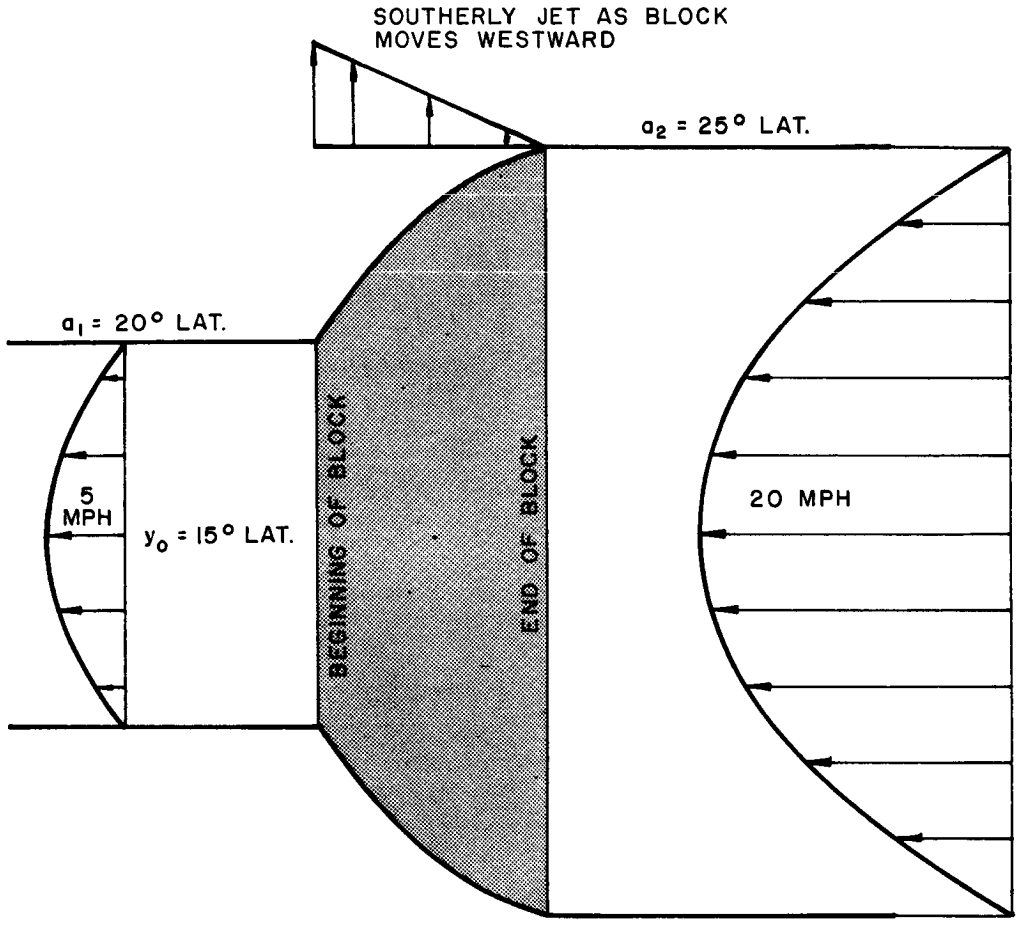

LEGEND

The wind distribution and the shape of a steady state block.

FIGURE VII-3

WINDS IN A BLOCK

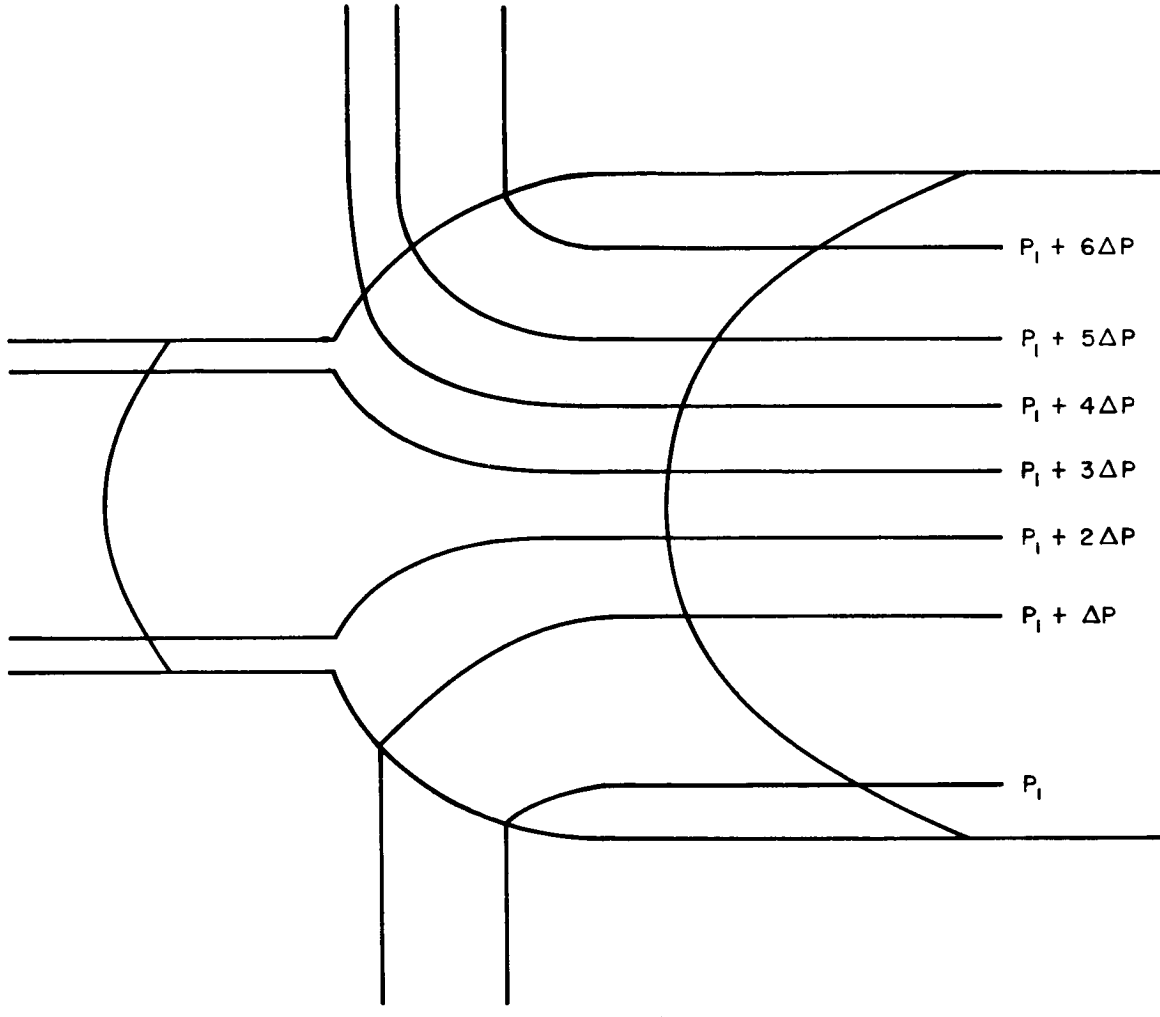

LEGEND

The height contours or isobars for Figure 3. The isobars are for 20 miles per hour at 15^{o} latitude.

FIGURE VII-4

ISOBARS IN A BLOCK

DERIVATIONS

The following notations illustrate the derivation of

$$\frac{\partial z}{\partial x} = z\sqrt{\frac{1}{z^2} - \frac{1}{z_1^2} + \frac{1}{z^2}\left(\frac{\partial z}{\partial x}\right) + \frac{2\beta}{V}\log\frac{z}{z_1}} \quad \text{where } z = a - y_o.$$

For all y in the block zone we have

$$u(y) = -\frac{\left(\beta + \frac{\partial^2 u_o}{\partial x^2}\right)}{2}\left[(a - y_o)^2 - (y - y_o)^2\right]$$

$$\frac{\partial u_o}{\partial x} = \frac{V}{a - y_o}\frac{\partial a}{\partial x} \text{ in the block.}$$

Thus,

$$\frac{\partial^2 u_o}{\partial x^2} = \frac{-V}{(a-y_o)^2}\left(\frac{\partial u}{\partial x}\right)^2 + \frac{V}{a - y_o}\frac{\partial^2 a}{\partial x^2}$$

This gives us

$$u_o = \frac{-\beta + \frac{\partial^2 u_o}{\partial x^2}}{2}(a - y_o)^2$$

or if we can ignore third derivatives

$$\frac{\partial u_o}{\partial x} = -\beta + \frac{\partial^2 u_o}{\partial x^2}\frac{\partial a}{\partial x}(a - y_o)$$

$$\frac{V}{a - y_o}\frac{\partial a}{\partial x} = -\left(\beta + \frac{\partial^2 u_o}{\partial x^2}\right)(a - y_o)\frac{\partial a}{\partial x}$$

$$\frac{V}{a-y_o}\frac{\partial a}{\partial x} = -\left(\beta - \frac{V}{(a-y_o)^2}\left(\frac{\partial a}{\partial x}\right)^2 + \frac{V}{a-y_o}\frac{\partial^2 a}{\partial x^2}\right)(a-y_o)\frac{\partial a}{\partial x}$$

$$\frac{V}{(a-y_o)^2} = -\left(\beta - \frac{V}{(a-y_o)^2}\left(\frac{\partial a}{\partial x}\right)^2 + \frac{V}{a-y_o}\frac{\partial^2 a}{\partial x^2}\right.$$

$$\frac{V}{(a-y_o)^2} + \beta = \frac{\partial}{\partial x}\frac{V\frac{\partial a}{\partial x}}{(a-y_o)}$$

$$\frac{V^2\frac{\partial a}{\partial x}}{(a-y_o)^3} + \beta\frac{V\frac{\partial a}{\partial x}}{a-y_o} = \frac{V\frac{\partial a}{\partial x}}{a-y_o}\frac{\partial}{\partial x}\frac{V\frac{\partial a}{\partial x}}{(a-y_o)}$$

$$\frac{V^2}{2(a-y_o)^2} - \frac{V^2}{2(a_1-y_o)^2} + \beta V \log\frac{(a-y_o)}{(a_1-y_o)} = \frac{1}{2}\left(\frac{V\frac{\partial a}{\partial x}}{a-y_o}\right)^2 - \frac{1}{2}\left(\frac{V\left(\frac{\partial a}{\partial x}\right)_1}{a_1-y_o}\right)^2$$

Setting $Z = a - y_o$, $Z_1 = a_1 - y_o$ we get

$$\frac{1}{z^2} - \frac{1}{z_1^2} + \frac{2\beta}{V}\log\frac{z}{z_1} = \frac{\left(\frac{\partial z}{\partial x}\right)^2}{z^2} - \frac{\left(\frac{\partial z}{\partial x}\right)^2}{z_1^2}$$

$$\frac{\partial z^2}{\partial x} = z^2\left(\frac{\left(\frac{\partial z}{\partial x}\right)_1^2}{z_1^2} + \frac{1}{z^2} - \frac{1}{z_1^2} + \frac{2\beta}{V}\log\frac{z}{z_1}\right)$$

$$\frac{\partial z^2}{\partial x} = z\sqrt{\frac{1}{z^2} - \frac{1}{z_1^2} + \frac{1}{z^2}\left(\frac{\partial z}{\partial x}\right) + \frac{2\beta}{V}\log\frac{z}{z_1}}$$

We obtain the pressure (or height contour) distribution as follows. Note that

$$\frac{\partial u}{\partial t} = -g\frac{\partial h}{\partial x} + fv \qquad \frac{\partial v}{\partial t} = -g\frac{\partial h}{\partial y} - fu$$

$$\frac{\partial h}{\partial x} = \frac{1}{g}\left(fv - \frac{\partial u}{\partial t}\right) = \frac{1}{g}\left(fv + V\frac{\partial u}{\partial x}\right)$$

$$\frac{\partial h}{\partial y} = -\frac{1}{g}\left(fu + \frac{\partial v}{\partial t}\right) = -\frac{1}{g}\left(fu - V\frac{\partial v}{\partial x}\right)$$

$$f = f_o + \beta z$$

$$\frac{\partial h}{\partial x} = \frac{1}{g}\left(f_o v + \beta z v + V\frac{\partial u}{\partial x}\right)$$

$$\frac{\partial h}{\partial y} = -\frac{1}{g}\left(f_o u + \beta z u - V\frac{\partial v}{\partial x}\right)$$

For a given Δh we have inside the block:

$$\Delta x = \frac{g\,\Delta h}{\left(f_o + \beta z + \frac{V}{v}\frac{\partial u}{\partial x}\right)v}$$

$$\Delta y = \frac{-g\,\Delta h}{\left(f_o + \beta z - \frac{V}{u}\frac{\partial v}{\partial x}\right)u}$$

Outside the block we have

$$\Delta y = \frac{-g\,\Delta h}{\left(f_o + \beta z\right)u}$$

Setting

$$\Delta y = \frac{-g \Delta h}{f u} \quad \text{we get} \quad y = \frac{f_o}{f_o + \beta z} \Delta y_o$$

Inside the block this becomes

$$\Delta y = \frac{f_o}{f_o + \beta z - \frac{V}{u} \frac{\partial v}{\partial x}} \Delta y_o$$

$$\Delta x = \frac{f_o}{f_o + \beta z + \frac{V}{v} \frac{\partial u}{\partial x}} \Delta x_o$$

TABLE OF $G(K, \gamma)$

γ \ K	0.0	0.2	0.4	0.6	0.8	0.9	1.0
-4	1	1.103	1.194	1.173	.965	.728	0
-8	1	1.214	1.419	1.453	1.225	.933	0
-20	1	1.499	1.942	2.078	1.793	1.375	0
-40	1	1.880	2.589	2.828	2.463	1.895	0
-80	1	2.472	3.545	3.918	3.432	2.645	0

REFERENCE

Freeman, Jr., J. C., 1956: Barotropic models of the planetary jet stream. A & M College of Texas Project 57, Contract AF 19(604)-559, 1-21.

LIST OF SYMBOLS

a	boundary of the easterlies
a_1	value of a ahead of block
a_2	value of a behind block
f	coriolis parameter
f_o	coriolis parameter at a fixed latitude
g	acceleration of gravity
$G(K,\alpha)$	function of K and α related to the slope of the block boundary
Δh	contour intervals of a constant pressure surface
K	value of the ratio $\frac{z}{z_2}$
K_o	the ratio, $\frac{z_1}{z_2}$
t	time
u	zonal velocity
u_o	zonal velocity at a fixed value of
v	north-south velocity
V	velocity of a block
x	east-west distance
Δx	x-distance between height contours
Δx_o	x-distance at $x = x_o$
y	north-south distance
Δy	y-distance between height contours
y_o	fixed north-south distance
Δy_o	y-distance at $y = y_o$

z	another measure of y for special purposes
z_1	fixed value of z (ahead of block)
z_2	another fixed value of z (behind block)
α	parameter in the slope function
β	north-south change of earth's vorticity

APPENDIX VIII

THOUGHTS DEVELOPED AFTER A DISCUSSION OF SOLAR WEATHER WITH THE STAFF MEMBERS OF THE SOUTHWEST CENTER FOR ADVANCED STUDIES

by

John C. Freeman, Jr.

THOUGHTS DEVELOPED AFTER A DISCUSSION OF SOLAR WEATHER WITH THE STAFF MEMBERS OF THE SOUTHWEST CENTER FOR ADVANCED STUDIES

The sun is a magnetically active body in which the perturbations in the magnetic field are larger than the over-all field which is poorly defined and almost unknown in detail.

Parker's (1959) theory of the solar wind has been confirmed with the source being within two or three solar radii of the sun. The magnetic field lines are carried by the solar wind but variations in the solar wind, weak magnetic influence and interaction lead to the carrying of a distorted solar wind field.

Since the radial motion of the solar wind is probably greater than the tangential and since the sun was rotating when the fields were forming, there may be a spiral-like shape to the field lines (see Figure VIII-1).

When high energy solar protons leave the sun as a result of a flare they must make their way through this torturous path to the earth and other measuring stations.

A flare has an organized enough magnetic field that it causes some organization of the magnetic field over part of the solar system, especially in a solid angle streaming out from it (see Figure VIII-2).

When there is a very strong stream of flares in a short time, they set up a Dessler and Parker (1959) spiral magnetic field with no breaks in the lines. (See Figure VIII-3) This new field is set up by a

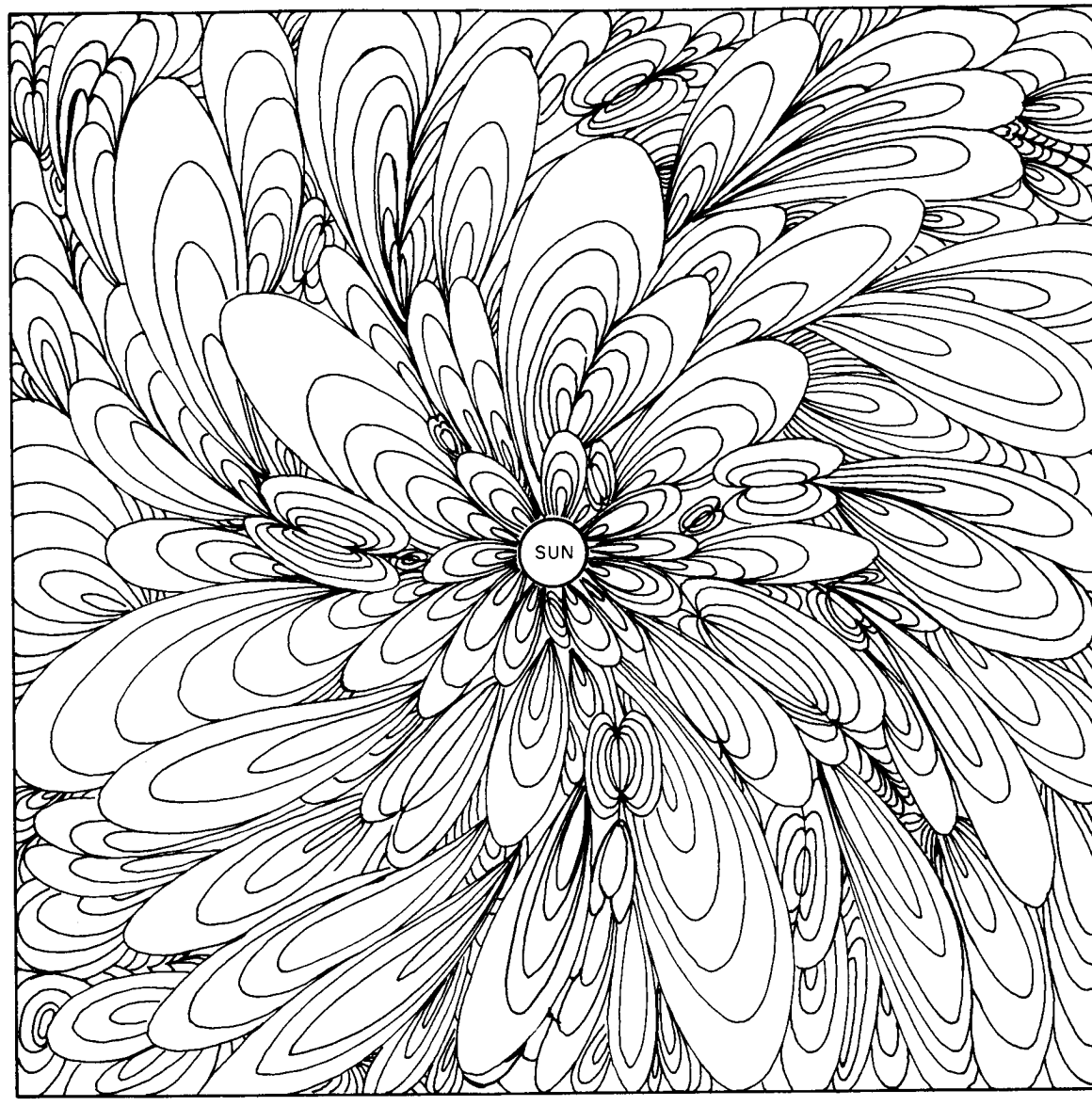

LEGEND

The spiral oriented "turbulent" magnetic field lines in the solar system.

FIGURE VIII-1

THE TURBULENT SOLAR SYSTEM

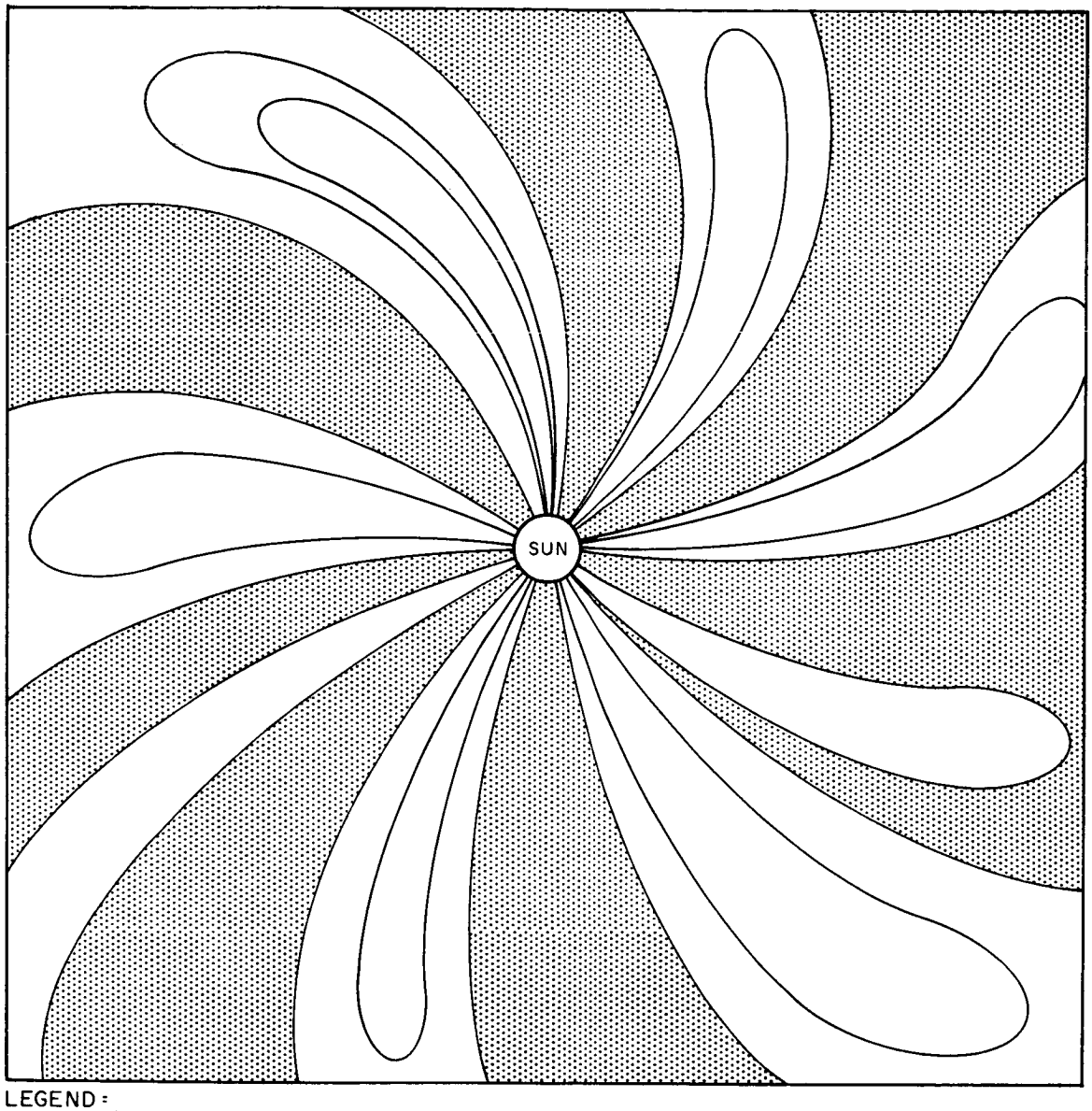

LEGEND

The pattern of the sun's magnetic field carried by a constant solar wind, after Parker and Dessler. This is proposed here as the pattern during a strong magnetic storm.

FIGURE VIII-2

THE SPIRAL MAGNETIC FIELD

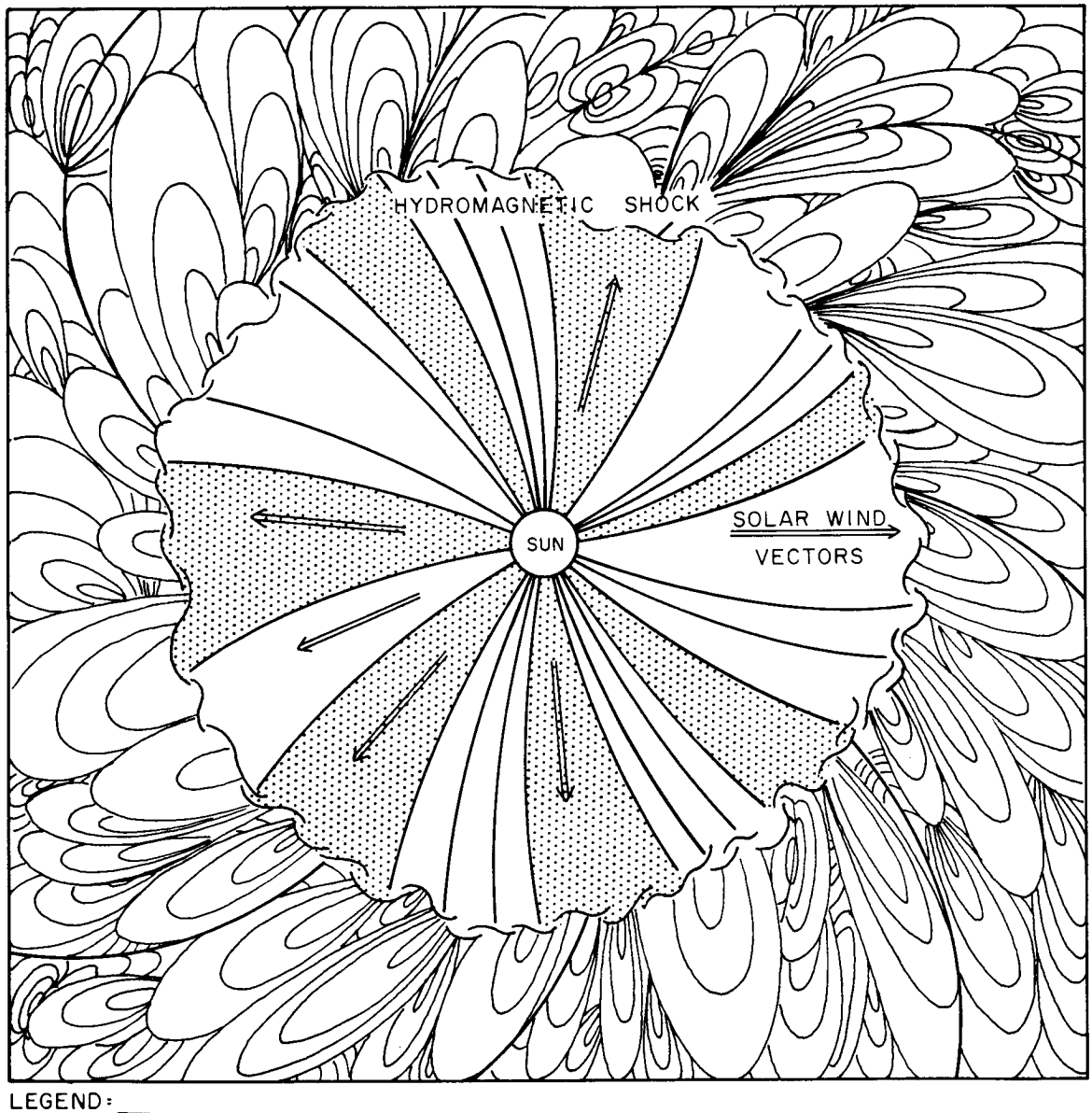

LEGEND:

DENOTES VERY WEAK MAGNETIC FIELD.

The hydromagnetic shock between the newly ordered strong magnetic field of the disturbed sun with strong solar wind and the "turbulent" old solar system magnetic field.

FIGURE VIII-3

STORM HYDROMAGNETIC SHOCK

hydromagnetic shock. Then a new storm causes a prompt arrival of high energy solar protons.

The fluid between the earth and sun is made up of confused weak dipoles moving with the "solar wind." The cell size of the dipoles would be expected to be about the size of the radii of confined plasma in solar flares or about 100 km. There is nothing expected in the plasma flow to increase the smallest scale of turbulence. It is true that the distance between particles is increasing because of divergence. There is no law that says that divergence increases the total scale of turbulence. The laws of turbulence indicate that smaller eddies are being created at all times. If the flow is stable, smaller eddies are dissipated by "viscosity."

If there is an equivalent of viscosity in this type of plasma flow it would be related to the cyclotron radius, and interactions of the type usually studied by turbulent theory. There seems to be a definite analogy as indicated by astronomers' photographs of nebulae and galaxies.

There is some heating of the atmosphere as a result of the absorption of the solar ultraviolet. In fact, this may be a principal source of heat in the region between 40 and 60 km. However, it could not be important as a source of heat in the winter time and at night. This heating would be very much like solar heating or eclipse cooling, or night cooling.

The heating that seems most effective is that, according to the theory of Dessler (1959), concerned with hydromagnetic waves that

originate in the high altitude area of the lines of magnetic force and travel down into the area near 100 km and dissipate their energy at about 100 km. This heating seems to be most effective at night and near the poles.

It was originally assumed that large numbers of solar protons entered the magnetosphere and caused disturbances. It is now "accepted" that the "cosmic rays" are excited in situ by hydromagnetic waves. (Dr. F. S. Johnson is primarily responsible for transmitting these remarks. No effort was made to distinguish between published and unpublished material or to identify original proponents.)

REFERENCES

Dessler, A. J., 1959: Ionospheric heating by hydromagnetic waves. J. Geophys. Res., 64, 397-401.

Dessler, A. J. and E. N. Parker, 1959: Hydromagnetic theory of geomagnetic storms. J. Geophys. Res., 64, 2239-2252.

Parker, E. N., 1959: Extension of the solar corona into interplanetary space. J. Geophys. Res., 64, 1675-1681.

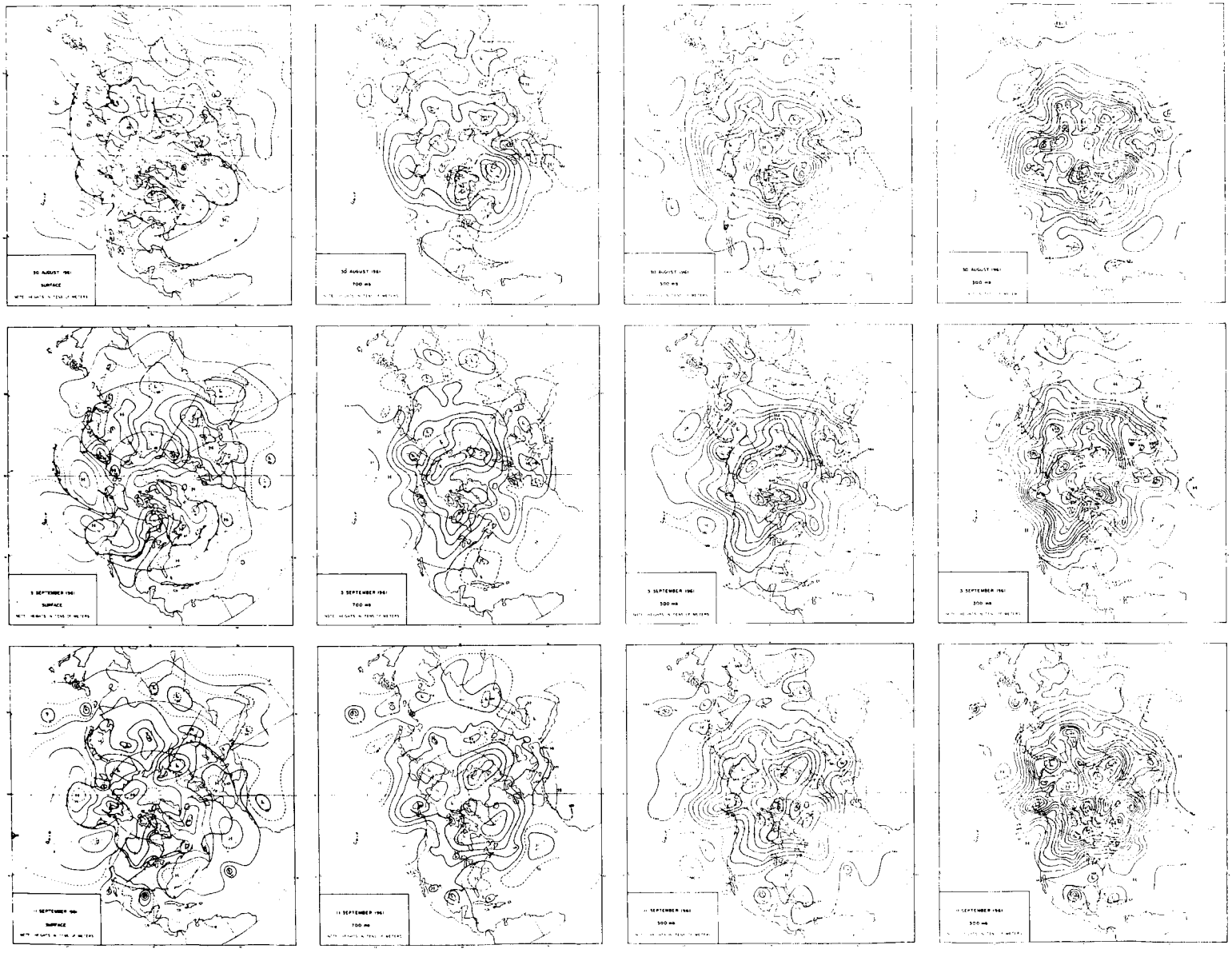

FIGURE 7
WEATHER ANALYSIS FOR AUGUST 30, SEPTEMBER 3, AND SEPTEMBER 11, 1961

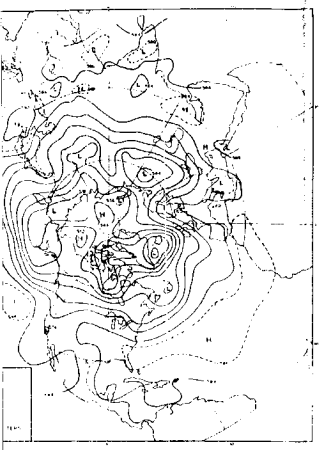

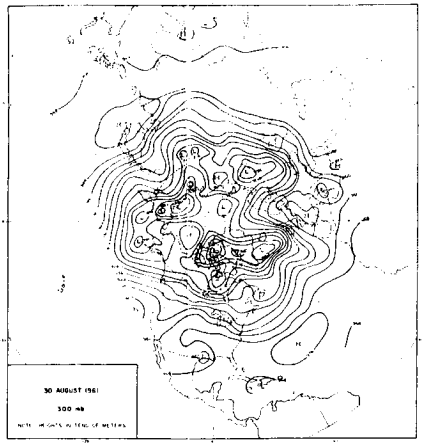
30 AUGUST 1961
300 mb

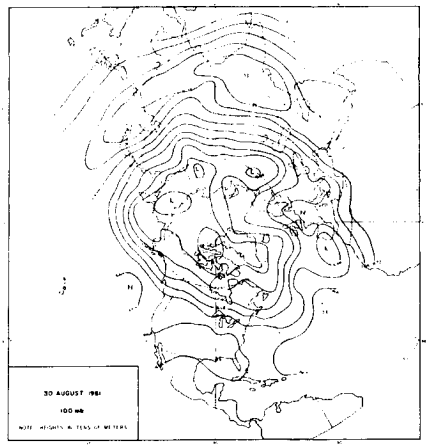
30 AUGUST 1961
100 mb

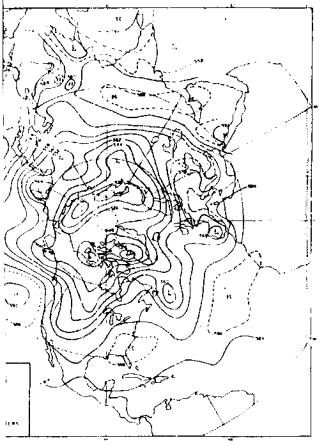

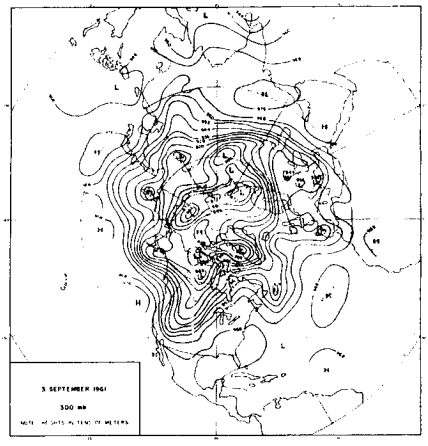
3 SEPTEMBER 1961
300 mb

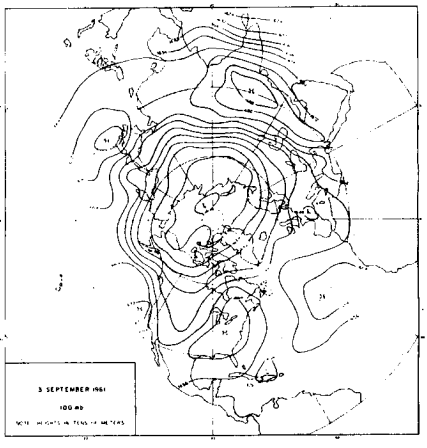
3 SEPTEMBER 1961
100 mb

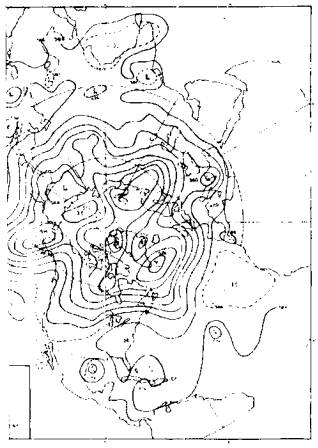

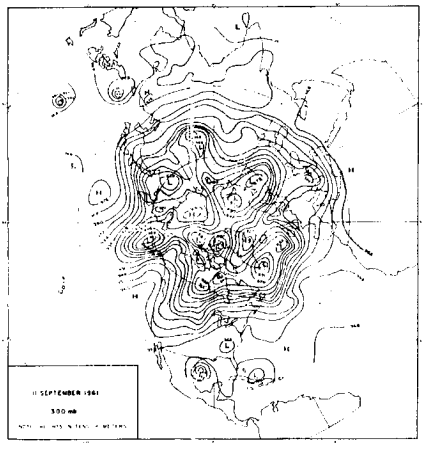
11 SEPTEMBER 1961
300 mb

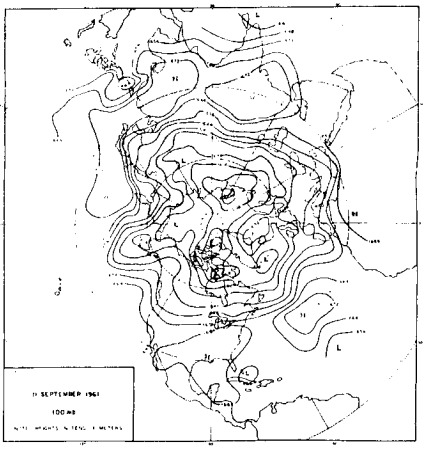
11 SEPTEMBER 1961
100 mb

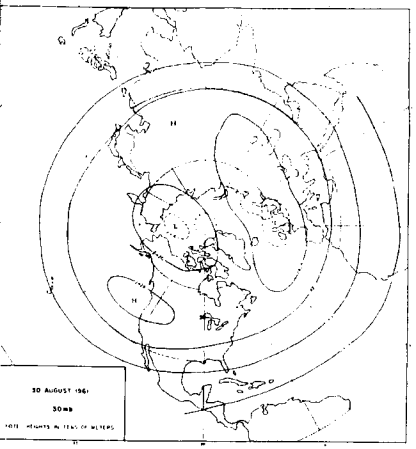
30 AUGUST 1961
30 mb

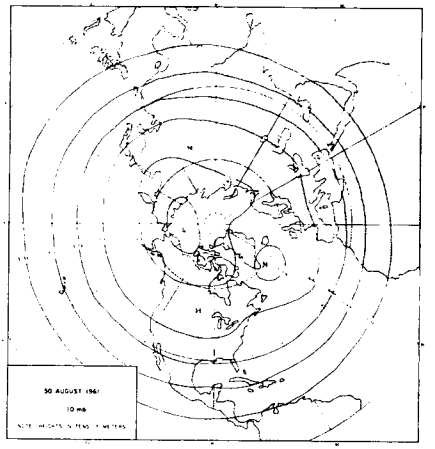
30 AUGUST 1961
10 mb

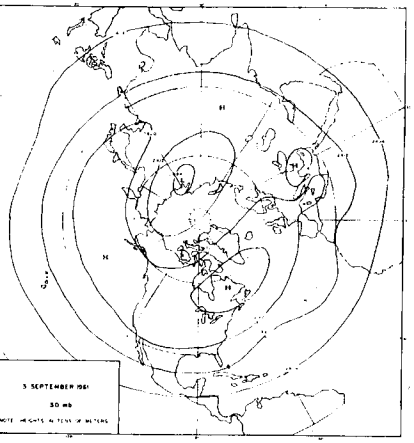
3 SEPTEMBER 1961
30 mb

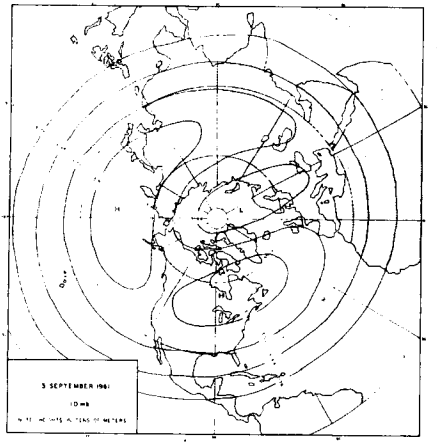
3 SEPTEMBER 1961
10 mb

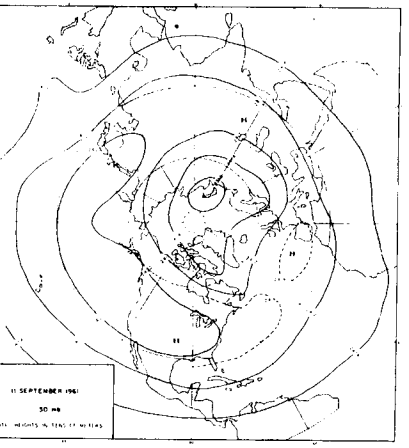
11 SEPTEMBER 1961
30 mb

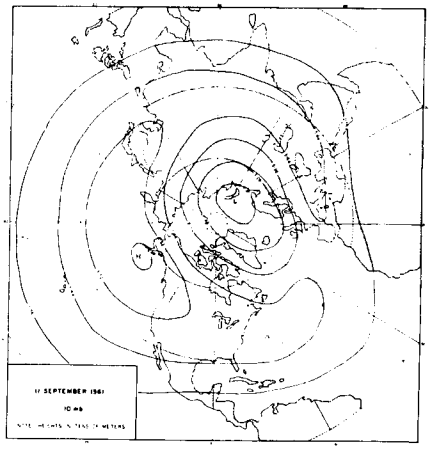
11 SEPTEMBER 1961
10 mb